

**SOLAR PV PLACEMENT AND SIZING FOR LINE STABILITY
ENHANCEMENT AND OPTIMAL OPERATING COST**

JAYIDAH BINTI MAT SALLEH

October 2019

**SOLAR PV PLACEMENT AND SIZING FOR LINE STABILITY
ENHANCEMENT AND OPTIMAL OPERATING COST**

JAYIDAH BINTI MAT SALLEH

**A Thesis Submitted to the College of Graduate Studies, Universiti
Tenaga Nasional in Fulfilment of the Requirements for the Degree of**

Master of Electrical Engineering

OCTOBER 2019

DECLARATION

I hereby declare that the thesis is my original work except for quotations and citations which have been duly acknowledged. I also declare that it has not been previously, and is not concurrently submitted for any other degree at Universiti Tenaga Nasional or at any other institutions. This thesis may be made available within the university library and may be photocopied and loaned to other libraries for the purpose of consultation.

JAYIDAH BINTI MAT SALLEH

Date : 02 October 2019

ABSTRACT

Nowadays, many countries have started to implement and installed solar photovoltaic (PV). Large penetrations of variable generation will have significant impacts on how scheduling is optimized to balance generation [1]. The initial designs of existing power systems were not integrating with any renewable energy (RE) including solar PV. So, the small scale of solar PV may not have any effect on these power systems. However, integrating large scale solar PV might raise several power quality issues including power system stability. Power system stability has become major attention where the main focus is on voltage stability [2]. Voltage stability is related on electrical grid capacity to balance the Total Power of Demand (P_D) and Total Power generated by Generator (P_{gnt}). Instability of the voltage can cause inability of the power system to meet the demand of reactive power. The lack of reactive power will cause instability in the power system. This paper present optimal placement and sizing of PV for stability enhancement and operating cost minimization. In this research, reactive power has gradually increased from 50 MVAR to 100 MVAR to 150 MVAR to 200 MVAR to 250 MVAR to 300 MVAR and to 350 MVAR and Fast Voltage Stability Index (FVSI) is applied to analyze voltage stability. The value of FVSI was used in order to determine the most sensitive line and corresponding weak bus in the system when increasing the reactive power. The results obtained from the voltage stability analysis using FVSI were utilized to predict system stability and identify most sensitive line corresponds to a load bus. The most sensitive line was indicated the unstable line. Then, Solar PV is applied to stabilize voltage stability of the power system. Economic Load Dispatch (ELD) is conducted to determine the optimal cost and loss [3]. DEIANT is conducted to optimize the total cost and the total loss after solar PV implementation. A performance comparison in terms of loss and cost minimization and voltage stability improvement was made when loss and cost minimization was taken to be the objective function. Simulation result indicates the effectiveness of the proposed technique for stability enhancement and operating cost minimization. From the results, solar PV capacity 100MW HIGH penetration produced the lowest total cost and total loss and FVSI result obtained the value start decrease nearest to 0.

ACKNOWLEDGMENT

In the Name of Allah, the Most Merciful, the Most Compassionate all praise be to Allah, the Lord of the worlds, and prayers and peace be upon Muhammad His servant and messenger.

First and foremost, I must acknowledge my limitless thanks to Allah, the Ever-Magnificent, the Ever-Thankful, for His help and bless. I am totally sure that this work would have never become truth without His guidance.

I would like to express my deepest gratitude and appreciation to my supervisor, Dr. Nur Azzammudin Bin Rahmat, for his invaluable advice and continuous guidance throughout the preparation of this dissertation.

My sincere thanks and gratefulness to Jabatan Perkhidmatan Awam Malaysia for providing financial support and opportunity for me to pursue and complete my study. I would like to extend my sincere thanks to all UNITEN staff that helped me a lot to complete this dissertation.

I would also like to extend my sincere thanks to my sisters, my friends, my classmates at the Universiti Tenaga Nasional and my boss and colleagues at the Jabatan Tenaga Manusia for their contributions.

This journey would not have been possible without support from my family. To my family, thank you for encouraging me in all of my pursuits and inspiring me to follow my dreams. I am especially grateful to my lovely husband En. Mohd Khairul Asyraf Bin Sabry and daughter Hannaan Qaisara Binti Mohd Khairul Asyraf for their support and understanding.

For my late mother and father Hjh. Meriam Binti Ibrahim and Hj. Mat Salleh bin Ahmad and my late mother-in-law Pn. Wan Teh binti Hashim, who always give me support to further my study as highest as I can. Al-Fatihah.

DEDICATION

This thesis is dedicated to:

The sake of Allah, my Creator and my Master,
My great teacher and messenger, Muhammad (May Allah bless
and grant him), who taught us the purpose of life,
My dearest husband, who leads me with light of hope and support,
My great parents and my kind mother-in-law (Al-Fatihah)
My sisters, who stands by me when things look bleak,
My beloved daughter Hannaan Qaisara, whom I can't force myself
to stop loving.
My friends who encourage and support me,
All the people in my life who touch my heart,
I dedicate this research.

TABLE OF CONTENTS

	Page
DECLARATION	ii
ABSTRACT	iii
ACKNOWLEDGEMENTS	iv
DEDICATION	v
TABLE OF CONTENTS	vi
LIST OF TABLES	x
LIST OF FIGURES	xiii
LIST OF SYMBOLS	xiv
LIST OF ABBREVIATIONS	xv
CHAPTER 1 INTRODUCTION	
1.1 Background	1
1.2 Problem Statement	3
1.3 Objective and Scope of Research	4
1.4 Summary of Chapter	4
1.5 Limitation of study	5
1.6 Summary	6
CHAPTER 2 LITERATURE REVIEW	
2.1 Introduction	7
2.2 Solar Photovoltaic	7
2.2.1 PV system	8
2.2.2 Solar PV in Malaysia	10
2.2.3 PV Potential in Malaysia	11
2.3 Impact of solar PV Implementation	14

2.4	Solar PV Implementation for this research	15
2.5	Voltage stability and voltage stability indices	16
2.5.1	Fast Voltage Stability Index (FVSI)	17
2.6	Economic Load Dispatch (ELD) and Optimization	21
2.7	Differential Evolution Immunized Ant Colony Optimization (DEIANT)	25
2.8	Summary	28
CHAPTER 3 METHODOLOGY		
3.1	Introduction	29
3.2	Research flow	29
3.3	Modeling Method	30
3.4	IEEE 26-Bus system	33
3.5	Newton-Raphson Power Flow Solution	37
3.6	FVSI Analysis	37
3.7	Solar PV Capacity and Output Power	38
3.8	Economic Load Dispatch (ELD)	39
3.9	Differential Evolution Immunized Ant Colony Optimization (DEIANT)	41
3.9.1	DEIANT Process	43
3.10	Summary	47
CHAPTER 4 RESULTS ANALYSIS AND DISCUSSIONS		
4.1	Introduction	48
4.2	Simulation Strategy	48
4.3	Simulation 1: Voltage Stability During Normal Condition	49
4.4	Simulation 2: Voltage Stability Studies Under Load Variations	51
4.5	Simulation 3: Voltage Stability Studies with PV Variations	53

4.5.1	Case 1: $Q_9=50\text{MVAR}$ with PV Variations	54
4.5.2	Case 2: $Q_9=150\text{MVAR}$ with PV Variations	55
4.5.3	Case 3: $Q_9=250\text{MVAR}$ with PV Variations	57
4.6	Simulation 4: Voltage Stability Under Worst Case Condition	59
4.7	Voltage Analysis	61
4.8	Economic Load Dispatch Before and After PV installation	63
4.8.1	Simulation 5: Economic Load Dispatch for 26 bus test system 50MVAR	64
4.8.2	Simulation 6: Economic Load Dispatch for 26 bus test system 150MVAR	67
4.8.3	Simulation 7: Economic Load Dispatch for 26 bus test system 250MVAR	70
4.8.4	Simulation 8: Economic Load Dispatch for 26 bus test system worst case	72
4.9	Optimization using DEIANT	75
4.9.1	Simulation 9: 50MVAR loading without and with solar PV Low irradiance level	76
4.9.2	Simulation 10: 50MVAR loading without PV and with PV Average irradiance level	77
4.9.3	Simulation 11: 50MVAR loading without PV and with PV High irradiance level	79
4.10	Summary	83
CHAPTER 5 CONCLUSION AND RECOMMENDATION		
5.1	Conclusion	85
5.2	Recommendation	86
5.3	Summary	86
REFERENCES		87

APPENDICES

93

Appendix A: Busdata and Linedata

Appendix B: FVSI Without and with solar PV

Appendix C: Voltage Profile for 26 Bus Test System

Appendix D: Economic Load Dispatch Before and After PV Placement

LIST OF TABLES

Table 2.1	New Generation Projects in the Peninsular 2017-2025	10
Table 2.2	Installed Capacity (MW) of Commissioned RE Installations	11
Table 2.3	Annual Power Generation (MWh) of Commissioned RE Installations	13
Table 2.4	PV active power output based on solar irradiance level with the penetration status	15
Table 2.5	Voltage stability indices	17
Table 2.6:	Economic Load Dispatch Methods	22
Table 2.7	Summary for DEIANT applications	27
Table 3.1	Distribution of the generators capacity total static load in the IEEE 26-Bus system	34
Table 3.2	Regulated Bus Data	34
Table 3.3	Transformer Data	35
Table 3.4	Shunt Capacitor Data	35
Table 3.5	Cost Coefficient of IEEE 26-Bus system	36
Table 3.6	Setting for base MVA, accuracy, and maximum iteration of IEEE 26-Bus system	36
Table 3.7	Generator Real Power Limit of IEEE 26-Bus system	36
Table 3.8	Summary of solar PV output power	39
Table 4.1	FVSI to indicate the stability status of IEEE 26 Bus Test System	49
Table 4.2	FVSI results for gradually increase MVAR at bus 9	51
Table 4.3	FVSI results for $Q_9=50\text{MVAR}$, without and with variations penetration status of solar PV	54
Table 4.4	FVSI results for $Q_9=150\text{MVAR}$, without and with variations penetration status of solar PV	56
Table 4.5	FVSI results for $Q_9=250\text{MVAR}$, without and with variations penetration status of solar PV	58
Table 4.6	FVSI result for $Q_9=350\text{MVAR}$, without and with	60

	variations penetration status of solar PV	
Table 4.7	Results for voltage profile under load variations with 100MW solar PV	62
Table 4.8	Total system loss and total generation cost, initial operating condition and optimal dispatch (50MVAR loading)	64
Table 4.9	Total optimal dispatch, total demand, total saving \$/h and total annual saving for initial operating condition and optimal dispatch (50MVAR loading)	66
Table 4.10	Total system loss and total generation cost, initial operating condition and optimal dispatch (150MVAR Loading)	68
Table 4.11	Total optimal dispatch, total demand, total saving \$/h and total annual saving for initial operating condition and optimal dispatch (150MVAR loading)	69
Table 4.12	Total system loss and total generation cost, initial operating condition and optimal dispatch (250MVAR loading)	70
Table 4.13	Total optimal dispatch, total demand, total saving \$/h and total annual saving for initial operating condition and optimal dispatch (250MVAR loading)	71
Table 4.14	Total system loss and total generation cost, initial operating condition and optimal dispatch (350MVAR loading)	73
Table 4.15	Total optimal dispatch, total demand, total saving \$/h and total annual saving for initial operating condition and optimal dispatch (350MVAR loading)	74
Table 4.16	DEIANT results with PV1 and PV2 with low penetration status	76
Table 4.17	DEIANT results with PV3 and PV4 with low penetration status	77
Table 4.18	DEIANT results with PV1 and PV2 with average penetration status	77

Table 4.19	DEIANT results with PV3 and PV4 with average penetration status	78
Table 4.20	DEIANT results with PV1 and PV2 with high penetration status	79
Table 4.21	DEIANT results with PV3 and PV4 with high penetration status	80
Table 4.22	DEIANT results without and with solar PV low irradiance level	81
Table 4.23	DEIANT results without and with solar PV average irradiance level	81
Table 4.24	DEIANT results without and with solar PV high irradiance level	82

LIST OF FIGURES

Figure 2.1	Process from a solar cell to a PV System	9
Figure 2.2:	Schematic Diagram of a grid-connected for PF system	10
Figure 2.3	Malaysia solar irradiance annually	12
Figure 2.4	2-Bus single line power system model	18
Figure 3.1	Research block diagram	30
Figure 3.2	The flowchart of the modeling process to prepare the simulation	32
Figure 3.3	One-Line Diagram 26 Bus Data	33
Figure 3.4	DEIANT Flowchart	42
Figure 3.5	Represents the random behavior of ant touring process	44
Figure 3.6	Cloning Process	45
Figure 3.7	Crossover Process	46
Figure 4.1	FVSI results for the most sensitive lines correspond to the load buses	52
Figure 4.2	Voltage profile for IEEE 26-Bus system under load variations	53
Figure 4.3	FVSI results for $Q_9=50\text{MVAR}$ reactive power loading without and with variations penetration status of solar PV	55
Figure 4.4	FVSI results for $Q_9=150\text{MVAR}$ reactive power loading without and with variations penetration status of solar PV	57
Figure 4.5	FVSI results for $Q_9=250\text{MVAR}$ reactive power loading without and with variations penetration status of solar PV	58
Figure 4.6	FVSI results for $Q_9=350\text{MVAR}$ reactive power loading without and with variations penetration status of solar PV	61
Figure 4.7	Voltage profile for IEEE 26-Bus system for $Q_9=50\text{MVAR}$ reactive power loading with 100MW solar PV	63

LIST OF SYMBOLS

P_D	Total Power Demand
P_{gtt}	Total Power generated by Generator
P_{Gen}	Power Generator
V_1	Voltage on Sending Buses
V_2	Voltage on Receiving Buses
P_i	Active power on the sending bus
Q_i	Reactive power on the sending bus
P_2	Active power on the receiving bus
Q_2	Reactive power on the receiving bus
P_1	Active power on the sending bus
Q_1	Reactive power on the sending bus
Q_9	Reactive power at bus 9
S_1	Apparent power on sending buses
S_2	Apparent power on receiving buses
δ	Angle different between sending and receiving buses

LIST OF ABBREVIATIONS

AVG	Average
ELD	Economic Load Dispatch
EED	Economic Emission Dispatch
EPP	Entry Point Projects
DEIANT	Differential Evolution Immunized Ant Colony Optimization
FiT	Fit-in-tariff
FVSI	Fast Voltage Stability Index
IEEE	Institute of Electrical and Electronic Engineer
MW	MegaWatt (Active Power)
MVAR	Mega Volt-Ampere Reactive (Reactive Power)
PV	Photovoltaic
RE	Renewable energy

CHAPTER 1

INTRODUCTION

1.1 Background

Malaysia has set to achieve the status of a developed country by 2020 through achieving sustainable development. To this end, Malaysia is on a need for sustainable energy, which is the main pillar of sustainable development. The major tools to achieve sustainable energy are renewable energy and energy efficiency [4]. The 11th Malaysia Plan (11MP 2016 – 2020) is the final stage of the ambitious plan for Malaysia to become a developed nation by 2020. The aim of the Malaysia Entry Point Projects (EPP) 10, building up renewable energy (RE) and solar power capacity is to leverage renewable energy as a feasible alternative to reduce Malaysia's dependence on fossil fuels, minimize carbon emissions, stimulate foreign direct investments, and contribute to job opportunity. In the National Renewable Energy Policy, solar power must provide at least 220MW to the total mix of capacity. A regulatory framework was also developed for the feed-in tariff (FiT) mechanism, which enables the sale of locally produced electricity to power utilities at fixed premiums for a certain period of time to assist the Government achieve its renewable energy targets [5].

According to [6] the challenges facing power utilities are to provide reliable power to customers has increased growth of load demand, technical constraints in power system and lack of active power generation. In addition, increased demand for load from the commercial, residential and industrial sectors may leads to voltage instability in power system network. This effect will cause voltage collapse. Therefore, a variety of methods have been used towards ensure the voltage stability can be maintained. Several of method has been introduced towards improving voltage stability in power system such as by integrating RE such as solar photovoltaic into the power system. An integration of RE into a power system causes

certain technical effects such as voltage instability, flicker effect and harmonic voltages and current [7]. This is because the initial designs of an existing power system network were not integrating with any RE including solar photovoltaic. So, the small-scale solar photovoltaic may not have an effect on this network but large-scale solar photovoltaic integration could raise several technical problems on power quality and power system stability to power system. Stability of the power system has been a major concern where the main focus is on voltage stability. Voltage stability is defined as the power system's ability to maintain a steady voltages at all buses in the system after experiencing some form of interference that leads to a voltage collapse [8].

Voltage instability occurs when the system generation fails to meet the load demand in the system [9]. The imbalance between the generation power and demand power can be due to system outage or limitations in reactive power sources or a combination of both. Insignificant voltage instability can result in voltage collapse, a process in which the sequence of events leading to voltage instability leads to erosion, or abnormal voltage in most power systems [10]. Voltage stability indices function to situate the present operation of a power system, predict future changes to the nature of the system, and evaluate a long-run development trend within predefined circumstances [11]. There are several methods that can be used to evaluate voltage stability indices such as fast voltage stability index (FVSI), Line stability index (Lmn) index is to evaluate the critical condition of lines, Line stability factor (LQP) index was developed that used for proving the voltage stability and others.

In Malaysia, indicators of energy have been established in the form of sustainable development through the recognition of energy policy priority areas such as guarantee sufficient and economic efficiency of energy supply, improve energy efficiency, improve social welfare, reduce the negative impact of energy generation on the environment and expansion and deployment of RE resources [12]. PV integration is seen as an attractive approach to reduce fuel cost, and save the environment. In order to assess its economic impact on the power system, it is crucial to conduct Economic Load Dispatch (ELD) with RE integration [13]. Therefore,

inappropriate integration of solar photovoltaic in random locations can cause power losses and voltage instability. So, this research highlight solar PV placement and sizing for line stability enhancement by evaluate using FVSI and optimal operating cost by using Differential Evolution Immunized Ant Colony Optimization (DEIANT).

1.2 Problem Statement

Solar photovoltaic receives great interest for its sustainable energy resources and low-cost installation[6]. Introduction to photovoltaic power generation otherwise can disturb power system stability if not properly planned. Therefore, researchers have done many researches on the effect of photovoltaic implementation to power system stability and integrity.

The impact of solar photovoltaic in power system stability depends on various factors for example solar photovoltaic installation latitude, meteorological factors, shading effect, and solar photovoltaic plant type integrated at various solar photovoltaic penetration level[6]. Therefore, proper placement and sizing of solar photovoltaic improves the stability of power system [14]. Most of the studies on stability of the power system after implementation of solar PV are not taking into account the impact on operating costs. Some researchers only studied operating costs regardless of the stability of the power system after installation of solar PV.

Therefore, a study on proper placement and sizing of solar PV to improve power system stability is required. There is also a need to use solar PV to reduce operating cost of conventional power plant.

This research will use fast voltage stability index (FVSI) to analyze the condition of voltage stability before and after the installations of solar photovoltaic in a power system. Then, economic load dispatch is conducted to analyze the total loss and the total cost of the power system before and after the installations of solar photovoltaic.

This is intended to meet the demand for specific loads and to minimize operating costs by optimal placement and sizing of solar photovoltaic.

1.3 Objective and Scope of Research

The aim of this research is to achieve optimal placement and sizing of solar photovoltaic for stability enhancement and operating cost minimization. Thus, several objectives are outlined to achieve the aim:

- i. To analyze power system stability under load variations using FVSI as stability indicator for IEEE 26 Bus Test System.
- ii. To evaluate the voltage stability before and after solar photovoltaic implementation using FVSI, at different irradiance level.
- iii. To determine optimal placement and sizing of solar photovoltaic that can improve power system stability, and minimize operating cost using DEIANT as an optimization tool.

1.4 Summary of Chapter

This thesis is divided into five chapters with appendixes.

Chapter 1:

This chapter explains on an introduction and background, problem statement, objective and scope of the research.

Chapter 2:

This chapter explains on the impact and effect implementation of the solar photovoltaic. This chapter also provides literature review of the research focusing on the voltage stability and voltage stability indices, fast voltage stability index (FVSI), economic load dispatch (ELD) and differential evolution immunized ant colony optimization (DEIANT).

Chapter 3:

This chapter outline the methodology used throughout the research. This chapter also covers simulation setup that includes modeling methodology for IEEE 26-Bus system and the computational method using MATLAB software. Newton-Raphson power flow, FVSI, economic load dispatch and DEIANT algorithm are discussed. The data of solar PV capacity and output power are also provided.

Chapter 4:

This chapter provides observations and results from simulation and mathematical method. It includes analysis of the results obtained and discussion about the voltage stability during normal condition, voltage stability studies under load variation, voltage stability studies with solar PV variations such as in low, average and high irradiance and voltage stability under worst-case condition. The results obtained and discussion of economic load dispatch before and after solar PV installation also provided. It also includes analysis of the results obtained and discussion on optimization using DEIANT for reactive power loading without and with solar PV low, average and high penetration status.

Chapter 5:

This chapter concludes research objectives and finding. The recommendations for future studies are also discussed.

1.5 Limitation of study

This research has some limitation that only for IEEE 26 Bus system and FVSI used as a voltage stability index. The reactive power gradually increased by bus 9. The solar PV with 10MW, 20MW, 40 MW and 100MW were used to control the voltage stability of the power system. ELD and DEIANT were used to calculate the total cost and total loss.

1.6 Summary

This chapter provided a comprehensive introduction including background, problem statement, objective and scope of research and summary of the chapter. The literature review will be defined in the next chapter.

CHAPTER 2

LITERATURE REVIEW

2.1 Introduction

In recent years, large amount of photovoltaic power generation has been presented into Malaysia energy mix. This is exactly encouraged by the introduction of the feed-in tariff (FiT) to Malaysia began as early as 2004 and Gazette of the RE and SEDA Bills on June 2011 [15]. However, introduction to photovoltaic power generation can disturb power system stability if it is not properly planned. Therefore, researchers have done many researches on the study of the effect of photovoltaic implementation on power systems. To meet the demand for specific loads and to minimize operating costs with voltage stability considerations has become a necessity to ensure power systems work efficiently, effectively and economically[16]. This chapter presents the literature review related to optimal placement and sizing of photovoltaic for stability enhancement and operating cost minimization. This chapter also discussed on solar photovoltaic implementation, voltage stability index and economic load dispatch. Furthermore, discussions on methods related to current studies are also presented.

2.2 Solar Photovoltaic

In year 1839, French physicist Edmund Becquerel had discovered the use of photovoltaic cells to utilize solar energy. This solar photovoltaic system consists of photovoltaic cells and equipment used to convert light energy into electricity. Since the source of light is the sun, it is called a solar cell. The word photovoltaic originates from the word photo which means light while voltaic refers to generating electricity. Thus, the photovoltaic process generates electricity directly from sunlight energy. Solar energy is radiant energy that is produced by the sun. In many parts of the world, direct solar radiation is one of the best prospective sources of energy. The

main ways to convert solar radiation into energy are active and passive solar design. Passive solar design is often based on the optimal design of buildings that capture the sun's energy in order to reduce the need for artificial light and heating [17]. The advantages of photovoltaic are characterized by zero discharge, silent operation, and long service life [15]. The photovoltaic also offer the ability for users to generate electricity in a more clean, quiet and reliable with low maintenance and no fuel costs [18]. Solar photovoltaic technology could harness the sun's energy to provide large-scale, domestically secure, and environmentally friendly electricity [19].

2.2.1 PV system

Solar cells convert sunlight directly into electricity without creating any water or air pollution. Figure 2.1 shows a complete process from solar cells to a PV system and the processes are as follows:

- i) Solar cells are constructed by at least two layers of semiconductor materials. A positive charge layer and a negative charge layer.
- ii) This process starts when the light enters the cell, the photon from the light absorbed by the semiconductor atom, the electrons will be released from the cell's negative layer then flows through the external circuit and returns to the positive layer. This flow of electrons produces electric current.
- iii) To increase their utility, dozens of individual solar cells are connected in a sealed with weatherproof package called a solar module.
- iv) Two solar modules are connected in series called a solar panel; the produce voltage is doubled while constant current.
- v) Two solar modules are connected in parallel; the produce current is doubled but constant voltage. To achieve the desired voltage and current solar modules are connected in series and parallel. It is called a solar array.
- vi) The combination of solar array produced a PV System.

The flexibility of the modular PV system allows the solar energy system to be manufactured to meet various electrical needs [15]. From the figure 2.1, shown a process from a solar cell to a PV system.

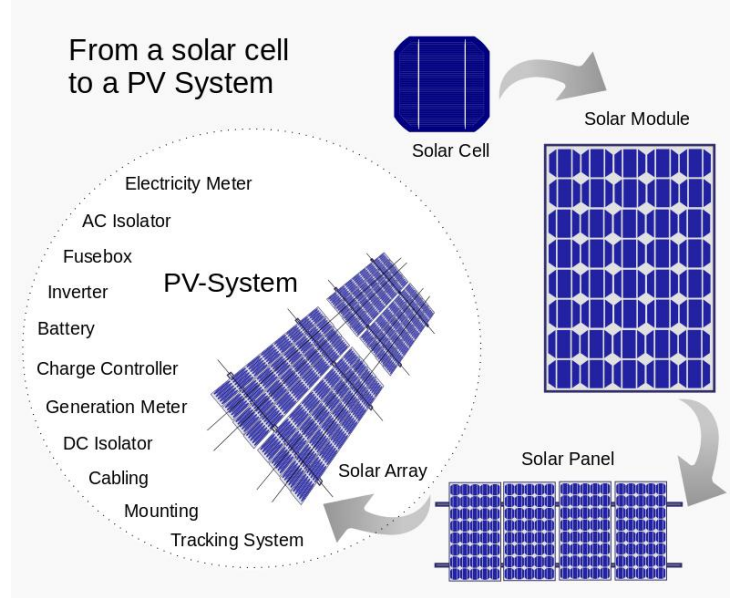


Figure 2.1: Process from a solar cell to a PV System [20]

While figure 2.2 shows a schematic diagram of a grid-connected PV system. The schematic diagram typically consists of components as follows:

- i) PV array;
- ii) DC link capacitor;
- iii) inverter with filter;
- iv) step-up transformer; and
- v) power grid.

The flow start when the DC power generated from the PV array charges the DC link capacitor. Then, the inverter converts the DC power into AC power that has a sinusoidal voltage and frequency related to the utility grid. The diode function is to blocks the reverse current flow through the PV array. Next, the transformer steps up the inverter voltage to the nominal value of the grid voltage and provides electrical isolation between the PV system and the grid. The harmonic filter eliminates the harmonic components other than the fundamental electrical frequency [21].

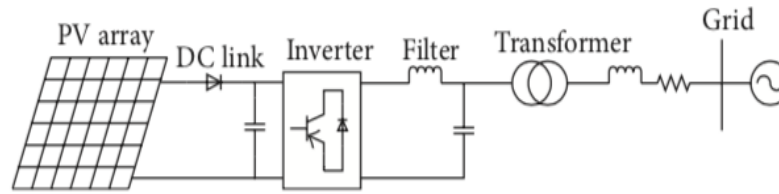


Figure 2.2: Schematic Diagram of a grid-connected for PF system

2.2.2 Solar PV in Malaysia

During the 21st Conference of Parties (COP 21) from the 30 November to 12 December 2015, Malaysia signed the Paris Agreement and pledged to reduce carbon emissions by 45% by 2030. Malaysia Government commits to increase renewable energy generation capacity by 20% by 2025. One initiative that has been taken to help achieve the goals of that pledge is the Large Scale Solar (LSS) programme. Tenaga Nasional Bhd (TNB)'s Large Scale Solar (LSS) project at Mukim Tanjung 12, Kuala Langat, Selangor has reached its initial operation date (IOD) with the first generated power transmitted to the National Grid last week. Work is progressing well for the solar plant to generate its full capacity of 50MW before year end. The plant, with 230,000 solar panels and 10 km of 132kV power and fiber optic underground cable, is Malaysia's first largest LSS project to date. New Generation Projects in the Peninsular 2017-2025 shown in table 2.1.

Table 2.1: New Generation Projects in the Peninsular 2017-2025

Renewable Energy	New Generation Projects	Capacity (MW)	Status
Solar	Edra Solar Sdn. Bhd Kuala Ketil, Kedah	50	Ongoing Construction
	Quantum Solar Park (Malaysia) Sdn. Bhd Kedah, Terengganu & Melaka	150	Ongoing Construction

The second ongoing construction for the solar plant project is at Kuala Ketil, Kedah with solar capacity is 50MW. Third, ongoing construction for the solar plant project

is at Kedah, Terengganu and Melaka by Quantum Solar Park with solar capacity is 150MW.

2.2.3 PV Potential in Malaysia

Several researchers have been published their review on studies the current potential for the solar energy development, initiatives and the renewable energy policies in Malaysia. The authors in [15] present an overview of the current perspective for renewable energy development in Malaysia. There are several potential renewable energy sources available in Malaysia such as solar, biomass, biogas, mini-hydro, and municipal solid waste. The government has introduced a comprehensive policy in implementing renewable energy.

Table 2.2: Installed Capacity (MW) of Commissioned RE Installations

Year	Biomass	Solar PV	Small Hydro	Biomass (Solid Waste)	Biogas (Landfill / Agri Waste)	Biogas	Geothermal	Total
2012	36.90	31.54	11.70	8.90	3.16	2.00	0.00	94.20
2013	0.00	106.93	0.00	0.00	3.20	3.38	0.00	113.51
2014	12.50	61.88	0.00	0.00	0.00	1.10	0.00	75.48
2015	13.80	60.33	6.60	7.00	5.40	0.00	0.00	93.13
2016	19.50	77.83	12.00	0.00	15.46	0.00	0.00	124.79
2017	0.00	38.64	0.00	0.00	22.54	0.00	0.00	61.18
2018	0.00	2.87	20.00	5.85	11.71	0.00	0.00	40.43
2019	0.00	0.01	0.00	0.00	1.50	0.00	0.00	1.51
Cumulative	82.70	380.03	50.30	21.75	62.97	6.48	0.00	604.23

The installed capacity (MW) of commissioned RE installations shown in table Table 2.2 explained the total RE capacities (in MW) granted with Feed-in Approvals under the FiT mechanism and which have achieved the FiT Commencement Date. The total cumulative installed photovoltaic (PV) capacity is approximately 380.03 MW. It is expected that solar energy has the potential to reach more than 6500 MW by 2030. There is approximately 82.70 MW in biomass and 62.97 MW in biogas (landfill/agri waste). The potential capacity of both biomass and biogas can become 1340 MW and 410 MW, respectively by 2028. The current mini-hydro generation is approximately 50.3 MW and should reach 490 MW by 2020. As for biomass (solid waste) power generation, the total cumulative capacity is 21.75 MW and can be 360 MW by 2020. The current biogas generation is approximately 6.48 MW.

By these constant efforts, Malaysia can be one of the largest producers in renewable and sustainable energy in the world. The solar energy outlook has been positive and is expected to exceed all other renewable energy sources in Malaysia by year 2050. This is because Malaysia is a tropical country where high solar irradiance is available throughout the year. Malaysia receives an average of 4.96kWh/m² of solar irradiance annually. This is shown in Figure 2.3.

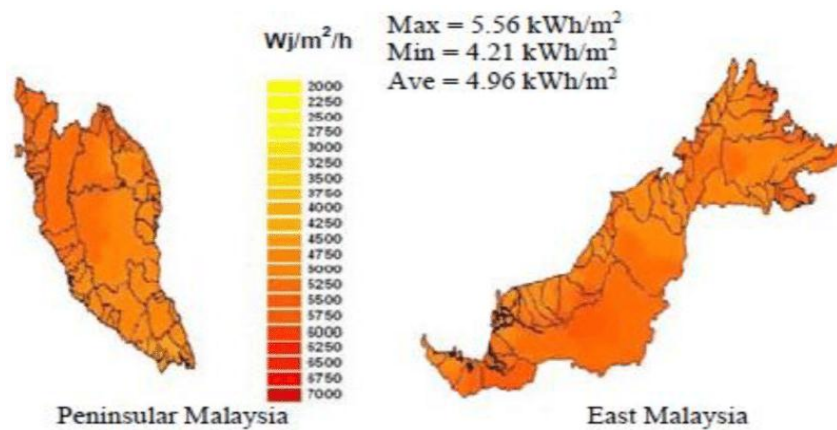


Figure 2.3: Malaysia solar irradiance annually

The Malaysian government has put in efforts to encourage the utilization of photovoltaic systems especially to the domestic users. The authors of state that Malaysia is likely to be one of the largest solar power producers in the world in the near future. These research efforts coupled with the government policy on solar

energy can stimulate the PV market growth substantially. The Malaysian government has also introduced solar energy programs such as Suria 1000, Malaysia Building Integrated Photovoltaic (MBIPV) and Feed-In Tariff (FiT) mechanism. The following table 2.3, show the amount of RE generated under the FiT system, in Megawatt-hours (MWh). The reading represents RE generated on an annual basis and for the respective on-going year. Readings are reported from year 2012 up to the year 2019.

Table 2.3: Annual Power Generation (MWh) of Commissioned RE Installations

Year	Solar PV	Biomass	Biogas (Landfill / Agri Waste)	Small Hydro	Biogas	Biomass (Solid Waste)	Geothermal
2019	64913.81	41997.24	40171.00	13148.15	2709.10	0.24	0.00
2018	462906.02	225468.05	225415.85	65377.23	15679.17	4102.42	0.00
2017	427736.03	247542.95	198985.22	74831.27	16319.90	19303.86	0.00
2016	318900.54	151385.22	70486.00	47798.28	17143.13	36751.74	0.00
2015	264096.44	192372.22	41122.39	55406.38	16988.66	18090.07	0.00
2014	184553.90	226196.38	31844.44	67567.90	19772.25	4347.83	0.00
2013	50875.29	209407.59	9804.10	79081.75	12962.68	11144.25	0.00
2012	5321.15	101309.87	7465.40	25629.78	98.11	3234.52	0.00

The total Annual Power Generation (MWh) of commissioned RE Installations for current year 2019 show Solar PV produced the highest power generation is approximately 64913.81MWh. Second is biomass produced the power generation is approximately 41997.24MWh. Third is biogas (landfill/agri waste) produced the power generation is approximately 40171.00MWh. Next is small hydro produced the power generation is approximately 13148.15MWh. Biogas produced the power generation is approximately 2709.10MWh. Last is biomass (solid waste) produced the power generation is approximately 0.24MWh.

2.3 Impact of solar PV Implementation

Several researchers have been published their review on studies on the impact of integrating solar PV generator into power system. According to [22] an integrating solar PV generator into power system improves the loading margin, voltage magnitude of the system and improves voltage stability. However it needs comprehensive design and analysis on the solar PV system and integrating techniques to ensure high quality and reliability of power supply. This can be supported by [6] the effects of solar PV generation on power system voltage stability are thoroughly examined based on various factors that influence system static and dynamic voltage stabilities. However, the efficiency of voltage stability analysis depends on the system design, application and scenarios. In placing more emphasis [23] claimed that high level of solar PV penetration can inject power to transmission network that can affect the voltage level and protection setting of the distribution system. The technical impacts of high PV penetration into distribution systems are mainly on the current and voltage profiles such as voltage stability, quality of power, power balancing, protection, losses in system and power factor [24].

Furthermore, in an observation based study by [25] solar PV generation provide energy at the load side of the distribution network can reduce the feeder active power loading and thus improving the voltage profile. Consequently, solar PV system can delay the operation time of shunt capacitors and series voltage regulators hence increasing their lifetime and reduce the losses in distribution feeders if optimally allocated and sized. The research effort in [26] revealed the solar PV impact on power system stability. The study explained about the stability issues such as voltage stability, transient stability and small signal stability that related to solar PV and existing generators for secure and reliable operation of the power system. The study in [27] concludes that the location, mode, and size of solar PV have a strong effect on static voltage stability. Voltage stability fails due to solar PV inverters operating in constant power factor mode during operation, while solar PV inverters operating in the voltage regulation mode may improve the system voltage stability [28]. To improve voltage stability and reducing power loss in a power system with PV generators, appropriate planning of PV generators is considered by optimal

placement of PV [29]. In this research the voltage stability before and after the placement of solar PV in a power system will be studied.

2.4 Solar PV Implementation for this research

In this research, the Solar PV output and capacity which has been provided in [14] will be used as a variation of PV integrated to instability buses. The data of solar irradiance as shown in Table 2.4 explained on the penetrations of solar PV that are categorized in accordance to the solar irradiation level. Furthermore, the output power of the solar PV panels also had shown at irradiance each level.

Table 2.4: PV active power output based on solar irradiance level with the penetration status

No.	Irradiance (W/m ²)	PV Output (MW)				Penetration Status
		10MW	20MW	40MW	100MW	
1	192	1.527	3.052	6.102	15.231	
2	393	3.699	7.399	14.789	36.842	
3	586	5.708	11.412	22.807	56.826	HIGH
4	539	5.204	10.403	20.805	51.939	
5	318	2.843	5.689	11.395	28.575	
6	470	4.475	8.941	17.891	44.652	AVERAGE
7	335	3.032	6.072	12.16	30.414	
8	240	1.993	3.991	8.002	20.019	
9	315	2.819	5.639	10.473	28.223	
10	112	0.859	1.734	3.485	8.721	LOW

Table 2.4 provided ten inputs point for solar irradiance data with different PV sizing from 10MW, 20MW, 40MW and 100MW. The PV output power entering the transmission system depends on the solar irradiance.

2.5 Voltage stability and voltage stability indices

Voltage stability has recently become the two important parameters of electric power quality describing the power system performance [6] [30]. Voltage stability refers to the ability of power system to maintain steady voltages at all buses in the system after being exposed to a disturbance from a given initial operating point [31]. Refer to [32] voltage instability occurs when there is an interruption, an increase in load demand, or a change in power system condition which in turn causes a progressive and uncontrolled decrease in voltage.

According to [33] voltage stability can be analyzed by dynamic or static approaches. Dynamic approaches require more computational time while static approaches summarize views of a system at different time frames. Many static techniques are used to analyze the voltage stability of a system. The research results based on repeated power flow using PV and QV curves whereas these methods involve repeated power flow solution and effect on time consuming [3]. So, voltage stability indices were developed to calculate faster assessment of voltage stability in power system. Voltage stability indices function to situate the present operation of a power system, predict future changes to the nature of the system, and evaluate a long-run development trend within predefined circumstances [11].

As stated in [33] voltage stability indices calculate a numeric value from the power flow solution (PFS) that indicates the voltage stability state of the power system. The previous voltage stability indices were based on Jacobian matrix. However, this method cannot precisely estimate the voltage collapse point because of non-linearity near the collapse point. Next voltage stability indices developed in [34] calculated index based on artificial neural network (ANN), which is to address voltage security. This method becomes more complex and not suitable for the large power system. Others voltage stability index develops such as L-index based on load flow solution, is inaccurate when loads are not type of constant power. Line stability index (Lmn) index is to evaluate the critical condition of lines. Lmn has to be kept less than unity in order to ensure voltage stability is maintained in a system. Lmn evaluated higher

than unity implies imaginary voltage is experienced on the receiving bus leading to voltage instability in the whole system [8].

Line stability factor (LQP) index was developed that used for proving the voltage stability state of lines via load flow solution. LQP must be kept less than 1.00 in order to maintain real roots of Q_i hence a stable system [35]. The equations for Lmn and LQP are described in table 2.5.

Table 2.5: Voltage stability indices

No.	Year	Author	Topic	Equation
1	1998	M.Moghavvemi, F.M.Omar [8]	Line stability index (Lmn)	$L_{mn} = \frac{4XQ_j}{[V_s \sin(\theta - \delta)]^2}$
2	1989	A.Mohamed, G.B.Jasmon, S.Yusoff [36]	Line stability factor (LQP)	$LQP = 4 \left(\frac{X_{ij}}{V_i^2} \right) \left(\frac{X_{ij}}{V_i^2} P_i^2 + Q_j \right)$

Among the various indices for voltage stability and voltage collapse prediction, the FVSI offers truthful, correct and consistent results. The most advantage of FVSI and Lmn is the easy and understandable numerical calculations and results are more demonstrative [37]. This research employs FVSI as voltage stability indicator, as discussed further on the following section.

2.5.1 Fast Voltage Stability Index (FVSI)

A study by [38], has derived Fast Voltage Stability Index (FVSI) to measure voltage stability of lines in power system. FVSI use mathematic formulation and implemented in MATLAB. FVSI is formulated based on 2-bus power system model as shown in Figure 2.4:

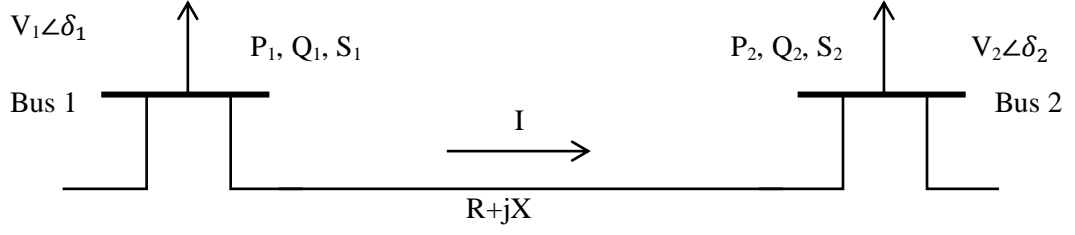


Figure 2.4: 2-Bus single line power system model [38]

Where;

V_1, V_2 = Voltage on sending and receiving buses

P_1, Q_1 = Active and reactive power on the sending bus

P_2, Q_2 = Active and reactive power on the receiving bus

S_1, S_2 = apparent power on sending and receiving buses

δ = angle different between sending and receiving buses

$$\delta = \delta_1 - \delta_2 \quad (\text{Equation 2.1})$$

The line impedance is noted as $Z = R+jX$ with the current that flows in the line is given by:

$$I = \frac{V_1 \angle 0 - V_2 \angle \delta}{R + jX} \quad (\text{Equation 2.2})$$

Taken V_1 as the reference and angle is shifted into 0, using the apparent power at bus 2, $S_2 = V_2 I_2^*$. So, after rearranged current flow, I can be written as:

$$I_2 = \left(\frac{S_2}{V_2} \right)^* = \frac{P_2 - jQ_2}{V_2 \angle -\delta} \quad (\text{Equation 2.3})$$

Equating both Equation 2.2 and Equation 2.3 can be written as:

$$\frac{V_1 \angle 0 - V_2 \angle \delta}{R + jX} = \frac{P_2 - jQ_2}{V_2 \angle -\delta} \quad (\text{Equation 2.4})$$

$$V_1 V_2 \angle -\delta - V_2^2 \angle 0 = (R + jX)(P_2 - jQ_2) \quad (\text{Equation 2.5})$$

$$V_1 V_2 (\cos \delta - j \sin \delta) - V_2^2 = (R + jX)(P_2 - jQ_2) \quad (\text{Equation 2.6})$$

Then, separate the real and imaginary parts of Equation 2.6 can be written as:

$$V_1 V_2 \cos \delta - V_2^2 = R P_2 + X Q_2 \quad (\text{Equation 2.7})$$

And,

$$-V_1 V_2 \sin \delta = X P_2 + R Q_2 \quad (\text{Equation 2.8})$$

Rearranging Equation 2.8 for P_2 :

$$P_2 = \frac{R}{X} Q_2 - \frac{V_1 V_2}{X} \sin \delta \quad (\text{Equation 2.9})$$

Substituting P_2 in Equation 2.7 can be written as:

$$V_1 V_2 \cos \delta - V_2^2 = R \left(\frac{R}{X} Q_2 - \frac{V_1 V_2}{X} \sin \delta \right) + X Q_2 \quad (\text{Equation 2.10})$$

$$V_2^2 + \frac{R^2}{X} Q_2 - \frac{R V_1 V_2}{X} \sin \delta - V_1 V_2 \cos \delta + X Q_2 = 0 \quad (\text{Equation 2.11})$$

Then, rearranging Equation 2.11 into the form $aV_2^2 + bV_2 + c = 0$ and the roots for V_2 will be,

$$a = 1, b = \left(\frac{R}{X} \sin \delta + \cos \delta \right) V_1 \text{ and } c = \left(x + \frac{R^2}{X} \right) Q_2$$

$$V_2 = \frac{\left(\frac{R}{X} \sin \delta + \cos \delta \right) V_1 \pm \sqrt{\left[\left(\frac{R}{X} \sin \delta + \cos \delta \right) V_1 \right]^2 - 4 \left(x + \frac{R^2}{X} \right) Q_2}}{2} \quad (\text{Equation 2.12})$$

To obtain real roots for V_2 , thus the following equation can be derived as

$$b^2 - 4ac \geq 0$$

So,

$$\frac{4(Z^2 Q_2 X)}{[(R \sin \delta + X \cos \delta) V_1]^2} \leq 1 \quad (\text{Equation 2.13})$$

Since δ is normally very small then,

$$\delta \approx 0, R \sin \delta \approx 0 \text{ and } X \cos \delta \approx X \quad (\text{Equation 2.14})$$

The assumptions in Equation 2.14 can be used to simplified Equation 2.13 can be written as:

$$\frac{4Z^2Q_2}{XV_1^2} \leq 1 \quad (\text{Equation 2.15})$$

By taking the symbols ‘*i*’ to substitute as the sending end and ‘*j*’ to substitute as receiving end, hence the Equation 2.15 used to define the FVSI for a line connecting bus ‘*i*’ and bus ‘*j*’ as below Equation 2.16

$$FVSI_{ij} = \frac{4Z_{ij}^2Q_j}{V_i^2X_{ij}} \quad (\text{Equation 2.16})$$

Where;

Z_{ij} = line impedance

X_{ij} = line reactance

V_i = voltage at the sending end

Q_j = reactive power at the receiving end

Fast voltage stability index (FVSI) suggested by [38] , was used to predict the voltage collapse point and contingency rankings of critical lines. The study [39] conclude that the voltage stability analysis procedure carried out using FVSI is efficient in defining the critical line referred to a critical outage, bus, the load ranking in the power system and weak bus beside. The highest FVSI value indicates a sensitive line referring to the bus, while the lowest reactive power loading shows the weak bus in the power system. In order to maintain line stability, FVSI value must be kept near to zero (0). If FVSI value is near to unity (1.0), it shows that the corresponding line is unstable. This can cause overall system to collapse and the reduction in voltage drop at heavily loaded bus.

Fast voltage stability index develop by [38] is a new voltage stability index refers to a line. The values of the line indices indicate the voltage stability condition in the system and it is used to rank the line outage contingency. In the voltage stability analysis, the line that gives index value closest to 1.00 will be taken as the most critical line corresponds to a bus that may lead to the whole system instability. Several of researchers have published their research on used of fast voltage stability

index as an indicator to utilize the voltage stability condition after load flow process is performed. According to [40] voltage stability index or proximity is the tool used to evaluate the voltage stability condition formulated based on a line or a bus. The line that exhibits FVSI closed to 1.00 implies that it is approaching its instability point. If FVSI goes beyond 1.00, one of the buses connected to the line will experience a sudden voltage drop leading to system collapse.

This can be supported by [41] that FVSI is used to determine the weak buses for the reactive power planning problem which involves process of simulation by voltage stability analysis based on the load variation. In placing more emphasis [42] claimed the FVSI close to unity can be described as a weakest bus. This can be supported by [43] that FVSI can be used as a tool for voltage stability indicator when the area that has the highest FVSI value would indicate the weakest branch in the system. Furthermore, an observation study in [16] described the weakest line when the FVSI of the line reached the value above 1.00. This research uses FVSI to analyze the condition of voltage stability before and after the implementation of solar photovoltaic in a power system.

2.6 Economic Load Dispatch (ELD)

ELD is referring towards the capabilities of the generator to allow real and reactive power vary within the certain limits to fulfill the load demand with minimum fuel cost [13]. In ELD, the total cost and the total loss are both the highest concern. When the loss is decrease, the total cost will reduce and vice versa. To fulfill the load demand, the strategic dispatch of electricity through the economic load dispatch is needed. Economic load dispatch is conducted to calculate the operation cost of power system. Several researches on ELD have been conducted. The dispatch strategy through a mathematical programming approach seeks to reduce to the minimum the fuel cost of conventional generators, the energy transactions, the regeneration of polluted emissions and, finally, includes the benefit in electricity demand reduction satisfying all restrictions through mathematical programming strategy [44].

In a study stated in [45] the economic dispatch with application of embedded generator will decrease the total losses and reduce the total cost of generation. This proves that with reduced of the total losses, the total generation is nearly equal to the total demand. So, all the power generated is applied to the load or demand and also reduces the generation cost.

According to [46] the author explained, usually the fuel cost function for generation has been represented as a quadratic function and resolved using classical optimization techniques, such as the lambda approach, the gradient method, linear programming, and Newton's methods. As mentioned in [47] there are several traditional approach to solve an ELD problem such as Newton methods, Gradient-based techniques, quadratic programming, and linear programming In research document in [47], the author highlight a traditional approach to solve the ELD by using Lambda iteration. While, in a study reported in [48] the author used a conventional Newton Raphson and Lagrangian multiplier algorithms and also proposed genetic algorithm (GA) as a comparative study of solution of ELD. However, the issue of these methods is convergence depending on the size of the power system, the initial guess, and the local minimum probability. According to [48] the author highlight the researchers have proposed various intelligent technique optimization algorithm for example particle swarm optimization (PSO), non-dominated sorting genetic algorithm, ant colony optimization (ACO), and differential evaluation immunized ant colony optimization (DEIANT) and others technique to obtain ELD. Table 2.6 shows some examples of methods of calculating economic load dispatch.

Table 2.6: Economic load dispatch methods

No.	Year	Author	Method	Merits	Demerits
1	2015	S. K. Dewangan, A. Jain, and a P. Huddar [49]	Lambda iteration	<ul style="list-style-type: none"> Most popular traditional technique to solve ELD problem for 	<ul style="list-style-type: none"> Computational procedure is complex.

No.	Year	Author	Method	Merits	Demerits
				<p>minimizing the cost of generating unit.</p> <ul style="list-style-type: none"> • Converges very fast. 	
2	2015	S. K. Mishra and S. K. Mishra [48]	Newton	<ul style="list-style-type: none"> • Solve the economic dispatch by observing that the aim is to always drive the gradient of function to zero. • Solve for the correction that is much closer to the minimum generation cost. 	<ul style="list-style-type: none"> • Convergence depends on initial guess, size of the system and the possibility of local minima.
3	2012	O. Abedinia, N. Amjady, and M. S. Naderi [50]	Genetic Algorithm (GA)	<ul style="list-style-type: none"> • Known as a global optimization technique. • Its efficiency and flexibility. • GA ensures colony evolves 	<ul style="list-style-type: none"> • Lacks a strong capacity of producing better offspring. • slow convergence near global optimum.

No.	Year	Author	Method	Merits	Demerits
				and solutions change continually.	<ul style="list-style-type: none"> • Trapped into local optimum. • Premature convergence of GA, its performance degrades, and its search capability reduces.
4		Sharma, Uma. Moses, Beaulah [51]	Particle swarm optimization (PSO)	<ul style="list-style-type: none"> • Simulation of a communal psychological metaphor instead of the existence of the suitable individual. • PSO has been effectively applied to determine the optimum allocation of power among committed units to minimize the total generation cost. • Offers high quality 	<ul style="list-style-type: none"> • PSO has got the disadvantage of getting caught up in local minimum while it handles heavy constraints in problems of optimisation due to restricted local or global search capabilities.

No.	Year	Author	Method	Merits	Demerits
				solutions, limited time of computation and stable convergence.	

In this research economic load dispatch is conducted to analyze the total loss and the total cost of the power system before and after the implementation of solar photovoltaic.

2.7 Differential Evolution Immunized Ant Colony Optimization (DEIANT)

In order to improve the performance of conventional Ant Colony Optimization (ACO), Differential Evolution Immunized Ant Colony Optimization (DEIANT) algorithm is developed. As stated in [13], conventional ACO algorithm was altered by integrating mutation and cloning process adopted from Differential Evolution and Artificial Immune System.

According to [52] the researcher used the DEIANT to optimize ELD in the power system. DEIANT engine has successfully improved the operating cost of generating units. The study concluded that DEIANT shown a very capable and proved the efficient. DEIANT is also faster compare to the ACO and the traditional ELD technique.

As state in [53] the researcher highlights the implementation of DEIANT technique in resolving economic and emission dispatch (EED). The new algorithm is the combination of cloning process from Artificial Immune System and Differential Evolution, Ant Colony Optimization. The study concluded that DEIANT is more superior to the traditional method, PSO, and ACO, and effectively minimize the

emission level. DEIANT also successfully perform better than in terms of solving the objective function and convergence speed

In a study reported in [54] a variety of intelligence techniques including Particle Swarm Optimization, Ant Colony Optimization, and DEIANT have been used to optimize the fuzzy unit commitment problem. From the study it can be concluded that DEIANT optimization technique has been verified to bear the best solution for unit commitment between the other two techniques. This can be supported by [55] has used DEIANT technique to optimize Fuzzy Combined-Emission Dispatch (FCED). The researcher compared DEIANT with Evolutionary Programming (EP) and Ant Colony Optimization (ACO) techniques in order to assess its performance. The study concluded the using of DEIANT is to optimize FCED problem achieved lower minimal emission level and reduce operating cost compare to EP and PSO.

In a study reported in [56] mentioned the use of DEIANT in resolving ELD problem with valve-point effect. A comparative study also involving EP and ACO. The study concluded that DEIANT is superior to the other compared methods in terms of calculating lower operating cost and power loss. Furthermore, in an observation based study by [57] explained the use of DEIANT technique in solving economic dispatch by considering prohibited operating zones. Comparing it with EP and ACO technique performed DEIANT technique. The study concluded that DEIANT executed the best in terms of calculating lower operating cost and loss.

The study conclude in [13] DEIANT is proposed as the optimization device to calculate the operating cost of power system with the integration of solar PV system. Solar PV integration significantly reduces fuel cost, as the technology will support the operation of existing conventional generators. From the study it can be concluded that DEIANT successfully optimizes ELD with photovoltaic integration. The summary for DEIANT applicatios are shown in table 2.7. In this research DEIANT is proposed to optimize operating costs through optimal placement and sizing of solar PV.

Table 2.7: Summary for DEIANT applications

No.	Year	Author	Topic	Application
1	2014	N. A. Rahmat, I. Musirin, A. F. Abidin, M. R. Ahmad [56]	Economic load dispatch with valve-point loading effect by using differential evolution immunized ant colony optimization technique	Differential Evolution Immunized Ant Colony Optimization (DEIANT) proposed in solving economic load dispatch problem with valve-point effect
2	2014	N. A. Rahmat, I. Musirin, A. F. Abidin [57]	Differential Evolution Immunized Ant Colony Optimization Technique (DEIANT) in solving economic dispatch by considering prohibited operating zones	Differential Evolution Immunized Ant Colony Optimization (DEIANT) proposed as a technique in solving economic dispatch by considering prohibited operating zones
3	2013	N. A. Rahmat, I. Musirin, A. F. Abidin [58]	Differential Evolution Immunized Ant Colony Optimization (DEIANT) Technique in Solving Weighted Economic Load Dispatch Problem	The ELD problem solved by Differential Evolution Immunized Ant Colony Optimization (DEIANT) technique. DEIANT technique outperforms the other techniques in terms of achieving lower operating cost and power loss.
4	2013	N. A. Rahmat, I.	Solving fuzzy	Developed

No.	Year	Author	Topic	Application
		Musirin, A. F. Abidin, S. A. Jumaat, W. N. Wan Abdul Munim [55]	combined-emission dispatch by using differential evolution immunized Ant Colony Optimization technique	optimization technique termed as Differential Evolution Immunized Ant Colony Optimization (DEIANT) technique is employed to optimize FCED
5	2013	N. A. Rahmat, I. Musirin, A. F. Abidin [53]	Differential Evolution Immunized Ant Colony Optimization (DEIANT) technique in solving economic emission dispatch	implementation of Differential Evolution Immunized Ant Colony Optimization (DEIANT) technique in solving economic emission dispatch

2.8 Summary

This chapter provided a comprehensive literature review on the impact PV implementation. The concept and application of voltage stability and stability indices were also review in this chapter. The literature review presented in this chapter also explained on Economic Load Dispatch. Based on these literatures, several gaps are identified. Most of the studies on stability of the power system after implementation of solar PV are not considering the impact on operating costs. Some researchers only studied operating costs regardless of the stability of the power system after installation of solar PV. Therefore, this study is conducted to study both the stability and operating costs of the power system after installation of solar PV.

CHAPTER 3

METHODOLOGY

3.1 Introduction

In this chapter, a methodology process of FVSI, ELD and optimization for optimal sizing and placement of solar PV will be discussed. The research will be carried out using MATLAB software as a simulation platform. IEEE 26-Bus system is selected as the test system.

3.2 Research Flow

Transmission system is implemented to export and import power from generators to the load. In an interconnected power system, the goal is to find the real and reactive power scheduling of each power plant in such a way as to minimize the operating cost. It means that the generator's real and reactive power are allowed to vary within certain limit as to meet a precise load demand and minimum fuel cost. In this research, the economic dispatch of generation for minimization of the total operating cost and loss will be evaluated by using MATLAB. By referring to figure 3.1 the IEEE 26-Bus system will be model using MATLAB as a test system for this simulation. Newton-Raphson power flow will be run and the reactive power will be increase gradually. FVSI will be run to determine the strongest and weakest line. The line that shows FVSI value closed to 1.00 indicates its approaching to voltage instability. PV will be installed at load bus as a solution to solve the voltage instability [59]. For this research the solar PV data output placing at bus 9, ELD and DEIANT optimization will be run to calculate the total loss and total cost.

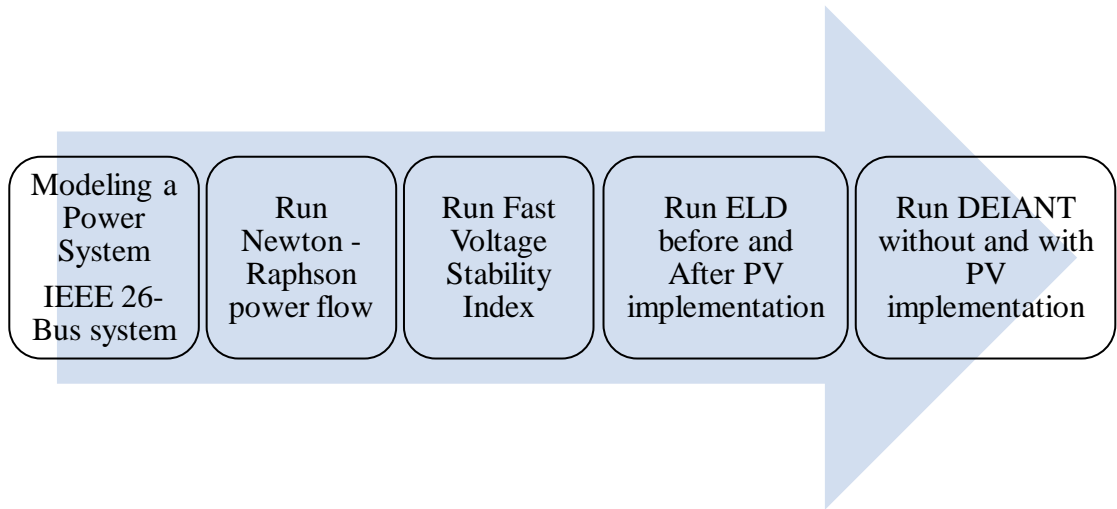


Figure 3.1: Research block diagram

3.3 Modeling Methodology

IEEE 26-Bus system is modeled in MATLAB. Bus 1 is selected as the slack bus with its voltage adjusted to $1.025\angle 0^\circ$ pu. Therefore, all parameters of bus 1 are maintained without any changes. The solar PV data output are obtain from [14]. ELD and optimization mathematically are used to minimize total loss and total cost. Figure 3.2 describes the flowchart of the modeling process to prepare the simulation. The following process as follows:

- i. Set the reactive power (MVAR) and run the power flow by Newton-Raphson method.
- ii. Results from the load solution is used to calculate the FVSI.
- iii. If the FVSI results indicate FVSI value smaller than 1.00, increase the reactive load (reactive power is gradually increased from 50 MVAR, 100 MVAR, 150 MVAR, 200 MVAR, 250 MVAR, 300 MVAR and 350 MVAR then repeats steps (ii) and (iii) until FVSI reaches 1.00 or result shown Nan (out of range). At this step the maximum loading of the particular bus is identified.
- iv. Install 4 types of solar PV (10MW, 20MW, 40MW and 100MW) into the power system to improve the stability of power system.

- v. Run FVSI, if the FVSI results indicate it value smaller than 1.00 or start to reduce to zero then proceed to step (vi) if the FVSI value show the increasing value to 1.00, repeats steps (ii), (iii), (iv) and (v).
- vi. Calculate the total cost and the total loss.
- vii. Run DEIANT for optimize the total cost and the total loss.

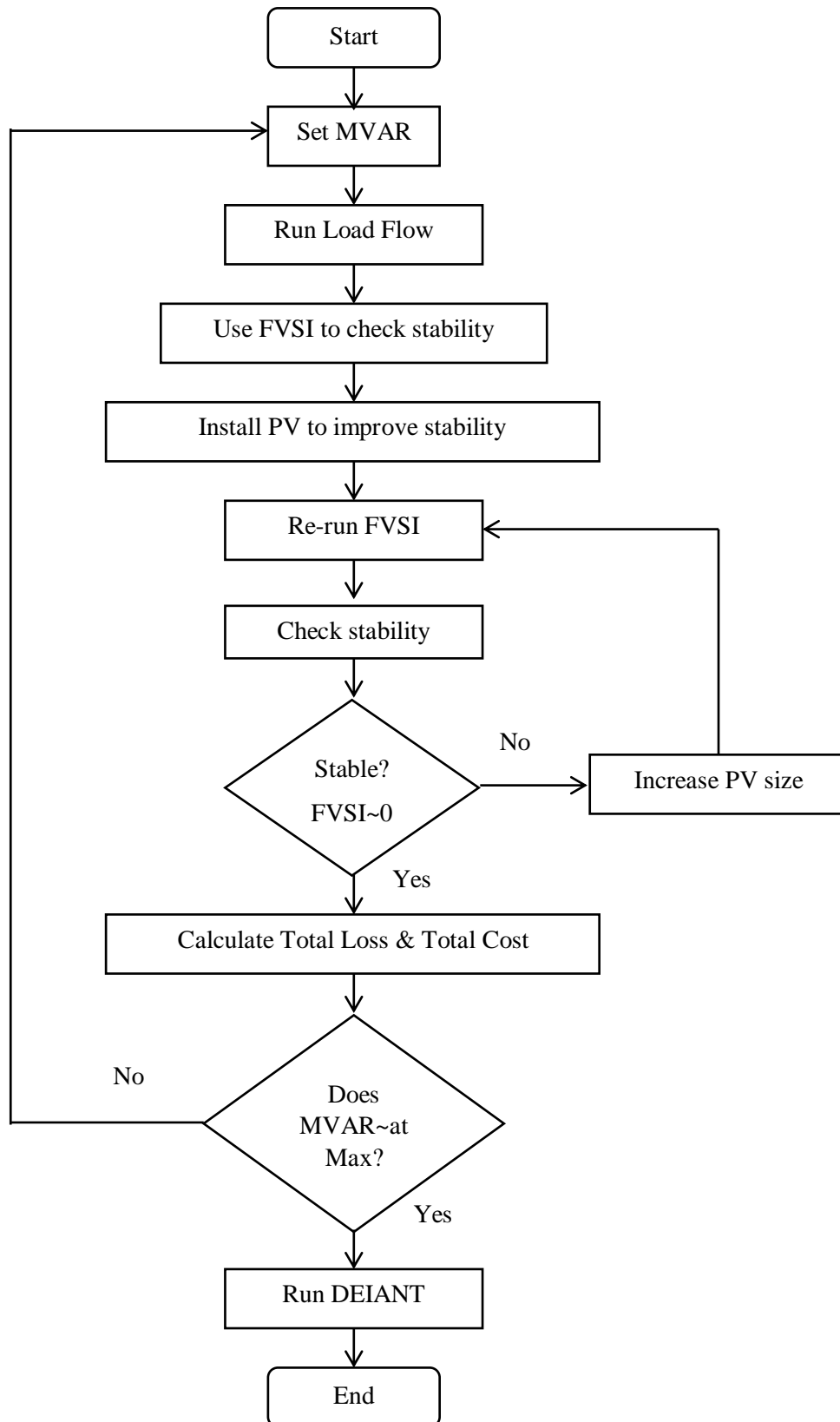


Figure 3.2: The flowchart of the modeling process to prepare the simulation

3.4 IEEE 26-Bus system

This research used IEEE 26-Bus system as a test system as shown in Figure 3.3. For numerous research such as short-circuit assessment, load flow studies, interrelated grid issues, the IEEE bus system is commonly used as a case study. This is because information from IEEE bus system is commonly used and simple to find. Furthermore, IEEE bus system information is an international standard that can be easily loaded to discover the research gap. This test system consists of 6 generator buses and 20 units of load buses.

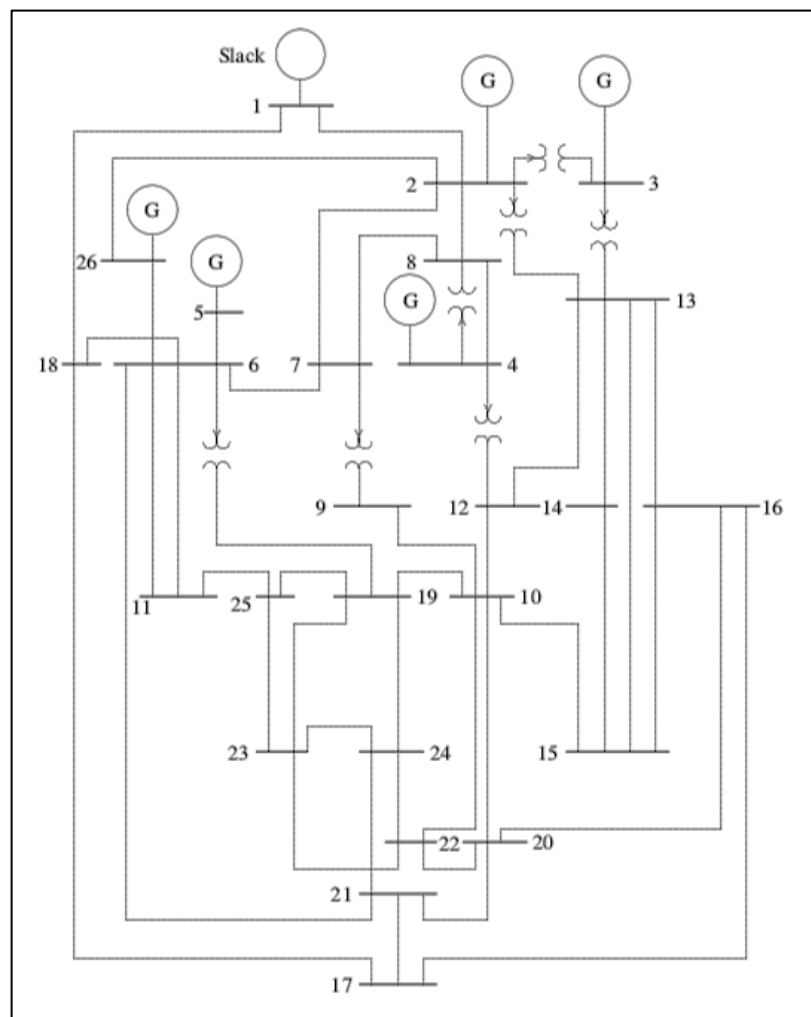


Figure 3.3: One-line diagram 26 bus data

Bus 1 is taken as the slack bus and it is adjusted to $1.025\angle 0^\circ$ pu. The buses are coded accordingly to represent them as slack bus, load bus or voltage-regulated bus.

The codes can be referred in the appendix A. Table 3.1 lists down the distribution of the generators and the total static load in the IEEE 26-Bus system:

Table 3.1: Distribution of the generators capacity total static load in the IEEE 26-Bus system

Bus no	PGen (MW)	QGen (MVAR)
1	51	41
2	22	15
3	64	50
4	25	10
5	50	30
26	40	20
Total Static Load	P = 252 MW	Q = 166 MVAR

The data for the generator buses also known as voltage-controlled buses are shown in Table 3.2.

Table 3.2: Regulated bus data

Bus No.	Min. MVAR Capacity	Max. MVAR Capacity	Voltage Magnitude
2	40	250	1.020
3	40	150	1.025
4	40	80	1.050
5	40	160	1.045
26	15	50	1.015

For transformer tap, the data setting as given in Table 3.3 the left bus number is assumed to be the tap side of the transformer

Table 3.3: Transformer data

Tx	Tap Setting Per Unit
Tx 1	0.960
Tx 2	0.960
Tx 3	1.017
Tx 4	1.050
Tx 5	1.050
Tx 6	0.950
Tx 7	0.950

The shunt capacitor setting are given in Table 3.4:

Table 3.4: Shunt capacitor data

Bus No.	MVAR
Bus 1	4.0
Bus 4	2.0
Bus 5	5.0
Bus 6	2.0
Bus 9	3.0
Bus 11	1.5
Bus 12	2.0
Bus 15	0.5
Bus 19	5.0

The cost coefficient, with P_i in MW are as given in Table 3.

Table 3.5: Cost coefficient of IEEE 26-Bus system

Generators	a	b	c
G_1	240	$7.0P_1$	$0.0070P_1^2$
G_2	200	$10.0P_2$	$0.0095P_2^2$
G_3	220	$8.5P_3$	$0.0090P_3^2$
G_4	200	$11.0P_4$	$0.0090P_4^2$
G_5	220	$10.5P_5$	$0.0080P_5^2$
G_{26}	190	$12.0P_6$	$0.0075P_6^2$

All the data such as regulated bus data, transformer data, and shunt capacitor data are compiled in matrix form known as busdata. The value for base MVA, accuracy, and maximum iteration are set as follow in Table 3.6:

Table 3.6: Setting for base MVA, accuracy, and maximum iteration of IEEE 26 Bus system

Data	Value
Base MVA	100
Accuracy	0.0001
Maximum iteration	10

For the generator's real power limits in MW are as given in Table 3.7.

Table 3.7: Generator real power limit of IEEE 26-Bus system

Generators	Minimum MW	Maximum MW
G_1	100	500
G_2	50	200
G_3	80	300
G_4	50	150
G_5	50	200
G_{26}	50	120

The busdata and linedata can be referred in the appendix A.

3.5 Newton-Raphson Power Flow Solution

Newton-Raphson power flow solution is faster than Gauss-Seidel method, which can solve non-linear algebraic equation. Power flow is used in the design and analysis of power system. It is the flow of active and reactive power from generating-end to the load through different branches of the network. In this study, preliminary power flow analysis is conducted to obtain load distribution and power loss before others test are conducted. The real and imaginary parts equations written as:

$$P_i = \sum_{j=1}^n |V_i| |V_j| |Y_{ij}| \cos(\theta_{ij} - \delta_i + \delta_j) \quad (\text{Equation 3.1})$$

$$Q_i = - \sum_{j=1}^n |V_i| |V_j| |Y_{ij}| \sin(\theta_{ij} - \delta_i + \delta_j) \quad (\text{Equation 3.2})$$

However, the scope of all simulations will be referring to the line impedance, line reactance, voltage at the sending end and reactive power at the receiving end in test system, which will be used for the FVSI calculation.

3.6 FVSI Analysis

FVSI in Equation 3.3 is proposed to evaluate the voltage stability condition in IEEE 26-Bus system. In order to obtain the voltage stability analysis, several steps are applied.

$$FVSI_{ij} = \frac{4Z_{ij}^2 Q_j}{V_i^2 X_{ij}} \quad (\text{Equation 3.3})$$

Where;

Z_{ij} = line impedance

X_{ij} = line reactance

V_i = voltage at the sending end

Q_j = reactive power at the receiving end

In order to maintain line stability, FVSI value must be kept near to zero (0). If FVSI value is near to unity (1.0), it shows that the corresponding line is unstable. This can cause overall system to collapse and the reduction in voltage drop at heavily loaded bus. Previous study by [40] proposed FVSI analysis by gradually increases the reactive power loading at bus 9. In this research, the developed FVSI is implemented according to the following procedure:

- i. Run the Power flow by Newton-Raphson method. Results from the load solution is used to calculate the FVSI.
- ii. If the FVSI results indicate it smaller than 1.00, increase the reactive load then repeats steps (ii) and (iii) until FVSI reaches 1.00 or result shown Nan (out of range) or until the load flow fails to give the results. Calculate FVSI for every load variation.
- iii. At this step the maximum loading of the particular bus is identified. Record the highest FVSI and the corresponding line.
- iv. Plot individual graph for FVSI versus reactive load variation at the tested load bus. This will identify the sensitive line with respect to the load bus.
- v. Repeat step (i) to (v) for other load buses in the system.

3.7 Solar PV Capacity and Output Power

The proposed solar PV capacity and output power used by [14] have improved system stability. The penetrations status indicates the highest (HIGH), lowest (LOW) and average (AVG) of the solar PV will be used in this research to insert into the power system. Table 3.8 shows the summary of solar PV output power used in this study.

Table 3.8: Summary of solar PV output power [14]

No.	Irradiance (W/m ²)	Solar PV Output Power (MW)				Penetration Status
		10MW	20MW	40MW	100MW	
1	586	5.708	11.412	22.807	56.826	HIGH
2	470	4.475	8.941	17.891	44.652	AVERAGE
3	112	0.859	1.734	3.485	8.721	LOW

From Table 3.9, for highest (HIGH) penetration status is about 586W/m² generating PV output 5.708MW for 10MW PV capacity, 11.412MW PV output power for 20MW PV capacity, 22.807MW PV output power for 40MW PV capacity and 56.826MW PV output power for 100MW PV capacity. While, for average (AVG) penetration status is about 470W/m² generating PV output 4.475MW for 10MW PV capacity, 8.941MW PV output power for 20MW PV capacity, 17.891MW PV output power for 40MW PV capacity and 44.652MW PV output power for 100MW PV capacity.

Last is for the lowest (LOW) penetration status is around 112W/m² generating PV output 0.859MW for 10MW PV capacity, 1.734MW PV output power for 20MW PV capacity, 3.485MW PV output power for 40MW PV capacity and 8.721MW PV output power for 100MW PV capacity.

In this research, the installation of PV is based on the power output data penetration status highest (HIGH), lowest (LOW) and average (AVG) data. These data will be integrated to instability buses calculated using FVSI.

3.8 Economic Load Dispatch (ELD)

In this study, ELD is conducted by integrating four types of photovoltaic into the power system. The purpose is to reduce the operating cost that normally is directly proportional to fuel cost. So, ELD is conducted to determine the optimal size of solar PV to be installed in the IEEE 26-Bus system. Furthermore, for this case, the start-up cost of solar PV is excluded in the operating cost [13]. The fundamental ELD will

only consider real power generation. This study simplifies ELD problem by setting aside prohibited operating zone, emission, penalty constraint, valve-point loading effect, and ramp-rates. This ELD technique is suitable to be computed at any generation level. The total operating cost is calculated by using the following quadratic function in equation 3.4 are taken from [13],

$$Cost_{GEN} = \sum_{i=1}^n C_i P_i = \sum_{i=1}^n a_i + b_i P_i + c_i P_i^2 \quad (\text{Equation 3.4})$$

Where $Cost_{GEN}$ is the total fuel cost, C_i is the fuel cost of generating P_i amount of output power. a_i , b_i and c_i is the fuel cost coefficient for P_i . The total generated power should equal to the total load demands, P_D plus power losses, P_{loss} as in Equation 3.5,

$$\sum_i^{n_g} P_i = P_D + P_{loss} \quad (\text{Equation 3.5})$$

The power loss is calculated by using Equation 3.6,

$$P_{loss} = \sum_i^n \sum_j^n P_i B_{ij} P_j + \sum_i^n B_{0i} P_i + B_{00} \quad (\text{Equation 3.6})$$

Where B_{ij} , B_{0i} , and B_{00} are the elements of loss coefficient matrix. Equation 3.7 satisfying the inequality constraint of generation limits for each unit,

$$P_{i(min)} \leq P_i \leq P_{i(max)} \quad (\text{Equation 3.7})$$

Where $P_{i(min)}$ and $P_{i(max)}$ are the minimum and maximum generating limit.

Based on Power balance equation [60], the relationship between load demand, P_D generated power, P_i and power output of the solar, P_V is equated as in Equation 3.8,

$$\sum_i^{n_g} P_i + P_{V(Solar\ PV)} = P_D \quad (\text{Equation 3.8})$$

The relationship between the total cost for the initial operating condition and the total cost with optimal dispatch is equated as in Equation 3.9,

$$\$/h = Total\ Cost\ Initial - Total\ Cost\ Optimal\ Dispatch \quad (\text{Equation 3.9})$$

Total annual saving is equated in Equation 3.10,

$$Total\ Annual\ Saving = \frac{\$}{h} * (8760) \quad (\text{Equation 3.10})$$

3.9 Differential Evolution Immunized Ant Colony Optimization (DEIANT)

In this research, DEIANT colony is applied as an optimization technique. DEIANT flowchart is shown in Figure 3.4 and discussed briefly as follows:

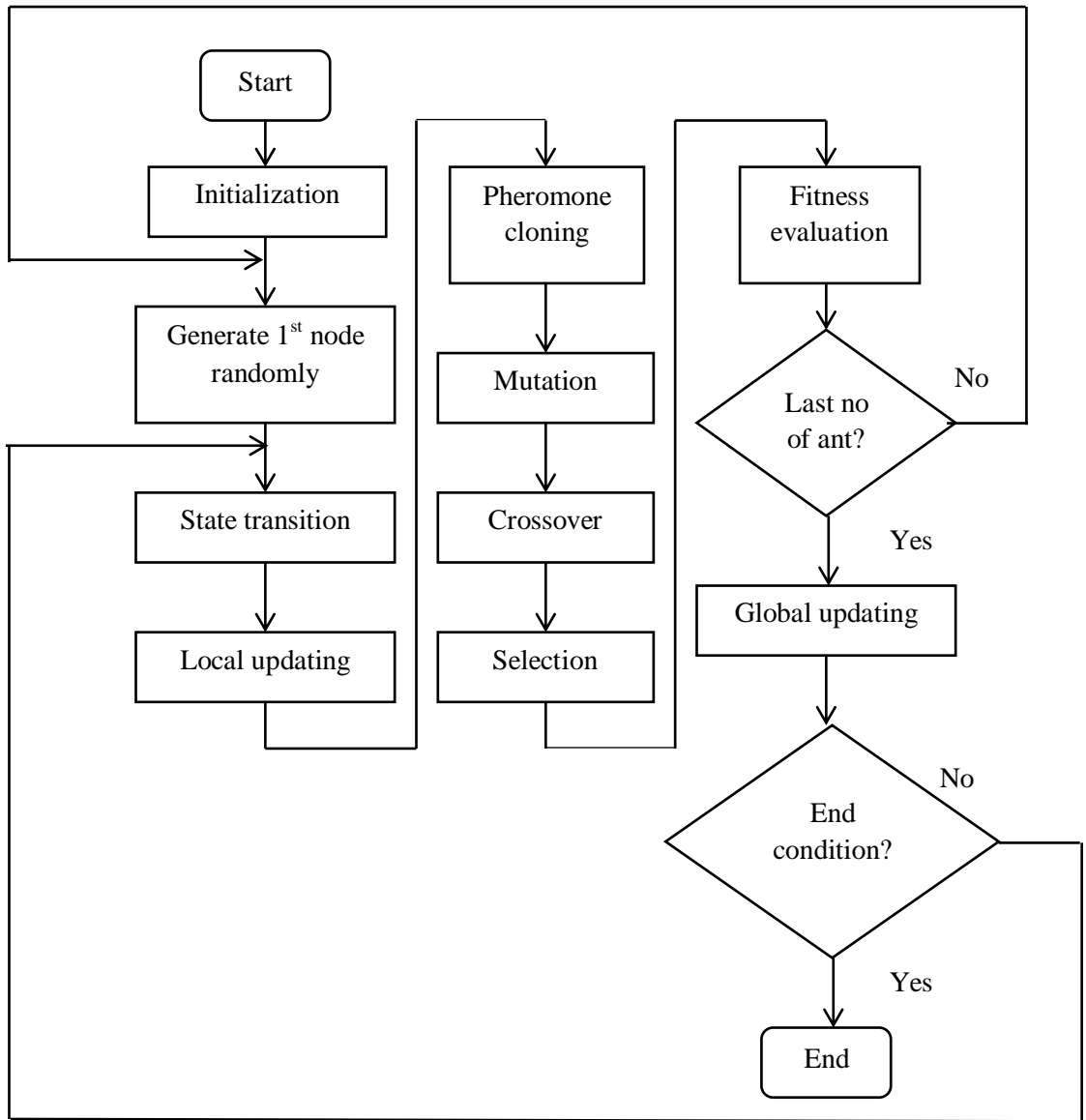


Figure 3.4: DEIANT Flowchart

From the figure 3.4, the flowchart process start as follows:

- i. Set all fixed value of the parameters. For DEIANT, the number of ants is set to five (5) ants and the number of nodes set to six (6) namely as Pg1, Pg2, Pg3, Pg4, Pg5 and Pg26. Then, set the cloning rate and lastly set the mutation factor. Next, set IEEE 26 Bus system such as for MVAR, MW Limit and cost.
- ii. At this step, the ant will hold new exploration and select node in tour. Different tour will be produced by different ants. The shortest path that

produce by ants will be choose as fitness solution. So, first tour namely as Pgtt 1, Pgtt 2, Pgtt 3, Pgtt 4, and Pgtt 5 will be produce at this step.

- iii. Next step is cloning process, at this step the selected tour of Pgtt 1, Pgtt 2, Pgtt 3, Pgtt 4, Pgtt 5 will be replicated.
- iv. Then, at mutation step Cloning tour will be altering by using Gaussian Distribution and will produce new tour of Pgtt 1*, Pgtt 2*, Pgtt 3*, Pgtt 4*, and Pgtt 5*.
- v. At crossover step clone tour and mutated tour combined together in matrix arrangement from decending order. Best elements are the best solution will be choosing to compute as an objective function.
- vi. Last step is objective function, at this step the ant tour has lowest evaporative point will be chosen as the best elements. The best element value of X will be multiplying by each Pgtt. The objective function will be used to minimize total loss and total cost.

3.9.1 DEIANT Process

The following are DEIANT processes:

i) Initialization

Firstly, set the number of ants and nodes. The cloning and mutation coefficient are also initialized. DEIANT is unique, in which a small number of search ants with a small number of nodes is enough to produce a desirable solution. For DEIANT, the fewer number of ants and node will make the algorithm faster. In this research, ant is set to five and node is set to six.

ii) Ant Tour

Figure 3.5 represents the random behaviour of ant touring process. This process called permutation strategy. In this process, the ant will hold new exploration and select the node in tour. Different tour will be produced by different ants. The shortest

path produces by ant which is the finest solution, will be put through towards the cloning process. In this study, the shortest path is produced by the summation of permutation that produces the lowest number of tours. Equation 3.11 and equation 3.12 represent permutation process.

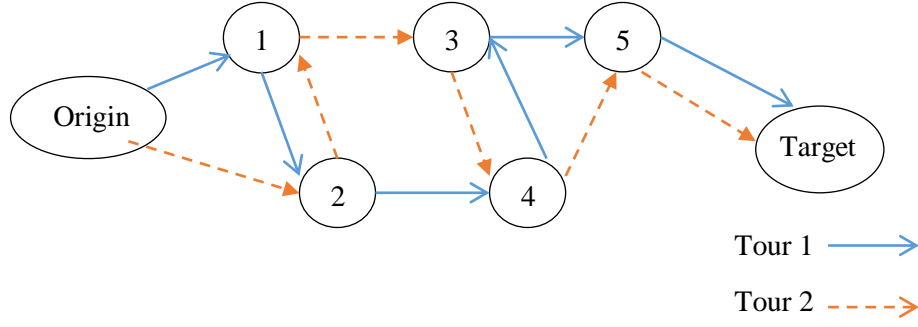


Figure 3.5: Represents the random behavior of ant touring process

$$n! = n^1, n^2, n^3 \dots n^m \quad (\text{Equation 3.11})$$

$$\sum_{m=1}^m n = n^1 + n^2 + n^3 \dots + n^m \quad (\text{Equation 3.12})$$

Where,

- n : number of nodes to be generated
- n^1, n^2, n^3, n^m : generated node
- m : m^{th} number of nodes

iii) Tour Cloning

The cloning process will determine the selected tour. Depending on the initialized cloning coefficient, the process will replicate the selected tour. In search of the desired path, the cloning process is requiring by compensating the number of small search agents (ants). Through this cloning process the number of ants is reduced but the variety of solutions may increase. Figure 3.6 shown the simple cloning process

start from the original tour that will be cloned into several identical copies called cloned tour. Then, the cloned tour will be mutated.

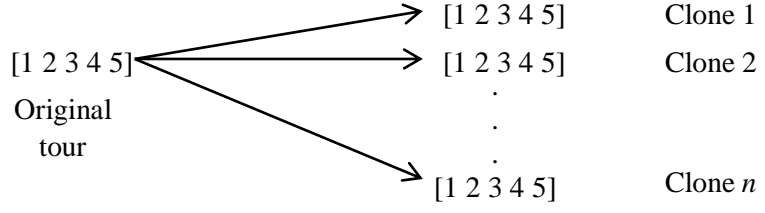


Figure 3.6: Cloning Process

iv) Tour Mutation

Gaussian or Normal distribution will be use in order to mutate the cloned tour. Refer to equation 3.13, Gaussian distribution is applied in the mutation process. The element of the cloned tour will be altering through this mutation process.

$$X_{i+m} = X_{i,j} + N\left(0, \beta(X_{jmax} - X_{jmin})\right) \cdot \frac{f_i}{f_{max}} \quad (\text{Equation 3.13})$$

Where,

X_{i+m} : Mutation function

X_{jmin} : Smallest node number

X_{jmax} : Largest node number

f_i : Travelled distance

f_{max} : Maximum distance

In this mutation process, variation of ant tour will be increased, and varieties of samples are going to be selected. The variation of ant tour depends on initial mutation coefficient. The mutated tour will be called as offspring tour and the cloned on as parent tour.

v) Crossover

Figure 3.7 showing the crossover process, which is combination of parent and offspring tours in a single matrix. This crossover process later will be conducted to enhance the tour's variation.

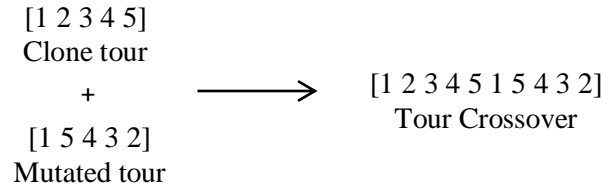


Figure 3.7: Crossover Process

vi) Tour Selection

Elements of a crossover-matrix arranged in descending order. The best elements are the best solution that will be compute for objective function.

vii) Objective Function Calculation

The best solution will have the lowest evaporation rate. The objective function is solved by calculating the control variable, represented by equation 3.14.

$$X = \frac{d}{d_{max}} \cdot X_{max} \quad (\text{Equation 3.14})$$

Where:

d : distance of ant tour

d_{max} : maximum distance

X_{max} : the maximum value of x

The value of X will be taken as the multiplier to the output of the generator for ELD computation. Total Loss and total cost minimized using the objective function.

viii) Termination

DEIANT process is halted when the best solution is obtained, or the maximum iteration is fully met. In this research, DEIANT is used to obtain an optimal placement and sizing of PV for operating cost minimization.

3.10 Summary

This chapter provided a comprehensive methodology to obtain an optimal placement and sizing of solar PV for stability enhancement and operating cost minimization. Modeling of the test system into the MATLAB software as preparations for the simulation process. Newton-Raphson power flow will be used to the test system as a load flow analysis. After test system in a steady state operation, Fast voltage stability index (FVSI) will be using to check the voltage stability index. Increasing in load demand will effect on stability of the test system so solar PV will integrate to the test system. Integrated of solar PV will effect on stability enhancement and operating cost. The simulation process will be defined in the next chapter.

CHAPTER 4

RESULTS ANALYSIS AND DISCUSSIONS

4.1 Introduction

Using MATLAB software, this simulation will be tested on test system with the integration of PV models to obtain an optimal placement and sizing of solar PV for stability enhancement and operating cost minimization. This chapter explains in detail the analysis and results that have been used for the implementation of this project. FVSI, total system loss before ELD, total generation cost initial operating condition, total system loss after ELD, total generation cost after ELD, total optimal dispatch of generation (Pg_{tt}), total demand (P_{dt}), totally different cost before and after, total annual saving cost (hr/year) and optimization using DEIANT will be the main parameters for the simulation results. The test system behavior with and without solar PV integration will be analyzed and discussed based on FVSI calculation.

4.2 Simulation Strategy

The first simulation is to run power flow of the test system. FVSI will function as a line-based voltage stability index that can determine the voltage stability condition of all lines in the test system. The second simulation is to run simulation at IEEE 26-Bus system without solar PV integration. Bus 9 (Q₉) is randomly selected [40] with the setting for reactive power is gradually increased from 50 MVAR to 100 MVAR to 150 MVAR to 200 MVAR to 250 MVAR to 300 MVAR and to worst case 350 MVAR until FVSI reaches 1.00 or result shown Nan (out of range). The numbers represent the new reactive power dispatch in this system, which functioned as the control parameters. The aim is to study the instability of the test systems without the integration of solar PV. FVSI calculation will be calculated. The ELD simulation

will determine the total cost and total loss of the test system without solar PV. The third simulation is to run simulation at IEEE 26-Bus system with solar PV integration. FVSI calculation will be calculated to check the stability status after solar PV integration. Then, the ELD simulation will be performed to determine the total cost and total loss of the test system with solar PV. DEIANT technique will be employs for optimization the total cost and total loss of test system with solar PV.

4.3 Simulation 1: Voltage Stability During Normal Condition

The FVSI analysis based on Equation 3.3 is conducted on IEEE 26-Bus system to demonstrate the stability of the system during normal condition. The FVSI reading shown in the Table 4.1 indicates the stability of the test system. A particular line is considered as stable if its FVSI is approaching 0.

Table 4.1: FVSI to indicate the stability status of IEEE 26-Bus system

Line No.	From Bus	To Bus	FVSI	Voltage
1	1	2	0.0195	1.0250
2	1	18	0.0184	1.0250
3	2	3	0.0963	1.0200
4	2	7	0.0141	1.0200
5	2	8	0.0048	1.0200
6	2	13	0.0074	1.0200
7	2	26	0.0196	1.0200
8	3	13	0.0757	1.0450
9	4	8	0.1949	1.0500
10	4	12	0.1877	1.0500
11	5	6	0.0674	1.0450
12	6	7	0.0209	1.0007
13	6	11	0.0109	0.9979
14	6	18	0.0215	1.0007

Line No.	From Bus	To Bus	FVSI	Voltage
15	6	19	0.0055	1.0007
16	6	21	0.0014	1.0007
17	7	8	0.0121	0.9953
18	7	9	0.0556	0.9953
19	8	12	0.0151	0.9983
20	9	10	0.0771	1.0104
21	10	12	0.0115	0.9909
22	10	19	0.0112	0.9909
23	10	20	0.0287	0.9909
24	10	22	0.0261	0.9909
25	11	25	0.0330	0.9751
26	11	26	0.0226	1.0150
27	12	14	0.0541	0.9943
28	12	15	0.0181	0.9943
29	13	14	0.0274	1.0224
30	13	15	0.0263	1.0224
31	13	16	0.0742	1.0224
32	14	15	0.0359	1.0081
33	15	16	0.0329	0.9988
34	16	17	0.0285	0.9901
36	17	18	0.1007	0.9827
37	17	21	0.0127	1.0075
38	19	23	0.1058	1.0046
39	19	24	0.1412	1.0046
40	19	25	0.1172	1.0046
36	17	18	0.1007	0.9827
41	20	21	0.0200	0.9830
42	20	22	0.0122	0.9830
43	21	24	0.0315	0.9771
44	22	23	0.0057	0.9796

Line No.	From Bus	To Bus	FVSI	Voltage
45	22	24	0.0400	0.9780
46	23	25	0.0118	0.9691

Based on the FVSI calculation obtained from the Table 4.1, shows the IEEE 26-Bus system is in a stable state where all buses values are near to zero.

4.4 Simulation 2: Voltage Stability Studies Under Load Variations

Next, reactive power loading is gradually increased. The aim of this simulation is to investigate the behavior of the test system under load variation. The loading conditions were divided into 7 MVAR levels; 50MVAR, 100MVAR, 150MVAR, 200MVAR, 250MVAR, 300MVAR and 350MVAR at a randomly selected bus 9 (Q₉) [40]. FVSI calculations were captured at every loading step to determine the weakest line.

Table 4.2: FVSI results for gradually increase MVAR at bus 9

Line No.	FVSI						
	50 MVAR	100 MVAR	150 MVAR	200 MVAR	250 MVAR	300 MVAR	350 MVAR
9	0.1948	0.2038	0.1988	0.2088	0.1972	0.1747	0.2027
10	0.1877	0.1933	0.1835	0.1884	0.1567	0.1280	0.1361
18	0.0554	0.0104	0.0447	0.0994	0.1679	0.2310	0.2888
20	0.0771	0.0333	0.0111	0.0620	0.1212	0.1777	0.2534
27	0.0540	0.0598	0.0617	0.0682	0.0871	0.1059	0.1184
36	0.1009	0.1036	0.1154	0.1179	0.1334	0.1386	0.1427
38	0.1057	0.1083	0.1128	0.1156	0.1238	0.1297	0.1316
39	0.1412	0.1441	0.1498	0.1531	0.1630	0.1684	0.1713
40	0.1173	0.1173	0.1166	0.1166	0.1159	0.1195	0.1185

Table 4.2 shows the FVSI of bus 9 increases proportionally with the increment in reactive power loading. Line 18 (from bus 7 to bus 9) is identified as the most sensitive line as its FVSI value is increase from 0.0554 to 0.2888 as the reactive power increases from 50MVAR to 350MVAR. Line 20 (from bus 9 to bus 10) is also identified as one of the sensitive lines as its FVSI value increases from 0.0771 to 0.2534 as the reactive power increases from 50MVAR to 350MVAR.

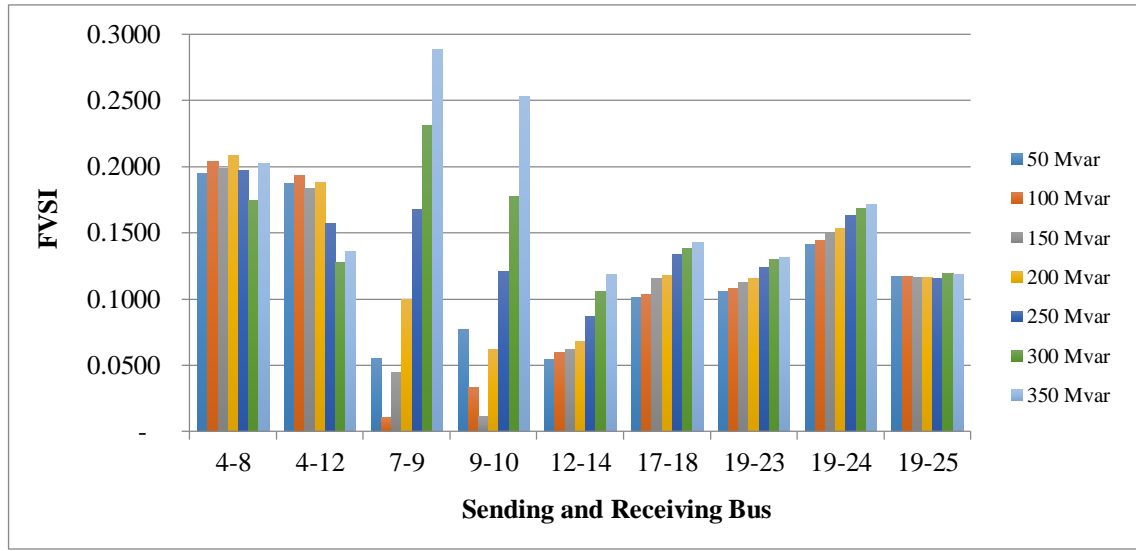


Figure 4.1: FVSI results for the most sensitive lines correspond to the load buses

Results taken from Table 4.2 are charted in Figure 4.1 to have clearer view on the effect of loading level to line stability. The FVSI value at Line 9 (from bus 4 to bus 8), line 10 (from bus 4 to bus 12), line 18 (from bus 7 to bus 9), line 20 (from bus 9 to bus 10), line 27 (from bus 12 to bus 14), line 36 (from bus 17 to bus 18), line 38 (from bus 19 to bus 23), line 39 (from bus 19 to bus 24), and line 40 (from bus 19 to bus 25) increases proportionally with the increment in reactive power loading. Figure 4.1 indicates that line 18 (from bus 7 to bus 9) has the highest FVSI when the line is loaded with 350MVAR.

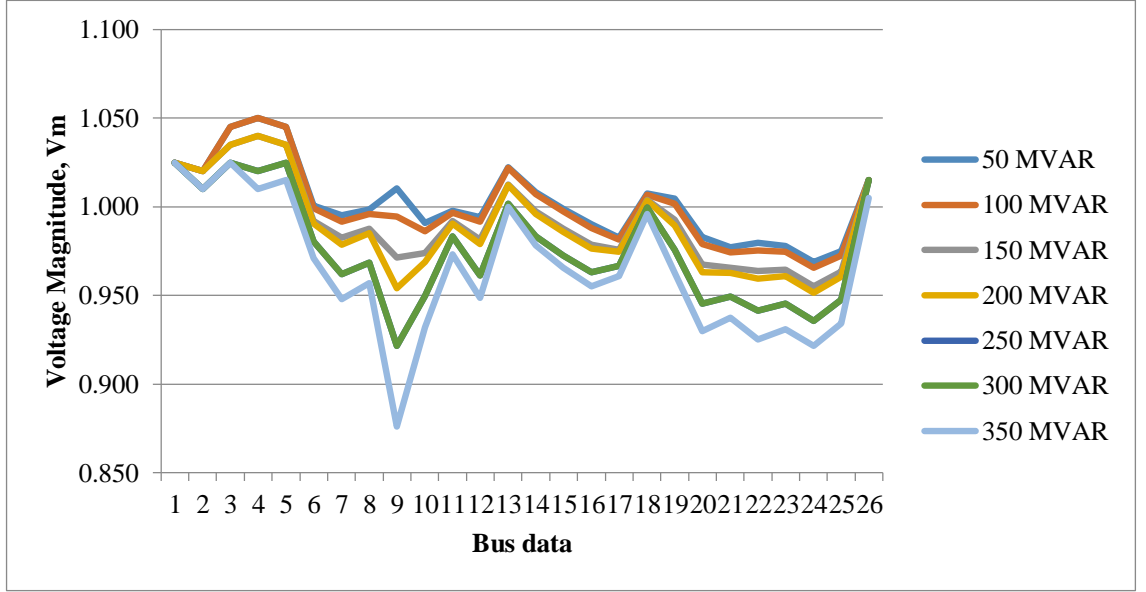


Figure 4.2: Voltage profile for IEEE 26-Bus system under load variations

Figure 4.2 shows the voltage profile under the variation of the load. Results indicate the voltage is degraded when the load increases.

4.5 Simulation 3: Voltage Stability Studies with PV Variations

This study was conducted to determine the optimal size and placement of solar PV to be injected into the IEEE 26-Bus system that can enhance the voltage stability after increasing the reactive power loading. By referring to Table 2.4, the PV will be sized to four different power capacities; 10MW, 20MW, 40MW and 100MW. Each of the solar PV output power is divided into three-penetration status; lowest (LOW), average (AVG) and highest (HIGH) irradiance level as in Table 3.8. Based on Table 4.2, five weakest lines are selected as a candidate to be assessed of their line stability after solar PV integration into the power system. They are selected based on their high FVSI values. Three cases were considered namely the case 1: $Q_9=50\text{MVAR}$, case 2: $Q_9=150\text{MVAR}$ and case 3: $Q_9=250\text{MVAR}$, Q_9 is referring to bus 9, where were investigated in this chapter.

4.5.1 Case 1: $Q_9=50\text{MVAR}$ with PV Variations

Tests were conducted by injecting the solar PV with capacity 10MW, 20MW, 40MW and 100MW into the power system. The results for FVSI values obtained at reactive power loading at bus 9 set to 50MVAR are tabulated in Table 4.3.

Table 4.3: FVSI results for $Q_9=50\text{MVAR}$, without and with variations penetration status of solar PV

Penetration status	PV output power	FVSI				
		Line 9	Line 10	Line 18	Line 20	Line 27
Without PV	NA	0.1948	0.1877	0.0554	0.0771	0.0540
10MW LOW	0.859	0.1947	0.1873	0.0559	0.0772	0.0540
10MW AVG	4.475	0.1946	0.1860	0.0576	0.0774	0.0538
10MW HIGH	5.708	0.1945	0.1856	0.0582	0.0774	0.0537
20MW LOW	1.734	0.1947	0.1870	0.0563	0.0772	0.0539
20MW AVG	8.941	0.1944	0.1844	0.0594	0.0775	0.0535
20MW HIGH	11.412	0.1943	0.1835	0.0601	0.0775	0.0534
40MW LOW	3.485	0.1946	0.1864	0.0572	0.0773	0.0538
40MW AVG	17.89	0.1941	0.1812	0.0614	0.0772	0.0530
40MW HIGH	22.807	0.1940	0.1794	0.0618	0.0769	0.0527
100MW LOW	8.721	0.1944	0.1845	0.0593	0.0775	0.0535
100MW AVG	44.652	0.1933	0.1717	0.0594	0.0753	0.0515
100MW HIGH	56.826	0.1932	0.1813	0.0573	0.0769	0.0349

The table 4.3 tabulates the FVSI results for five weakest lines such as line 9 (from bus 4 to bus 8), line 10 (from bus 4 to bus 12), line 18 (from bus 7 to bus 9), line 20 (from bus 9 to bus 10), and line 27 (from bus 12 to bus 14). From the table, it is observed that at the application of voltage stability improvement as the objective function after installation of 100MW solar PV with high penetration status have significantly improved the voltage stability condition indicated by the reduction in FVSI values for line 9, line 10, line 18, line 20 and line 27 from 0.1948, 0.1877, 0.0554, 0.0771 and 0.0540 to 0.1932, 0.1813, 0.0573, 0.0769 and 0.0349

respectively. This would mean that 100MW solar PV with high penetration status provided sufficient solar PV output power when injected into the power system. So as to identify the FVSI results after solar PV placement into the power system, the FVSI results from Table 4.3 was extracted on the chart as shown in Figure 4.3.

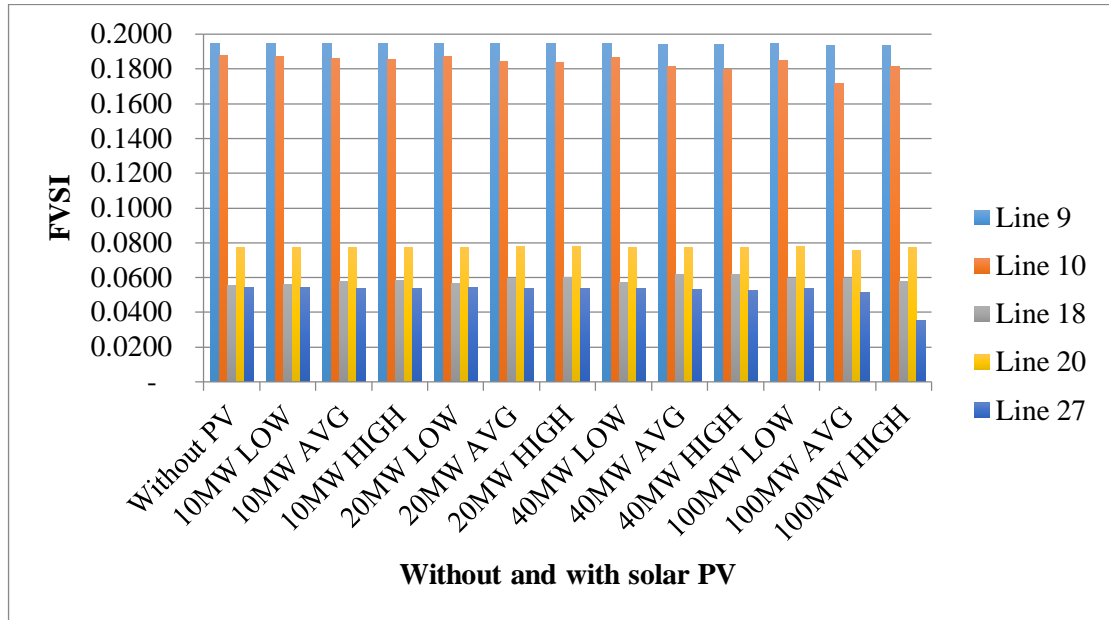


Figure 4.3: FVSI results for $Q_9=50\text{MVAR}$ reactive power loading without and with different penetration status of solar PV

4.5.2 Case 2: $Q_9=150\text{MVAR}$ with PV Variations

Further tests were conducted by injecting the solar PV with capacity 10MW, 20MW, 40MW and 100MW into the power system. The results for FVSI values obtain at reactive power loading at bus 9 set to 150MVAR are tabulated in Table 4.4.

Table 4.4: FVSI results for $Q_0=150\text{MVAR}$, without and with variations penetration status of solar PV

Penetration status	PV output power	FVSI				
		Line 9	Line 10	Line 18	Line 20	Line 27
Without PV	NA	0.1988	0.1835	0.0447	0.0111	0.0617
10MW LOW	0.859	0.1987	0.1828	0.0450	0.0111	0.0616
10MW AVG	4.475	0.1985	0.1798	0.0453	0.0108	0.0611
10MW HIGH	5.708	0.1984	0.1788	0.0452	0.0107	0.0609
20MW LOW	1.734	0.1987	0.1828	0.0450	0.0111	0.0616
20MW AVG	8.941	0.1985	0.1798	0.0453	0.0108	0.0611
20MW HIGH	11.412	0.1984	0.1788	0.0452	0.0107	0.0609
40MW LOW	3.485	0.1987	0.1821	0.0451	0.0110	0.0614
40MW AVG	17.89	0.1982	0.1761	0.0446	0.0105	0.0606
40MW HIGH	22.807	0.1981	0.1741	0.0437	0.0103	0.0603
100MW LOW	8.721	0.1985	0.1799	0.0453	0.0108	0.0611
100MW AVG	44.652	0.1975	0.1658	0.0383	0.0095	0.0591
100MW HIGH	56.826	0.1972	0.1615	0.0357	0.0092	0.0585

The table 4.4 tabulates the FVSI results for five weakest lines such as line 9 (from bus 4 to bus 8), line 10 (from bus 4 to bus 12), line 18 (from bus 7 to bus 9), line 20 (from bus 9 to bus 10), and line 27 (from bus 12 to bus 14). From the table, it is observed that at the application of voltage stability improvement as the objective function after installation of 100MW solar PV with high penetration status have significantly improved the voltage stability condition indicated by the reduction in FVSI values for line 9, line 10, line 18, line 20 and line 27 from 0.1988, 0.1835, 0.0447, 0.0111 and 0.0617 to 0.1972, 0.1615, 0.0357, 0.0092 and 0.0585 respectively. This would mean that solar PV 100MW high penetration status provided sufficient solar PV output power when injected into the power system.

So as to identify the FVSI results after solar PV placement into the power system, the FVSI results from Table 4.4 was extracted on the chart as shown in Figure 4.4. It is observed that the FVSI at the 100MW solar PV during low penetration status, the

FVSI value is increased compared to the 40MW solar PV during average and high penetration status. This is because the of 100MW solar PV only produced approximately 8.721 MW of output power.

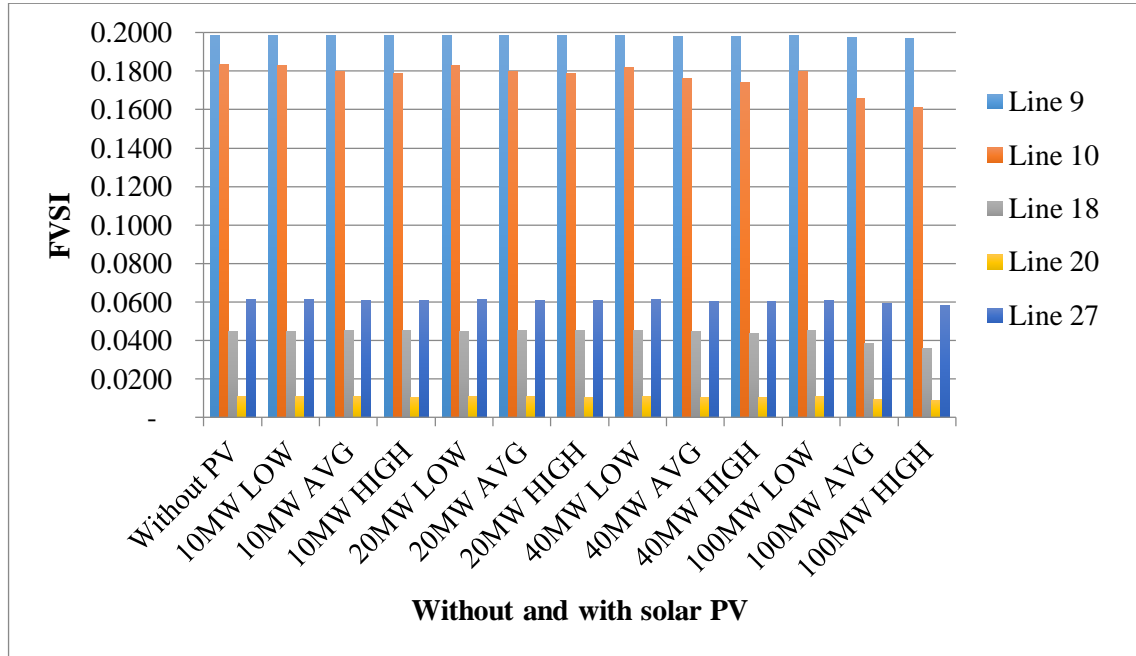


Figure 4.4: FVSI results for $Q_9=150\text{MVAR}$ reactive power loading without and with variations penetration status of solar PV

4.5.3 Case 3: $Q_9=250\text{MVAR}$ with PV Variations

Additional tests were conducted by injecting the solar PV with capacity 10MW, 20MW, 40MW and 100MW into the power system. The results for FVSI values obtain at reactive power loading at bus 9 set to 250MVAR are tabulated in Table 4.5.

Table 4.5: FVSI results for $Q_0=250\text{MVAR}$, without and with variations penetration status of solar PV

Penetration status	PV output power	FVSI				
		Line 9	Line 10	Line 18	Line 20	Line 27
Without PV	NA	0.1972	0.1567	0.1679	0.1212	0.0871
10MW LOW	0.859	0.1972	0.1564	0.1677	0.1213	0.0870
10MW AVG	4.475	0.1971	0.1548	0.1662	0.1216	0.0868
10MW HIGH	5.708	0.1971	0.1542	0.1655	0.1216	0.0867
20MW LOW	1.734	0.1972	0.1560	0.1674	0.1214	0.0870
20MW AVG	8.941	0.1970	0.1529	0.1632	0.1216	0.0865
20MW HIGH	11.412	0.1970	0.1518	0.1610	0.1215	0.0864
40MW LOW	3.485	0.1971	0.1552	0.1667	0.1215	0.0869
40MW AVG	17.89	0.1968	0.1492	0.1543	0.1210	0.0860
40MW HIGH	22.807	0.1968	0.1473	0.1485	0.1204	0.0858
100MW LOW	8.721	0.1970	0.1530	0.1633	0.1216	0.0866
100MW AVG	44.652	0.1964	0.1396	0.1246	0.1186	0.0848
100MW HIGH	56.826	0.1829	0.1299	0.1184	0.1135	0.0815

The table 4.5 tabulates the FVSI results for five weakest lines such as line 9 (from bus 4 to bus 8), line 10 (from bus 4 to bus 12), line 18 (from bus 7 to bus 9), line 20 (from bus 9 to bus 10), and line 27 (from bus 12 to bus 14). From the table, it is observed that at the application of voltage stability improvement as the objective function after installation of 100MW solar PV with high penetration status have significantly improved the voltage stability condition indicated by the reduction in FVSI values for line 9, line 10, line 18, line 20 and line 27 from 0.1972, 0.1567, 0.1679, 0.1212 and 0.0871 to 0.1829, 0.1299, 0.1184, 0.1135 and 0.0815 respectively. This would mean that solar PV 100MW high penetration status provided sufficient solar PV output power when injected into the power system.

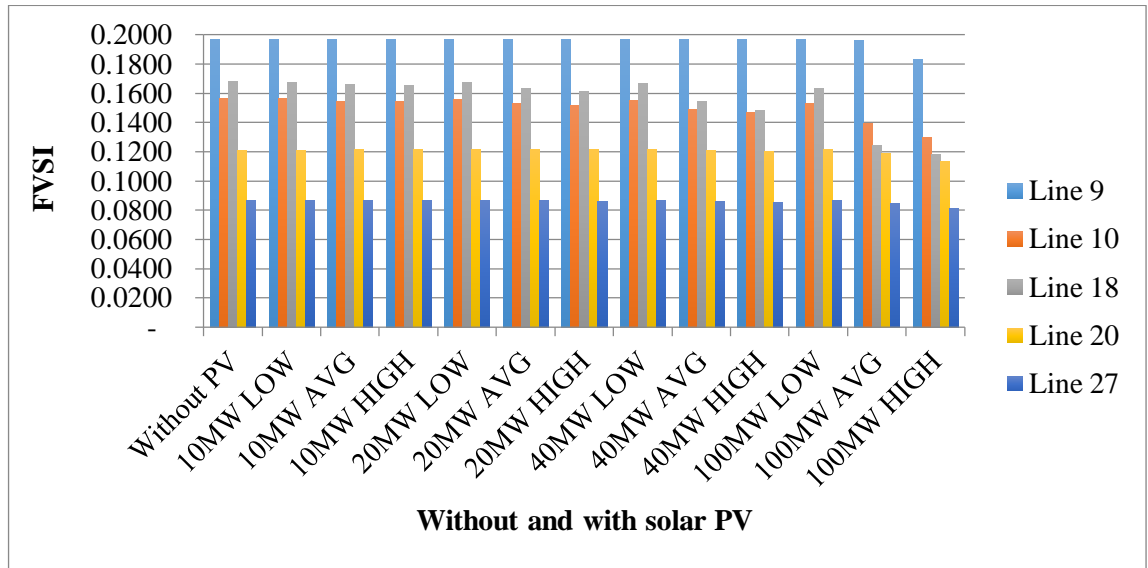


Figure 4.5: FVSI results for $Q_9=250\text{MVAR}$ reactive power loading without and with variations penetration status of solar PV

In order to identify the FVSI results after solar PV placement into the power system, the results from Table 4.5 was extracted on the chart as shown in Figure 4.5. It is observed that at the 100MW solar PV during low penetration status, the FVSI value is increased compared to the 40MW solar PV during average and high penetration status. This is because the of 100MW solar PV produced approximately 8.721 MW of output power.

The FVSI results for $Q_9=100\text{MVAR}$, $Q_9=200\text{MVAR}$ and $Q_9=300\text{MVAR}$ can be referred in the appendix B.

4.6 Simulation 4: Voltage Stability Under Worst Case Condition

This study is conducted to determine the best PV size to be installed in the 26-Bus test system that can enhance the test system voltage stability under worse case condition. For this power system, the maximum loading is 350MVAR. By referring to Table 2.4, the PV will be sized to four different power capacities; 10MW, 20MW, 40MW and 100MW. Each of the PV output power is divided into three irradiance level; lowest (LOW) irradiance level, average (AVG) irradiance and the highest

(HIGH) irradiance level as in Table 3.8. Based on Table 4.2, five weakest lines are selected as a candidate to be assessed of their line stability after solar PV integration into the power system. They are selected based on their high FVSI value.

Tests were conducted by injecting the solar PV with capacity 10MW, 20MW, 40MW and 100MW into the power system. The results for FVSI values obtained at reactive power loading at bus 9 set to 350MVAR are tabulated in Table 4.6.

Table 4.6: FVSI result for $Q_9=350\text{MVAR}$, without and with variations penetration status of solar PV

Penetration status	PV output power	FVSI				
		Line 9	Line 10	Line 18	Line 20	Line 27
Without PV	NA	0.2027	0.1361	0.2888	0.2534	0.1184
10MW LOW	0.859	0.2027	0.1358	0.2870	0.2536	0.1184
10MW AVG	4.475	0.2027	0.1344	0.2786	0.2545	0.1182
10MW HIGH	5.708	0.2027	0.1339	0.2755	0.2547	0.1182
20MW LOW	1.734	0.2027	0.1354	0.2850	0.2539	0.1183
20MW AVG	8.941	0.2027	0.1328	0.2669	0.2549	0.1180
20MW HIGH	11.412	0.2026	0.1319	0.2600	0.2549	0.1179
40MW LOW	3.485	0.2027	0.1348	0.2810	0.2543	0.1183
40MW AVG	17.89	0.2026	0.1298	0.2415	0.2543	0.1177
40MW HIGH	22.807	0.1856	0.1200	0.2301	0.2454	0.1128
100MW LOW	8.721	0.2027	0.1328	0.2675	0.2549	0.1180
100MW AVG	44.652	0.1855	0.1147	0.1895	0.2440	0.1122
100MW HIGH	56.826	0.1855	0.1125	0.1862	0.2441	0.1120

The table 4.6 tabulates the FVSI results for five weakest lines such as line 9 (from bus 4 to bus 8), line 10 (from bus 4 to bus 12), line 18 (from bus 7 to bus 9), line 20 (from bus 9 to bus 10), and line 27 (from bus 12 to bus 14). From the table, it is observed that at the application of voltage stability improvement as the objective function after installation of 100MW solar PV with high penetration status have significantly improved the voltage stability condition indicated by the reduction in

FVSI values for line 9, line 10, line 18, line 20 and line 27 from 0.2027, 0.1361, 0.2888, 0.2534 and 0.1184 to 0.1855, 0.1125, 0.1862, 0.2441 and 0.1120 respectively. At this point, line 18 gives the lowest comparison FVSI value of 0.1862. It is also observed that as the solar PV increases by penetration status, the FVSI results evaluated for each line starts to decrease. This would mean that solar penetration status would cause the power system to be closer to its stability.

In order identify the FVSI results after solar PV placement into the power system, the FVSI results from Table 4.6 was extracted on the chart as shown in Figure 4.6.

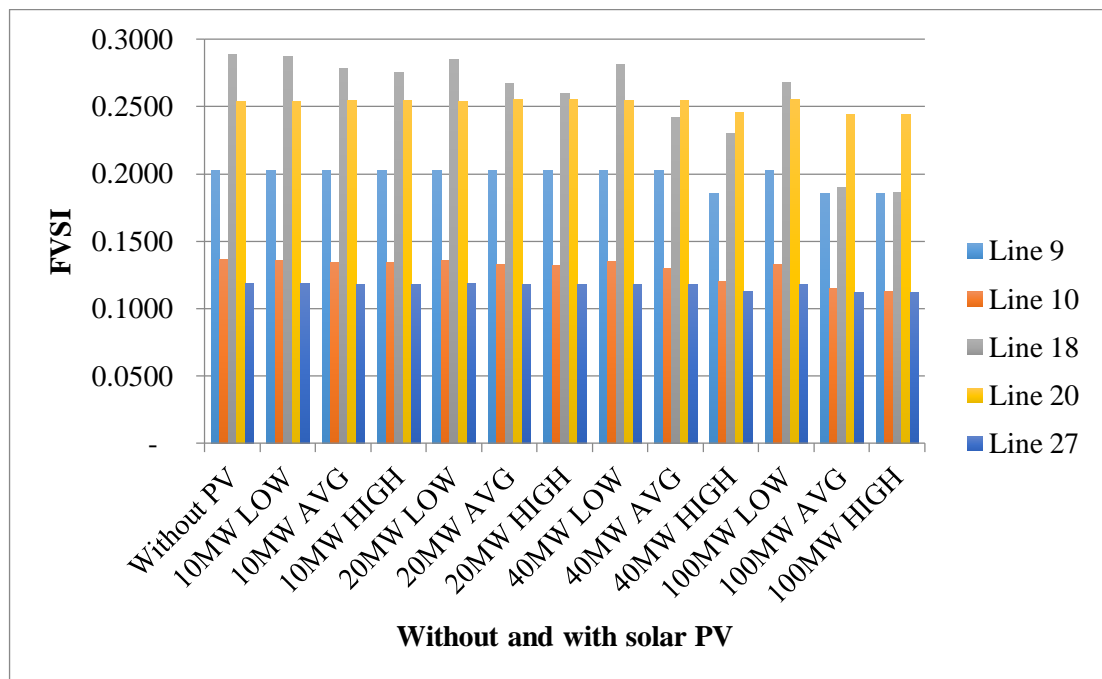


Figure 4.6: FVSI results for $Q_9=350\text{MVAR}$ reactive power loading without and with variations penetration status of solar PV

4.7 Voltage Analysis

The voltage profiles were investigated by highlighting the voltage magnitude with 100MW solar PV installed. The voltage profiles are tabulated in table 4.7.

Table 4.7: Results for voltage profile under load variation with 100MW solar PV

Bus No.	Voltage Magnitude (Vm)							
	50 MVAR	100MW HIGH	150 MVAR	100MW HIGH	250 MVAR	100MW HIGH	350 MVAR	100MW HIGH
1	1.025	1.025	1.025	1.025	1.025	1.025	1.025	1.025
2	1.020	1.030	1.020	1.020	1.010	1.020	1.010	1.020
3	1.045	1.045	1.035	1.035	1.025	1.025	1.025	1.025
4	1.050	1.060	1.040	1.040	1.020	1.020	1.010	1.010
5	1.045	1.045	1.035	1.035	1.025	1.025	1.015	1.025
6	1.001	1.004	0.992	0.993	0.981	0.982	0.971	0.976
7	0.995	1.003	0.983	0.984	0.962	0.967	0.948	0.954
8	0.998	1.007	0.988	0.988	0.968	0.973	0.957	0.962
9	1.010	1.019	0.971	0.973	0.922	0.927	0.876	0.883
10	0.991	0.999	0.974	0.975	0.950	0.953	0.932	0.937
11	0.998	1.000	0.992	0.992	0.984	0.985	0.973	0.977
12	0.994	1.002	0.982	0.982	0.961	0.964	0.949	0.952
13	1.022	1.024	1.013	1.013	1.002	1.002	1.000	1.001
14	1.008	1.011	0.997	0.998	0.983	0.984	0.978	0.980
15	0.999	1.003	0.988	0.988	0.972	0.974	0.966	0.968
16	0.990	0.994	0.979	0.979	0.963	0.965	0.955	0.957
17	0.983	0.985	0.976	0.976	0.967	0.967	0.961	0.963
18	1.007	1.009	1.004	1.004	0.999	1.000	0.996	0.998
19	1.005	1.009	0.993	0.993	0.976	0.978	0.963	0.967
20	0.983	0.990	0.968	0.969	0.945	0.948	0.930	0.934
21	0.977	0.982	0.966	0.966	0.950	0.951	0.938	0.942
22	0.980	0.986	0.964	0.965	0.942	0.944	0.925	0.930
23	0.978	0.984	0.965	0.966	0.946	0.948	0.931	0.936
24	0.969	0.975	0.955	0.956	0.936	0.938	0.921	0.926
25	0.975	0.980	0.964	0.964	0.947	0.949	0.934	0.938
26	1.015	1.015	1.015	1.015	1.015	1.015	1.005	1.005

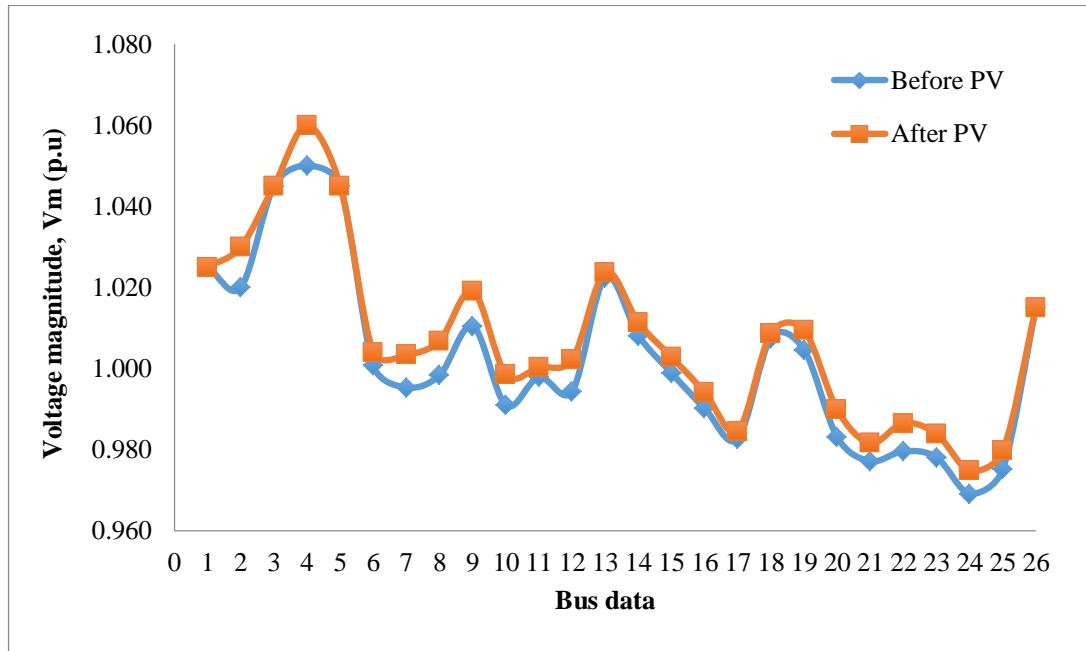


Figure 4.7: Voltage profile for IEEE 26-Bus system for $Q_9=50\text{MVAR}$ reactive power loading with 100MW solar PV

The voltage profile of the IEEE 26-Bus system for the cases $Q_9=50\text{MVAR}$ reactive power loading with 100MW solar PV is shown in the figure 4.7. It is observed that the voltage profile is started to improve. For example the voltage at bus 8 improved from 0.998 p.u. to 1.007 p.u. The voltage profile with and without solar PV is obtained in order to improve the system performance.

The voltage magnitude results for $Q_9=150\text{MVAR}$ and $Q_9=250\text{MVAR}$ and $Q_9=350\text{MVAR}$ can be referred in the appendix C.

4.8 Economic Load Dispatch Before and After PV installation

ELD is conducted at IEEE 26-Bus test system to study the economic load dispatch before and after installation variations of PV. By referring to Table 2.4, the solar PV will be sized to four different power capacities; 10MW, 20MW, 40MW and 100MW. Each of the PV output power is divided into three-penetration status; lowest (LOW), average (AVG) and the highest (HIGH) irradiance level as in Table 3.8. Four cases

were considered namely the case 1: $Q_9=50\text{MVAR}$, case 2: $Q_9=150\text{MVAR}$, case 3: $Q_9=250\text{MVAR}$ and worst case is case 4: $Q_9=350\text{MVAR}$.

4.8.1 Simulation 5: Economic Load Dispatch for 26 bus test system 50MVAR

Table 4.8 tabulates the results of total generation cost and total system loss for the condition without solar PV and with solar PV 10MW, 20MW, 40MW and 100MW are injected into the power system at 50MVAR loading. For the condition without solar PV, the total generation cost initial operating condition is approximately 15,689.30 \$/h and the total system loss is approximately 26.16MW. The total generation cost with optimal dispatch of generation is 15,448.00 \$/h and the total system loss is approximately 12.80MW.

Based on the Table 4.8, it could be seen that when 100MW HIGH is injected into the power system, the total generation cost and total system loss seems to be much lower compared to the test system without solar PV. The total generation cost initial operating condition is approximately 14,900.73 \$/h and the total system loss is approximately 23.78MW. The total generation cost with optimal dispatch of generation is 14,683.00 \$/h and the total system loss is approximately 11.74MW.

Table 4.8: Total system loss and total generation cost, initial operating condition and optimal dispatch (50MVAR loading)

Without and With PV	Total System Loss (MW) initial operating condition	Total System Loss (MW), optimal dispatch	Total Generation Cost, (\$/h) initial operating condition	Total Generation Cost, (\$/h) optimal dispatch
Without PV	26.15	12.80	15,689.30	15,448.00
10MW LOW	26.11	12.79	15,677.23	15,436.00
10MW AVG	25.94	12.73	15,626.49	15,387.00

Without and With PV	Total System Loss (MW) initial operating condition	Total System Loss (MW), optimal dispatch	Total Generation Cost, (\$/h) initial operating condition	Total Generation Cost, (\$/h) optimal dispatch
10MW HIGH	25.88	12.71	15,609.20	15,371.00
20MW LOW	26.07	12.77	15,664.95	15,424.00
20MW AVG	25.73	12.65	15,563.93	15,327.00
20MW HIGH	25.61	12.61	15,529.37	15,294.00
40MW LOW	25.98	12.74	15,640.37	15,401.00
40MW AVG	25.31	12.51	15,438.94	15,206.00
40MW HIGH	25.09	12.43	15,370.51	15,140.00
100MW LOW	25.74	12.66	15,567.01	15,330.00
100MW AVG	24.19	12.11	15,068.13	14,848.00
100MW HIGH	23.78	11.74	14,900.73	14,683.00

Based on Table 4.9, when four types of solar PV are installed into the power system, load demand is re-dispatched among the generators such as G_1 , G_2 , G_3 , G_4 , G_5 and G_{26} and the solar PV units. Promptly, the loads simultaneously supply by the existing conventional generators and the solar PV units. For example, the result for load demand without PV is 1263MW, after solar PV 100MW HIGH is installed into the power system; generators only supply 1206.20MW from the load demand another load demand approximately 56.826MW is supplied by solar PV unit.

Table 4.9: Total optimal dispatch, total demand, total saving \$/h and total annual saving for initial operating condition and optimal dispatch (50MVAR loading)

Without and With PV	Total Optimal Dispatch of Generation (Pg_{tt}), MW	PV Output Power, MW	Total Demand, (P_{dt}), MW	Total Different Cost before and After, (\$/h)	Total Annual Saving Cost hr/year, (\$/h)
Without PV	1275.80	-	1263	241.30	2,113,803.63
10MW LOW	1274.90	0.859	1262.10	241.23	2,113,208.51
10MW AVG	1271.30	4.475	1258.50	239.49	2,097,897.59
10MW HIGH	1270	5.708	1257.30	238.20	2,086,642.84
20MW LOW	1274.00	1.734	1261.30	240.95	2,110,687.65
20MW AVG	1266.70	8.941	1254.10	236.93	2,075,474.12
20MW HIGH	1264.20	11.412	1251.60	235.37	2,061,822.87
40MW LOW	1272.30	3.485	1259.50	239.37	2,096,894.08
40MW AVG	1257.60	17.891	1245.10	232.94	2,040,571.01
40MW HIGH	1252.60	22.807	1240.20	230.51	2,019,264.29
100MW LOW	1266.90	8.721	1254.30	237.01	2,076,163.86
100MW AVG	1230.50	44.652	1218.30	220.13	1,928,323.92
100MW HIGH	1217.90	56.826	1206.20	217.73	1,907,319.42

Furthermore, for power system without solar PV Table 4.9 which are also tabulated show results of a savings of 241.30 \$/h and the total annual savings is approximately 2,113,803.63 \$/h. However, when four types of solar PV are installed into the power system this results in a saving of power system and the total annual savings starts to decrease. For example, for 100MW HIGH, this results in a savings of 217.73 \$/h with the total annual savings is approximately 1,907,319.42 \$/h. the example calculation of a saving/hour and the total annual savings for 100MW HIGH shown using equation 3.9 and equation 3.10.

$$\begin{aligned}
\frac{\$}{h} &= \text{Total Cost Initial} - \text{Total Cost Optimal Dispatch} \\
&= 14,900.73 - 14,683.00 \\
&= \$217.73
\end{aligned}$$

$$\begin{aligned}
\text{Total Annual Saving} &= \frac{\$}{h} * (8760) \\
&= 217.73 * (8760) \\
&= \$1,907,314.80
\end{aligned}$$

4.8.2 Simulation 6: Economic Load Dispatch for 26 bus test system 150MVAR

Table 4.10 tabulates the results of total generation cost and total system loss for the condition without solar PV and with solar PV 10MW, 20MW, 40MW and 100MW is injected into the test system at 150MVAR loading. For the condition without solar PV, the total generation cost initial operating condition is approximately 15,854.96 \$/h and the total system loss is approximately 31.50MW. The total generation cost with optimal dispatch of generation is 15,463.39 \$/h and the total system loss is approximately 13.97MW.

Based on the Table 4.10, it could be seen that when four types of solar PV are injected into the power system, the total generation cost and total system loss seems to be much lower compared to the test system without solar PV. For example, when 100MW HIGH is injected into the power system, the total generation cost initial operating condition is approximately 15,049.55 \$/h and the total system loss is approximately 29.18MW. The total generation cost with optimal dispatch of generation is 14,700.72 \$/h and the total system loss is approximately 13.09MW.

Table 4.10: Total system loss and total generation cost, initial operating condition and optimal dispatch (150MVAR Loading)

Without and With PV	Total System Loss (MW) initial operating condition	Total System Loss (MW), optimal dispatch	Total Generation Cost, (\$/h) initial operating condition	Total Generation Cost, (\$/h) optimal dispatch
Without PV	31.50	13.97	15,854.96	15,463.39
10MW LOW	31.43	13.95	15,842.58	15,451.77
10MW AVG	31.50	13.89	15,790.30	15,402.89
10MW HIGH	31.43	13.87	15,772.59	15,386.24
20MW LOW	31.37	13.94	15,829.98	15,439.94
20MW AVG	31.23	13.82	15,726.21	15,342.59
20MW HIGH	31.07	13.77	15,690.83	15,309.26
40MW LOW	31.56	13.91	15,804.53	15,416.27
40MW AVG	30.68	13.67	15,598.30	15,221.98
40MW HIGH	30.39	13.59	15,528.33	15,155.85
100MW LOW	31.24	13.82	15,729.37	15,345.56
100MW AVG	29.14	13.26	15,219.88	14,863.10
100MW HIGH	29.18	13.09	15,049.55	14,700.72

Based on Table 4.11, when four types of solar PV are installed into the power system, load demand is re-dispatched among the generators such as G_1 , G_2 , G_3 , G_4 , G_5 and G_{26} and the solar PV units. Promptly, the loads simultaneously supply by the existing conventional generators and the solar PV units. For example, the result for load demand without solar PV is 1263MW, after solar PV 100MW HIGH is installed into the power system; generators only supply 1206.20MW from the load demand another load demand approximately 56.826MW is supplied by solar PV unit.

Table 4.11: Total optimal dispatch, total demand, total saving \$/h and total annual saving for initial operating condition and optimal dispatch (150MVAR loading)

Without and With PV	Total Optimal Dispatch of Generation (Pgtt), MW	PV Output Power, MW	Total Demand, (Pdt), MW	Total Different Cost before and After, (\$/h)	Total Annual Saving Cost hr/year, (\$/h)
Without PV	1277	-	1263	391.96	3,433,569.76
10MW LOW	1276.10	0.859	1262.10	390.58	3,421,497.94
10MW AVG	1272.40	4.475	1258.50	387.30	3,392,767.81
10MW HIGH	1271.20	5.708	1257.30	386.59	3,386,534.22
20MW LOW	1275.20	1.734	1261.30	389.98	3,416,241.42
20MW AVG	1267.90	8.941	1254.10	383.21	3,356,943.25
20MW HIGH	1265.40	11.412	1251.60	381.83	3,344,804.33
40MW LOW	1272.30	3.485	1259.50	388.53	3,403,547.88
40MW AVG	1258.80	17.891	1245.10	376.30	3,296,348.96
40MW HIGH	1253.80	22.807	1240.20	372.33	3,261,584.04
100MW LOW	1268.10	8.721	1254.30	383.37	3,358,284.03
100MW AVG	1231.60	44.652	1218.30	356.88	3,126,302.52
100MW HIGH	1219.30	56.826	1206.20	348.55	3,053,281.04

Furthermore, for power system without solar PV Table 4.11 also tabulates this results in a savings of 391.96 \$/h and the total annual savings is approximately 3,433,569.76 \$/h. However, when four types of PV are installed into the power system this results in a saving of power system and the total annual savings starts to decrease. For example, for 100MW HIGH, this results in a savings of 348.55 \$/h with the total annual savings is approximately 3,053,281.04 \$/h.

4.8.3 Simulation 7: Economic Load Dispatch for 26 bus test system 250MVAR

Table 4.12 tabulates the results of total generation cost and total system loss for the condition without solar PV and with solar PV 10MW, 20MW, 40MW and 100MW is injected into the test system at 250MVAR loading. For the condition without solar PV, the total generation cost initial operating condition is approximately 15,911.00 \$/h and the total system loss is approximately 32.15MW. The total generation cost with optimal dispatch of generation is 15,504.04 \$/h and the total system loss is approximately 16.90MW.

Based on the Table 4.12, it could be seen that when four types of solar PV are injected into the power system, the total generation cost and total system loss seems to be much lower compared to the test system without solar PV. For example, when 100MW HIGH is injected into the power system, the total generation cost initial operating condition is approximately 15,105.09 \$/h and the total system loss is approximately 27.94MW. The total generation cost with economic load dispatch of generation is 14,738.33 \$/h and the total system loss is approximately 15.86MW.

Table 4.12: Total system loss and total generation cost, initial operating condition and optimal dispatch (250MVAR loading)

Without and With PV	Total System Loss (MW) initial operating condition	Total System Loss (MW), optimal dispatch	Total Generation Cost, (\$/h) initial operating condition	Total Generation Cost, (\$/h) optimal dispatch
Without PV	32.15	16.90	15,911.00	15,504.04
10MW LOW	32.05	16.89	15,898.59	15,492.41
10MW AVG	31.63	16.82	15,846.48	15,443.48
10MW HIGH	31.49	16.80	15,828.77	15,426.81
20MW LOW	31.95	16.87	15,885.95	15,480.57
20MW AVG	29.85	16.75	15,781.54	15,383.12

Without and With PV	Total System Loss (MW) initial operating condition	Total System Loss (MW), optimal dispatch	Total Generation Cost, (\$/h) initial operating condition	Total Generation Cost, (\$/h) optimal dispatch
20MW HIGH	29.70	16.71	15,746.07	15,349.75
40MW LOW	31.75	16.84	15,860.72	15,456.87
40MW AVG	29.29	16.60	15,653.36	15,262.37
40MW HIGH	28.99	16.52	15,583.32	15,196.18
100MW LOW	29.86	16.75	15,784.70	15,386.09
100MW AVG	27.72	16.19	15,275.08	14,903.17
100MW HIGH	27.94	15.86	15,105.09	14,738.33

Based on Table 4.13, when four types of solar PV are installed into the power system, load demand is re-dispatched among the generators such as G_1 , G_2 , G_3 , G_4 , G_5 and G_{26} and the solar PV units. Promptly, the loads simultaneously supply by the existing conventional generators and the solar PV units. For example, the result for load demand without solar PV is 1263MW, after solar PV 100MW HIGH is installed into the power system; generators only supply 1206.20MW from the load demand another load demand approximately 56.826MW is supplied by solar PV unit.

Table 4.13: Total optimal dispatch, total demand, total saving \$/h and total annual saving for initial operating condition and optimal dispatch (250MVAR loading)

Without and With PV	Total Optimal Dispatch of Generation (Pg_{tt}), MW	PV Output Power, MW	Total Demand, (P_{dt}), MW	Total Different Cost before and After, (\$/h)	Total Annual Saving Cost hr/year, (\$/h)
Without PV	1279.90	-	1263	407.00	3,565,363.23

Without and With PV	Total Optimal Dispatch of Generation (Pgtt), MW	PV Output Power, MW	Total Demand, (Pdt), MW	Total Different Cost before and After, (\$/h)	Total Annual Saving Cost hr/year, (\$/h)
10MW LOW	1279	0.859	1262.10	406.59	3,561,688.69
10MW AVG	1275.30	4.475	1258.50	403.48	3,534,459.44
10MW HIGH	1274.10	5.708	1257.30	401.77	3,519,524.39
20MW LOW	1278.10	1.734	1261.30	404.95	3,547,369.28
20MW AVG	1270.80	8.941	1254.10	398.54	3,491,186.04
20MW HIGH	1268.30	11.412	1251.60	396.07	3,469,533.94
40MW LOW	1276.40	3.485	1259.50	403.72	3,536,551.74
40MW AVG	1257.60	17.891	1245.10	391.36	3,428,344.03
40MW HIGH	1252.60	22.807	1240.20	387.32	3,392,907.97
100MW LOW	1271	8.721	1254.30	398.70	3,492,598.78
100MW AVG	1234.50	44.652	1218.30	372.08	3,259,446.14
100MW HIGH	1222	56.826	1206.20	367.09	3,215,738.29

Furthermore, for power system without solar PV Table 4.13 also tabulates this results in a savings of 407.00 \$/h and the total annual savings is approximately 3,565,363.23 \$/h. However, when four types of solar PV are installed into the power system this results in a saving of power system and the total annual savings starts to decrease. For example, for 100MW HIGH, this results in a savings of 367.09 \$/h with the total annual savings of operating cost is approximately 3,215,738.29 \$/h.

4.8.4 Simulation 8: Economic Load Dispatch for 26 bus test system worst case

Table 4.14 tabulates the results of total generation cost and total system loss for the condition without solar PV and with solar PV 10MW, 20MW, 40MW and 100MW is injected into the test system at 350MVAR loading. For the condition without solar

PV, the total generation cost initial operating condition is approximately 16,233.93 \$/h and the total system loss is approximately 60.20MW. The total generation cost with optimal dispatch of generation is 15,548.00 \$/h and the total system loss is approximately 20.13MW.

Based on the Table 4.14, it could be seen that when four types of solar PV are injected into the power system, the total generation cost and total system loss seems to be much lower compared to the test system without solar PV. For example, when 100MW HIGH is injected into the power system, the total generation cost initial operating condition is approximately 15,273.07 \$/h and the total system loss is approximately 32.16MW. The total generation cost with economic load dispatch of generation is 14,787.00 \$/h and the total system loss is approximately 19.34MW.

Table 4.14: Total system loss and total generation cost, initial operating condition and optimal dispatch (350MVAR loading)

Without and With PV	Total System Loss (MW) initial operating condition	Total System Loss (MW), optimal dispatch	Total Generation Cost, (\$/h) initial operating condition	Total Generation Cost, (\$/h) optimal dispatch
Without PV	60.20	20.13	16,233.93	15,548.00
10MW LOW	59.30	20.12	16,214.17	15,537.00
10MW AVG	55.72	20.05	16,133.88	15,488.00
10MW HIGH	54.57	20.03	16,107.49	15,471.00
20MW LOW	58.41	20.10	16,194.32	15,525.00
20MW AVG	51.72	19.97	16,040.49	15,427.00
20MW HIGH	49.67	19.93	15,991.25	15,394.00
40MW LOW	56.67	20.07	16,155.42	15,501.00
40MW AVG	44.82	19.81	15,869.30	15,306.00
40MW HIGH	41.56	19.87	15,782.84	15,243.00
100MW LOW	51.90	19.97	16,044.95	15,430.00

Without and With PV	Total System Loss (MW) initial operating condition	Total System Loss (MW), optimal dispatch	Total Generation Cost, (\$/h) initial operating condition	Total Generation Cost, (\$/h) optimal dispatch
100MW AVG	32.85	19.52	15,446.65	14,950.00
100MW HIGH	32.16	19.34	15,273.07	14,787.00

Based on Table 4.15, when four types of solar PV are installed into the power system, load demand is re-dispatched among the generators such as G_1 , G_2 , G_3 , G_4 , G_5 and G_{26} and the solar PV units. Promptly, the loads simultaneously supply by the existing conventional generators and the solar PV units. For example, the result for load demand without solar PV is 1263MW, after solar PV 100MW HIGH is installed into the power system; generators only supply 1206.20MW from the load demand another load demand approximately 56.826MW is supplied by solar PV unit.

Table 4.15: Total optimal dispatch, total demand, total saving \$/h and total annual saving for initial operating condition and optimal dispatch (350MVAR loading)

Without and With PV	Total Optimal Dispatch of Generation (P_{gtt}), MW	PV Output Power, MW	Total Demand, (P_{dt}), MW	Total Different Cost before and After, (\$/h)	Total Annual Saving Cost hr/year, (\$/h)
Without PV	1283.10	-	1263	685.93	6,008,723.30
10MW LOW	1282.30	0.859	1262.10	677.17	5,932,007.71
10MW AVG	1278.60	4.475	1258.50	645.88	5,657,906.24
10MW HIGH	1277.30	5.708	1257.30	636.49	5,575,683.32
20MW LOW	1281.40	1.734	1261.30	669.32	5,863,276.19
20MW AVG	1274	8.941	1254.10	613.49	5,374,164.15

Without and With PV	Total Optimal Dispatch of Generation (Pgtt), MW	PV Output Power, MW	Total Demand, (Pdt), MW	Total Different Cost before and After, (\$/h)	Total Annual Saving Cost hr/year, (\$/h)
20MW HIGH	1271.50	11.412	1251.60	597.25	5,231,904.60
40MW LOW	1279.60	3.485	1259.50	654.42	5,732,705.30
40MW AVG	1264.90	17.891	1245.10	563.30	4,934,500.16
40MW HIGH	1260.10	22.807	1240.20	539.84	4,728,972.60
100MW LOW	1274	8.721	1254.30	614.95	5,386,989.04
100MW AVG	1238	44.652	1218.30	496.65	4,350,690.73
100MW HIGH	1226	56.826	1206.20	486.07	4,257,970.29

Furthermore, for power system without solar PV Table 4.15 also tabulates this results in a savings of 685.93 \$/h and the total annual savings is approximately 6,008,723.30 \$/h. However, when four types of solar PV are installed into the power system this results in a saving of power system and the total annual savings starts to decrease. For example, for 100MW HIGH, this results in a savings of 486.07 \$/h with the total annual savings is approximately 4,257,970.29 \$/h.

The economic load dispatch before and after solar PV placement results can be referred in the appendix D.

4.9 Optimization using DEIANT

This simulation is to study the optimization using DEIANT before and after installation variations of solar PV for 50MVAR Loading with total loss and total cost minimization as the objective function.

4.9.1 Simulation 9: 50MVAR loading without and with solar PV Low irradiance level

The DEIANT was implemented in MATLAB software. Comparative studies between optimal dispatch without PV, with PV and DEIANT were conducted to prove the performance of DEIANT in solved the problem of ELD. The optimal dispatch without PV is set as the reference for the comparison purpose. The objective function

Table 4.16: DEIANT results with PV1 and PV2 with low penetration status

Technique	Optimal Dispatch Without PV	PV1 PV Capacity = 10MW PV Output = 0.859MW		PV2 PV Capacity = 20MW PV Output = 1.734MW	
		Optimal Dispatch	DEIANT	Optimal Dispatch	DEIANT
G₁ (MW)	447.6919	447.5197	482.56	447.3443	449.33
G₂ (MW)	173.1938	173.0661	90.36	172.9361	193.50
G₃ (MW)	263.4859	263.3521	292.25	263.2158	235.67
G₄ (MW)	138.8143	138.6592	118.02	138.5013	109.59
G₅ (MW)	165.5883	165.4372	181.72	165.2832	178.97
G₂₆ (MW)	87.026	86.8925	105.96	86.7566	102.61
Total Cost (\$/h)	15,448.00	15,436.00	15,463.47	15,424.00	15,381.65
Total Loss (MW)	12.80	12.79	8.73	12.77	8.40

Table 4.16 and 4.17 tabulates the total cost and total loss produced by each generator after integrated with four types of PV in low irradiance level. By comparing to optimal dispatch without and with PV, DEIANT results successfully minimize the total cost and the loss. For example, DEIANT results minimize the total cost to 15,309.08 \$/h and minimize the total loss to 9.37MW after PV4 integrated into the power system.

Table 4.17: DEIANT results with PV3 and PV4 with low penetration status

Technique	Optimal Dispatch Without PV	PV3 PV Capacity = 40MW PV Output = 3.485MW		PV4 PV Capacity = 100MW PV Output = 8.721MW	
		Optimal Dispatch	DEIANT	Optimal Dispatch	DEIANT
G₁ (MW)	447.6919	446.9934	429.88	445.9443	467.48
G₂ (MW)	173.1938	172.676	153.35	171.8983	165.1012
G₃ (MW)	263.4859	262.943	234.49	262.1276	236.2241
G₄ (MW)	138.8143	138.1854	148.71	137.2412	131.0117
G₅ (MW)	165.5883	164.9751	193.16	164.0531	146.4505
G₂₆ (MW)	87.026	86.4845	109.59	85.6709	117.3799
Total Cost (\$/h)	15,448.00	15,401.00	15,384.31	15,330.00	15,309.08
Total Loss (MW)	12.80	12.74	9.66	12.66	9.37

4.9.2 Simulation 10: 50MVAR loading without PV and with PV Average irradiance level

Next, by comparing to optimal dispatch without and with PV during an average irradiance level of PV with DEIANT, Table 4.18 and 4.19 tabulates DEIANT results successfully minimize the total cost and the loss the total cost.

Table 4.18: DEIANT results with PV1 and PV2 with average penetration status

Technique	Optimal Dispatch Without PV	PV1 PV Capacity = 10MW PV Output = 0.859MW		PV2 PV Capacity = 20MW PV Output = 1.734MW	
		Optimal Dispatch	DEIANT	Optimal Dispatch	DEIANT
G₁ (MW)	447.6919	446.795	478.15	445.9003	467.48

Technique	Optimal Dispatch Without PV	PV1 PV Capacity = 10MW PV Output = 0.859MW		PV2 PV Capacity = 20MW PV Output = 1.734MW	
		Optimal Dispatch	DEIANT	Optimal Dispatch	DEIANT
G₂ (MW)	173.1938	172.5289	197.58	171.8656	165.10
G₃ (MW)	263.4859	262.7888	275.32	262.0934	236.22
G₄ (MW)	138.8143	138.0068	87.01	137.2015	131.01
G₅ (MW)	165.5883	164.8008	169.42	164.0144	146.45
G₂₆ (MW)	87.026	86.3307	60.95	85.6367	117.38
Total Cost (\$/h)	15,448.00	15,387.00	15,379.62	15,327.00	15,309.08
Total Loss (MW)	12.80	12.73	9.91	12.65	9.59

For example, DEIANT results minimize the total cost to 14,840.00 \$/h and minimize the total loss to 9.02MW after PV4 integrated into the power system.

Table 4.19: DEIANT results with PV3 and PV4 with average penetration status

Technique	Optimal Dispatch Without PV	PV3 PV Capacity = 40MW PV Output = 3.485MW		PV4 PV Capacity = 100MW PV Output = 8.721MW	
		Optimal Dispatch	DEIANT	Optimal Dispatch	DEIANT
G₁ (MW)	447.6919	444.1086	463.38	438.7607	460.80
G₂ (MW)	173.1938	170.5374	77.34	166.5736	178.007
G₃ (MW)	263.4859	260.7009	288.58	256.546	247.1334
G₄ (MW)	138.8143	135.5898	142.44	130.7856	73.395
G₅ (MW)	165.5883	162.4368	183.44	157.7093	199.7435
G₂₆ (MW)	87.026	84.2457	98.92	80.0843	68.2898
Total Cost (\$/h)	15,448.00	15,206.00	15,254.55	14,848.00	14,840.10

Technique	Optimal Dispatch Without PV	PV3 PV Capacity = 40MW PV Output = 3.485MW		PV4 PV Capacity = 100MW PV Output = 8.721MW	
		Optimal Dispatch	DEIANT	Optimal Dispatch	DEIANT
Total Loss (MW)	12.80	12.51	8.99	12.11	9.02

4.9.3 Simulation 11: 50MVAR loading without PV and with PV High irradiance level

Finally, the comparisons are made between optimal dispatch without PV and with PV during high irradiance level of PV with DEIANT, Table 4.20 and 4.21 tabulates DEIANT results successfully minimize the total cost and the loss the total cost.

Table 4.20: DEIANT results with PV1 and PV2 with high penetration status

Technique	Optimal Dispatch Without PV	PV1 PV Capacity = 10MW PV Output = 0.859MW		PV2 PV Capacity = 20MW PV Output = 1.734MW	
		Optimal Dispatch	DEIANT	Optimal Dispatch	DEIANT
G₁ (MW)	447.6919	446.5479	425.22	445.4054	488.21
G₂ (MW)	173.1938	172.3457	181.7288	171.4988	133.1697
G₃ (MW)	263.4859	262.5967	249.2592	261.7088	274.9143
G₄ (MW)	138.8143	137.7844	113.5205	136.7563	106.2727
G₅ (MW)	165.5883	164.5837	184.4786	163.579	164.1099
G₂₆ (MW)	87.026	86.1391	111.4889	85.2527	94.4657
Total Cost (\$/h)	15,448.00	15,371.00	15,326.19	15,294.00	15,282.81
Total Loss (MW)	12.80	12.71	8.40	12.61	9.55

For example, DEIANT computed the lowest total cost to 14,723.00 \$/h and minimize the total loss to 8.64MW when PV4 integrated into the power system.

Table 4.21: DEIANT results with PV3 and PV4 with high penetration status

Technique	Optimal Dispatch Without PV	PV3 PV Capacity = 40MW PV Output = 3.485MW		PV4 PV Capacity = 100MW PV Output = 8.721MW	
		Optimal Dispatch	DEIANT	Optimal Dispatch	DEIANT
G₁ (MW)	447.6919	443.1251	471.12	440.0786	494.33
G₂ (MW)	173.1938	169.8084	143.1027	156.5072	143.8065
G₃ (MW)	263.4859	259.9367	266.4623	255.9525	234.3811
G₄ (MW)	138.8143	134.7055	136.9146	128.5543	51.3617
G₅ (MW)	165.5883	161.5693	159.3413	157.7495	179.1862
G₂₆ (MW)	87.026	83.4816	72.9469	79.0691	111.7541
Total Cost (\$/h)	15,448.00	15,140.00	15,117.31	14,683.00	14,723.73
Total Loss (MW)	12.80	12.43	9.70	11.74	8.64

It means that, at PV4 with solar PV capacity 100MW HIGH penetration produced the lowest total cost and total loss compared to PV1, PV2 and PV3. The summaries of DEIANT results for the total cost and total loss tabulates in table 4.22, 4.23 and 4.24.

Table 4.22: Optimization results without and with solar PV low irradiance level

Technique	Optimal Dispatch Without PV	PV1 PV Capacity = 10MW PV Output = 0.859MW		PV2 PV Capacity = 20MW PV Output = 1.734MW		PV3 PV Capacity = 40MW PV Output = 3.485MW		PV4 PV Capacity = 100MW PV Output = 8.721MW	
		Pre-optimization	Post-optimization (DEIANT)	Pre-optimization	Post-optimization (DEIANT)	Pre-optimization	Post-optimization (DEIANT)	Pre-optimization	Post-optimization (DEIANT)
Total Cost (\$/h)	15,448.00	15,436.00	15,463.47	15,424.00	15,381.65	15,401.00	15,384.31	15,330.00	15,309.08
Total Loss (MW)	12.80	12.79	8.73	12.77	8.40	12.74	9.66	12.66	9.37

Table 4.23: Optimization results without PV and with PV average irradiance level

Technique	Optimal Dispatch Without PV	PV1 PV Capacity = 10MW PV Output = 0.859MW		PV2 PV Capacity = 20MW PV Output = 1.734MW		PV3 PV Capacity = 40MW PV Output = 3.485MW		PV4 PV Capacity = 100MW PV Output = 8.721MW	
		pre-optimization	post-optimization (DEIANT)	pre-optimization	post-optimization (DEIANT)	pre-optimization	post-optimization (DEIANT)	pre-optimization	post-optimization (DEIANT)
Total Cost (\$/h)	15,448.00	15,387.00	15,379.62	15,327.00	15,309.08	15,206.00	15,254.55	14,848.00	14,840.10
Total Loss (MW)	12.80	12.73	9.91	12.65	9.59	12.51	8.99	12.11	9.02

Table 4.24: Optimization results without PV and with PV high irradiance level

Technique	Optimal Dispatch Without PV	PV1 PV Capacity = 10MW PV Output = 0.859MW		PV2 PV Capacity = 20MW PV Output = 1.734MW		PV3 PV Capacity = 40MW PV Output = 3.485MW		PV4 PV Capacity = 100MW PV Output = 8.721MW	
		pre-optimization	post-optimization (DEIANT)	pre-optimization	post-optimization (DEIANT)	pre-optimization	post-optimization (DEIANT)	pre-optimization	post-optimization (DEIANT)
Total Cost (\$/h)	15,448.00	15,371.00	15,326.19	15,294.00	15,282.81	15,140.00	15,117.31	14,683.00	14,723.73
Total Loss (MW)	12.80	12.71	8.40	12.61	9.55	12.43	9.70	11.74	8.64

4.10 Summary

This chapter presented the application of FVSI provided a comprehensive result to obtain an optimal placement and sizing of solar PV for stability enhancement and the application of DEIANT for operating cost minimization. From the simulation 1 until simulation 4, the analysis on the power system stability under load variations at bus 9, the FVSI analysis has identified the FVSI value is approaching 1 when increasing in reactive power loading that caused voltage instability to the power system. However, an integrated solar PV at bus 9 the FVSI is start to reduced especially on the highest solar PV output power (solar PV with 100MW capacity) at highest penetration status. FVSI values for line 9, line 10, line 18, line 20 and line 27 are decreasing their values from 0.2027, 0.1361, 0.2888, 0.2534 and 0.1184 to 0.1855, 0.1125, 0.1862, 0.2441 and 0.1120 respectively. Looking back at the impact of solar PV towards the power system, the penetration of solar PV did improve the stability of the system. Next, in the simulation from 5 until 8 simulation, the ELD analysis using Newton-Raphson method has identified the minimization of total cost and the total loss before and after solar PV placement in the power system. For example, at 100MW HIGH solar PV is injected into the power system, the total generation cost initial operating condition is approximately 15,273.07 \$/h and the total system loss is approximately 32.16MW. The total generation cost with economic load dispatch of generation is 14,787.00 \$/h and the total system loss is approximately 19.34MW. In this simulation the total demand, total different cost and total annual saving also have been analysis. For example, the result for load demand without solar PV is 1263MW, after solar PV 100MW HIGH is installed into the power system, generators only supply 1206.20MW from the load demand another load demand approximately 56.826MW is supplied by solar PV unit. Then on simulation 9 until simulation 11, it is proven that DEIANT successfully optimizes the operating cost and the total loss of the IEEE 26-Bus system. For example, after 100MW HIGH solar PV is injected into the power system, DEIANT computed the lowest total cost to 14,723.00 \$/h and minimize the total loss to 8.64MW.

CHAPTER 5

CONCLUSION AND RECOMMENDATION

5.1 Conclusion

This thesis presents a solar PV placement and sizing for line stability enhancement and optimal operating cost. This study involved the application of FVSI for voltage stability analysis. This study also ELD and DEIANT for loss and cost minimization. This research was conducted on IEEE 26-Bus system, which the system contains with six generators. The objectives are to analyze power system stability under load variations using FVSI as stability indicator, to evaluate the voltage stability before and after solar photovoltaic implementation using FVSI and to determine optimal placement and sizing of solar photovoltaic and for enhancing power system stability and minimizing operating cost.

In the beginning of the thesis, voltage stability analysis using FVSI was conducted to the test systems by gradually increasing the reactive power loading on a load bus 9 and FVSI was calculated for every line in the test system as the indicator to voltage stability condition. A line evaluated with FVSI value close to unity implies that the line has reached its voltage stability limit, beyond which voltage instability will occur leading to voltage collapse in the whole system. Results obtained from the voltage stability analysis showed that line 18 (from bus 7 to bus 9) was identified as the most sensitive line with FVSI value increased from 0.0554 to 0.2888 after the reactive power gradually increased from 50MVAR to 350MVAR. Comparative studies for FVSI were also conducted between the FVSI results obtained before and after PV implementation. Results obtained from the voltage stability analysis showed FVSI value at line 18 (from bus 7 to bus 9) was identified reduced from 0.2888 to 0.1862 after integrated of 100MW solar PV with high penetration status. This FVSI successfully reduced after PV implementation. In this research, the DEIANT algorithm is proposed to optimize economic dispatch before and after PV

implementation. This technique is used to compare the total cost and total loss between optimal dispatches without PV, with PV with DEIANT. DEIANT technique is successfully reduced the total cost and the total loss of PV. DEIANT computed the lowest total cost to 14,723.00 \$/h and minimize the total loss to 8.64MW after 100MW HIGH is injected into the power system. So, it can be concluded PV with high irradiance level is able to stabilize the power system at minimal operating cost.

5.2 Recommendation

There are several suggestions for further research as below:

- i) To use the concept highlighted in this research to study optimal placement and sizing of large scale solar farm. FVSI can be used to determine line stability for solar farm injection.
- ii) Using others voltage stability index such as LMN and LQP to compare the best voltage stability index that suitable for the power system.
- iii) DEIANT algorithm is applying to optimize power flow and reduces total cost and total loss when the power system is subjected to heavy reactive power loading.

5.3 Summary

This chapter provided a complete conclusion and several suggestions for further research.

REFERENCES

- [1] J. C. Su and I. Adaji, "Wind and Solar Integration – An Operational Planning View Point," 2019.
- [2] M. Mathew, S. Ghosh, D. Suresh Babu, and A. A. Ansari, "" An Assessment of Voltage Stability based on Line Voltage Stability Indices and its Enhancement Using TCSC "," *IOSR J. Electr. Electron. Eng. Ver. I*, vol. 10, no. 6, pp. 2278–1676, 2015.
- [3] A. Parthasarathy and R. Dhanasekaran, "Economic Load Dispatch with Optimal Power Flow Using Modified," vol. 10, no. 12, pp. 1–6, 2017.
- [4] M. A. W. M. S. N. Samsudin, M. M. Rahman, "Power Generation Sources in Malaysia : Status and Prospects for Sustainable Development," *J. Adv. Rev. Sci. Res.*, vol. 25, September, pp. 11–28, 2016.
- [5] KeTTHA, "National Renewable Energy Policy," *Natl. Renew. energy Policy*, no. November, p. 90, 2008.
- [6] Z. KAMARUZZAMAN, "Effect of grid-connected photovoltaic systems on static and dynamic voltage stability with analysis techniques - a review," *Przegląd Elektrotechniczny*, vol. 1, no. 6, pp. 136–140, 2015.
- [7] J. Paska, P. Biczal, and M. Kłos, "Technical and economic aspects of electricity storage systems co-operating with renewable energy sources," *2009 10th Int. Conf. Electr. Power Qual. Util. EPQU'09*, pp. 1–6, 2009.
- [8] I. Musiri and T. K. Abdul Rahman, "On-line voltage stability based contingency ranking using fast voltage stability index (FVSI)," *Proc. IEEE Power Eng. Soc. Transm. Distrib. Conf.*, vol. 2, ASIA PACIFIC, pp. 1118–1123, 2002.
- [9] S. E. E. Profile, "Stability Improvement of Power System by Using PI &," March 2013, 2018.
- [10] R. Verayiah and A. Iyadurai, "A Comparison Study on Types of PV for Grid Connected Photovoltaic Power," *Indones. J. Electr. Eng. Comput. Sci.*, vol. 6, no. 2, p. 349, 2017.
- [11] M. S. S. Danish, T. Senjyu, S. M. S. Danish, N. R. Sabory, K. Narayanan, and

- P. Mandal, "A recap of voltage stability indices in the past three decades," *Energies*, vol. 12, no. 8, pp. 1–18, 2019.
- [12] M. A. Hannan, R. A. Begum, M. G. Abdolrasol, M. S. Hossain Lipu, A. Mohamed, and M. M. Rashid, "Review of baseline studies on energy policies and indicators in Malaysia for future sustainable energy development," *Renew. Sustain. Energy Rev.*, vol. 94, August 2017, pp. 551–564, 2018.
- [13] N. A. Rahmat, N. F. A. Aziz, M. H. Mansor, and I. Musirin, "Optimizing Economic Load Dispatch with Renewable Energy Sources via Differential Evolution Immunized Ant Colony Optimization Technique," *Int. J. Adv. Sci. Eng. Inf. Technol.*, vol. 7, no. 6, p. 2012, 2017.
- [14] A. W. H. Sie, I. Z. Abidin, and H. Hashim, "A methodology to determine suitable placement of solar photovoltaic sources in the transmission system taking into account Voltage Stability Index (VSI)," *Conf. Proceeding - 2014 IEEE Int. Conf. Power Energy, PECon 2014*, pp. 226–230, 2014.
- [15] SEDA, "Seda Portal," *SEDA Malaysia*. 2017. Available: <https://www3.seda.gov.my>
- [16] M. K. Mohamad Zamani *et al.*, "Active and reactive power scheduling optimization using firefly algorithm to improve voltage stability under load demand variation," *Indones. J. Electr. Eng. Comput. Sci.*, vol. 9, no. 2, pp. 365–372, 2018.
- [17] A. Alcayde, F. G. Montoya, J. Gómez, F. Manzano-Agugliaro, R. Baños, and C. Gil, "Optimization methods applied to renewable and sustainable energy: A review," *Renew. Sustain. Energy Rev.*, vol. 15, no. 4, pp. 1753–1766, 2011.
- [18] D. Q. Hung, "Smart Integration of Distributed Renewable Generation and Battery Energy Storage," 2014.
- [19] M. R. Islam, R. Saidur, N. A. Rahim, K. H. Solangi, and E. Tower, "Usage of Solar Energy and Its Status in Malaysia," *Eng. e-Transaction*, vol. 5, no. 1, pp. 6–10, 2010.
- [20] "From a solar cell to a PV system," *Wikipedia*. 2014. Available: https://en.wikipedia.org/wiki/Solar_panel
- [21] A. F. A. Kadir, T. Khatib, and W. Elmenreich, "Integrating photovoltaic systems in power system: Power quality impacts and optimal planning challenges," *Int. J. Photoenergy*, 2014.

- [22] Z. A. Kamaruzzaman and A. Mohamed, "Impact of grid-connected photovoltaic generator using P-V curve and improved voltage stability index," *Conf. Proceeding - 2014 IEEE Int. Conf. Power Energy, PECon 2014*, pp. 196–200, 2014.
- [23] M. Karimi, H. Mokhlis, K. Naidu, S. Uddin, and A. H. A. Bakar, "Photovoltaic penetration issues and impacts in distribution network - A review," *Renew. Sustain. Energy Rev.*, vol. 53, pp. 594–605, 2016.
- [24] P. Chaudhary and M. Rizwan, "Voltage regulation mitigation techniques in distribution system with high PV penetration: A review," *Renew. Sustain. Energy Rev.*, vol. 82, no. September 2017, pp. 3279–3287, 2018.
- [25] M. S. Elnozahy and M. M. A. Salama, "Technical impacts of grid-connected photovoltaic systems on electrical networks - A review," *J. Renew. Sustain. Energy*, vol. 5, no. 3, 2013.
- [26] R. Shah, N. Mithulananthan, R. C. Bansal, and V. K. Ramachandaramurthy, "A review of key power system stability challenges for large-scale PV integration," *Renew. Sustain. Energy Rev.*, vol. 41, pp. 1423–1436, 2015.
- [27] R. Shah, N. Mithulananathan, R. Bansal, K. Y. Lee, and A. Lomi, "Influence of large-scale PV on voltage stability of sub-transmission system," *Int. J. Electr. Eng. Informatics*, vol. 4, no. 1, pp. 148–161, 2012.
- [28] D. L. Talavera, F. J. Muñoz-Rodríguez, G. Jimenez-Castillo, and C. Rus-Casas, "A new approach to sizing the photovoltaic generator in self-consumption systems based on cost-competitiveness, maximizing direct self-consumption," *Renew. Energy*, vol. 130, pp. 1021–1035, 2019.
- [29] Z. A. Kamaruzzaman, A. Mohamed, and R. Mohamed, "Optimal placement of grid-connected photovoltaic generators in a power system for voltage stability enhancement," *Indones. J. Electr. Eng. Comput. Sci.*, vol. 13, no. 1, p. 339, 2019.
- [30] H. M. Sultan, A. A. Zaki Diab, O. N. Kuznetsov, Z. M. Ali, and O. Abdalla, "Evaluation of the impact of high penetration levels of PV power plants on the capacity, frequency and voltage stability of Egypt's unified grid," *Energies*, vol. 12, no. 3, pp. 1–22, 2019.
- [31] W. Suampun, "Voltage Stability Analysis of Grid-connected Photovoltaic Power Systems Using CPFLOW," *Procedia Comput. Sci.*, vol. 86, March, pp.

301–304, 2016.

- [32] Prabha Kundur, "Power System Stability And Control," in Power System Engineering Series, ISBN 0-07-035958-X, New York: McGraw Hill, 1993.
- [33] S. Ratra, R. Tiwari, and K. R. Niazi, "Voltage stability assessment in power systems using line voltage stability index," *Comput. Electr. Eng.*, vol. 70, pp. 199–211, 2018.
- [34] D. Devaraj and J. Preetha Roselyn, "On-line voltage stability assessment using radial basis function network model with reduced input features," *Int. J. Electr. Power Energy Syst.*, vol. 33, no. 9, pp. 1550–1555, 2011.
- [35] N. A. M. Ismail, A. A. M. Zin, A. Khairuddin, and S. Khokhar, "A comparison of voltage stability indices," *Proc. 2014 IEEE 8th Int. Power Eng. Optim. Conf. PEOCO 2014*, pp. 30–34, 2014.
- [36] A. Mohamed, G. B. Jasmon, and S. Yusof, "A static voltage collapse indicator," *J. Ind. Technol.*, vol. 7, no. 1, pp. 73–85, 1998.
- [37] N. Shekhawat, A. K. Gupta, and A. Kumar Sharma, "Voltage Stability Assessment Using Line Stability Indices," *3rd Int. Conf. Work. Recent Adv. Innov. Eng. ICRAIE 2018*, vol. 2018, November, pp. 1–4, 2019.
- [38] I. Bin Musirin, "Universiti Teknologi MARA New Techniques for Voltage Stability Assessment and Improvement in Power System," 2003.
- [39] I. Musirin and T. K. Abdul Rahman, "Novel fast voltage stability index (FVSI) for voltage stability analysis in power transmission system," *2002 Student Conf. Res. Dev. Glob. Res. Dev. Electr. Electron. Eng. SCORED 2002 - Proc*, October 2018, pp. 265–268, 2002.
- [40] F. I. H. Hassim, I. Musirin, and T. K. A. Rahman, "Voltage stability margin enhancement using Evolutionary Programming (EP)," *SCORED 2006 - Proc. 2006 4th Student Conf. Res. Dev. "Towards Enhancing Res. Excell. Reg., SCORED*, pp. 235–240, 2006.
- [41] K. R. V. Dr.G.V.Marutheswar, "Fast Voltage Stability Index Based Optimal Reactive Power Planning Using Differential Evolution," *Electr. Electron. Eng. An Int. J. Vol 3, No 1, Febr. 2014 FAST*, vol. 3, no. 1, pp. 51–60, 2014.
- [42] S. K. Nandha Kumar and P. Renuga, "FVSI based reactive power planning using evolutionary programming," *2010 IEEE Int. Conf. Commun. Control Comput. Technol. ICCCT 2010*, pp. 265–269, 2010.

- [43] A. Ramasamy, R. Verayiah, H. I. Zainal Abidin, and I. Musirin, "A study on FVSI index as an indicator for Under Voltage Load Shedding (UVLS)," *ICEE 2009 - Proceeding 2009 3rd Int. Conf. Energy Environ. Adv. Towar. Glob. Sustain.*, December, pp. 84–87, 2009.
- [44] F. D. Santillán-Lemus, H. Minor-Popocatl, O. Aguilar-Mejía, and R. Tapia-Olvera, "Optimal economic dispatch in microgrids with renewable energy sources," *Energies*, vol. 12, no. 1, 2019.
- [45] G. H. Hwang, K. B. Ching, and M. Z. Samsuddin, "Economic Dispatch Studies for IEEE 14-Bus Distribution," 2009.
- [46] J. Lin, C. L. Chen, S. F. Tsai, and C. Yuan, "New intelligent particle swarm optimization algorithm for solving economic dispatch with valve-point effects," *J. Mar. Sci. Technol.*, vol. 23, no. 1, pp. 44–53, 2015.
- [47] A. Dhamanda, A. Dutt, S. Prakash, and A. K. Bhardwaj, "A Traditional Approach to Solve Economic Load Dispatch Problem of Thermal Generating Unit Using MATLAB Programming," vol. 2, no. 9, pp. 3147–3152, 2013.
- [48] S. K. Mishra and S. K. Mishra, "A Comparative Study of Solution of Economic Load Dispatch Problem in Power Systems in the Environmental Perspective," *Procedia Comput. Sci.*, vol. 48, pp. 96–100, 2015.
- [49] S. K. Dewangan, A. Jain, and a P. Huddar, "A Traditional Approach to Solve Economic Load Dispatch Problem Considering the Generator Constraints," *IOSR J. Electr. Electron. Eng. Ver. III*, vol. 10, no. 2, pp. 2278–1676, 2015.
- [50] O. Abedinia, N. Amjady, and M. S. Naderi, "Multi-objective Environmental/Economic Dispatch using firefly technique," *2012 11th Int. Conf. Environ. Electr. Eng. IEEEIC 2012 - Conf. Proc.*, pp. 461–466, 2012.
- [51] U. Sharma and B. Moses, "Analysis and optimization of economic load dispatch using soft computing techniques," *Int. Conf. Electr. Electron. Optim. Tech. ICEEOT 2016*, pp. 4035–4040, 2016.
- [52] N. A. Rahmat and I. Musirin, "Differential Evolution Ant Colony Optimization (DEACO) technique in solving economic load dispatch problem," *2012 IEEE Int. Power Eng. Optim. Conf. PEOCO 2012 - Conf. Proc.*, June, pp. 263–268, 2012.
- [53] N. A. Rahmat, I. Musirin, and A. F. Abidin, "Differential Evolution Immunized Ant Colony Optimization (DEIANT) technique in solving

- economic emission dispatch,” *Proc. 2013 Int. Conf. Technol. Informatics, Manag. Eng. Environ. TIME-E 2013*, pp. 198–202, 2013.
- [54] N. A. Rahmat, I. Musirin, and A. F. Abidin, “Fuzzy unit commitment for cost minimization in power system planning,” *Proc. 2013 IEEE 7th Int. Power Eng. Optim. Conf. PEOCO 2013*, June, pp. 680–685, 2013.
- [55] N. A. Rahmat, I. Musirin, A. F. Abidin, S. A. Jumaat, and W. N. Wan Abdul Munim, “Solving fuzzy combined-emission dispatch by using differential evolution immunized Ant Colony Optimization technique,” *2013 IEEE Jordan Conf. Appl. Electr. Eng. Comput. Technol. AEECT 2013*, pp. 1–6, 2013.
- [56] N. A. Rahmat, I. Musirin, A. F. Abidin, and M. R. Ahmad, “Economic load dispatch with valve-point loading effect by using differential evolution immunized ant colony optimization technique,” *2014 Australas. Univ. Power Eng. Conf. AUPEC 2014 - Proc.*, October, pp. 1–6, 2014.
- [57] N. A. Rahmat, I. Musirin, and A. F. Abidin, “Differential Evolution Immunized Ant Colony Optimization Technique (DEIANT) in solving economic dispatch by considering prohibited operating zones,” *Proc. 2014 IEEE 8th Int. Power Eng. Optim. Conf. PEOCO 2014*, vol. 2, no. March, pp. 455–460, 2014.
- [58] A. F. A. N. A. Rahmat, I. Musirin, “Asian Bulletin,” *Asian Bull. Eng. Sci. Technol. (ABEST)*, vol. 22, no. 2, pp. f1–f2, 2013.
- [59] I. Musirin and T. K. Abdul Rahman, “Estimating maximum loadability for weak bus identification using FVSI,” *IEEE Power Eng. Rev.*, 2002.
- [60] W. A. Augusteen, S. Geetha, and R. Rengaraj, “Economic dispatch incorporation solar energy using particle swarm optimization,” *2016 3rd Int. Conf. Electr. Energy Syst. ICEES 2016*, pp. 67–73, 2016.

APPENDICES

Appendix A: Busdata and Linedata

```
clear
clc
basemva = 100; accuracy = 0.0001; maxiter = 10;
%      Bus Bus Voltage Angle ---Load---- -----Generator----- Static MVAR
%      No  code Mag.   Degree MW   MVAR MW   MVAR Qmin Qmax  +Qc/-
Ql
busdata=[1  1  1.025  0.0  51  41  0  0  0  0  4
          2  2  1.020  0.0  22  15  79  0  40 250  0
          3  2  1.025  0.0  64  50  20  0  40 150  0
          4  2  1.050  0.0  25  10 100  0  25  80  2
          5  2  1.045  0.0  50  30 300  0  40 160  5
          6  0  1.00  0.0  76  29  0  0  0  0  2
          7  0  1.00  0.0  0  0  0  0  0  0  0
          8  0  1.00  0.0  0  0  0  0  0  0  0
          9  0  1.00  0.0  89  50  0  0  0  0  3
         10  0  1.00  0.0  0  0  0  0  0  0  0
         11  0  1.00  0.0  25  15  0  0  0  0 1.5
         12  0  1.00  0.0  89  48  00 00  0  0  2
         13  0  1.00  0.0  31  15  0  0  0  0  0
         14  0  1.00  0.0  24  12  0  0  0  0  0
         15  0  1.00  0.0  70  31  0  0  0  0 0.5
         16  0  1.00  0.0  55  27  0  0  0  0  0
         17  0  1.00  0.0  78  38  0  0  0  0  0
         18  0  1.00  0.0 153  67  0  0  0  0  0
         19  0  1.00  0.0  75  15  0  0  0  0  5
         20  0  1.00  0.0  48  27  0  0  0  0  0
         21  0  1.00  0.0  46  23  0  0  0  0  0
         22  0  1.00  0.0  45  22  0  0  0  0  0
         23  0  1.00  0.0  25  12  0  0  0  0  0
```

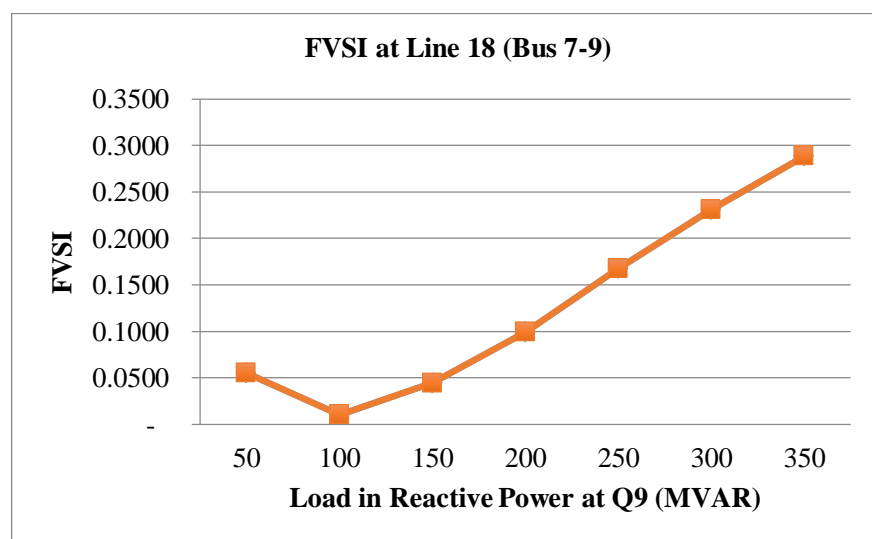
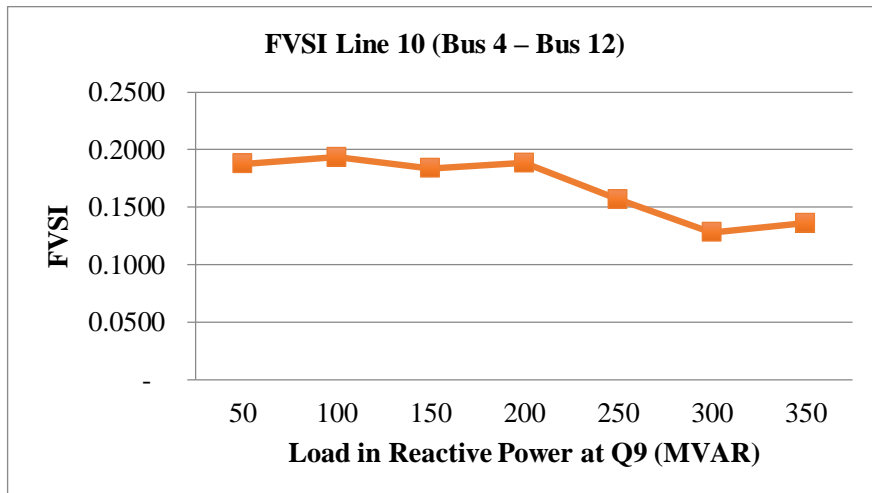
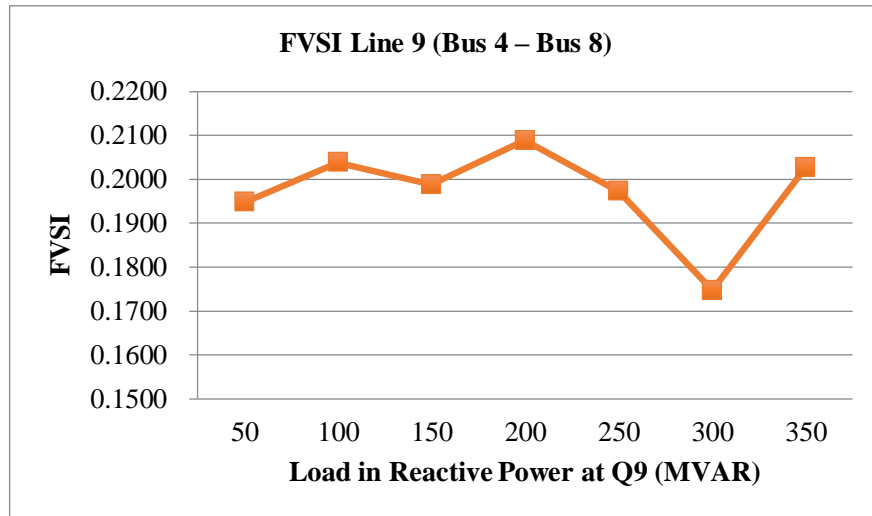
```

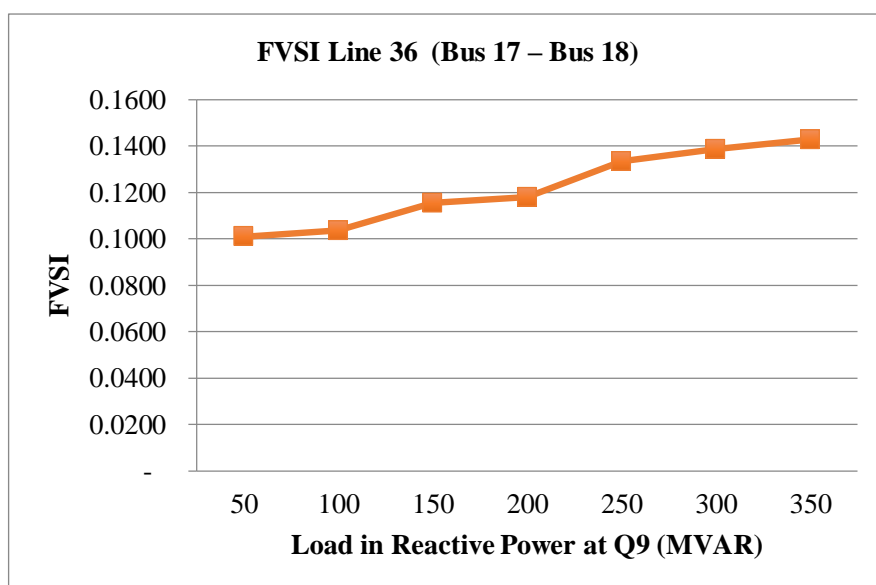
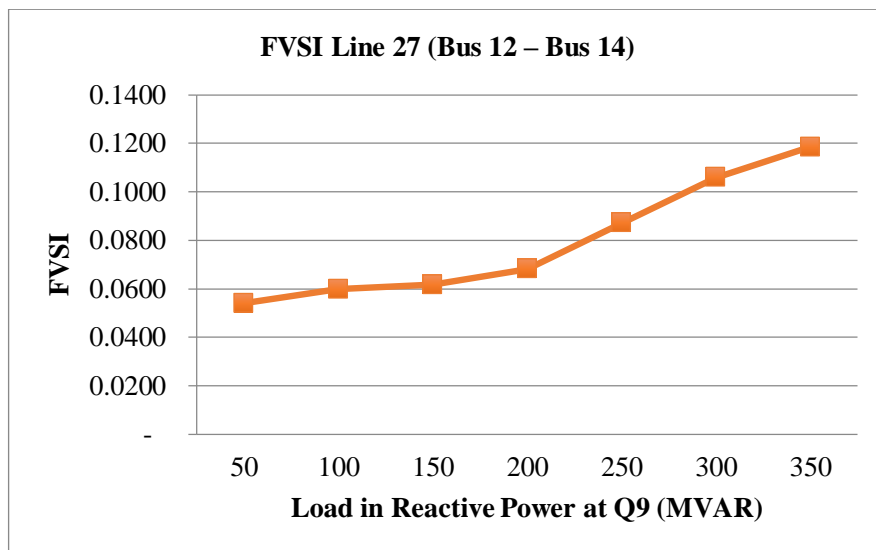
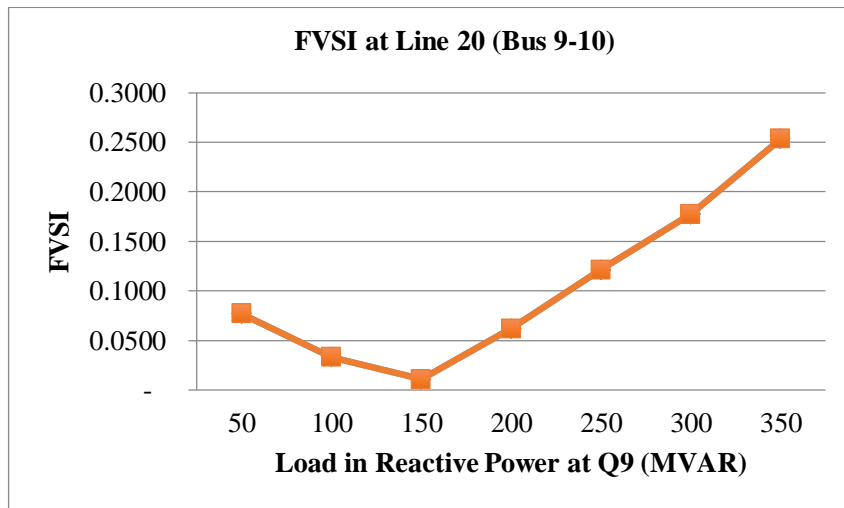
24 0 1.00 0.0 54 27 0 0 0 0 0
25 0 1.00 0.0 28 13 0 0 0 0 0
26 2 1.015 0.0 40 20 60 0 15 50 0];
%                               Line code
%      Bus bus  R    X    1/2 B  = 1 for lines
%      nl nr p.u.  p.u.  p.u.   > 1 or < 1 tr. tap at bus nl
linedata=[1 2 0.00055 0.00480 0.03000 1
1 18 0.00130 0.01150 0.06000 1
2 3 0.00146 0.05130 0.05000 0.96
2 7 0.01030 0.05860 0.01800 1
2 8 0.00740 0.03210 0.03900 1
2 13 0.00357 0.09670 0.02500 0.96
2 26 0.03230 0.19670 0.00000 1
3 13 0.00070 0.00548 0.00050 1.017
4 8 0.00080 0.02400 0.00010 1.050
4 12 0.00160 0.02070 0.01500 1.050
5 6 0.00690 0.03000 0.09900 1
6 7 0.00535 0.03060 0.00105 1
6 11 0.00970 0.05700 0.00010 1
6 18 0.00374 0.02220 0.00120 1
6 19 0.00350 0.06600 0.04500 0.95
6 21 0.00500 0.09000 0.02260 1
7 8 0.00120 0.00693 0.00010 1
7 9 0.00095 0.04290 0.02500 0.95
8 12 0.00200 0.01800 0.02000 1
9 10 0.00104 0.04930 0.00100 1
10 12 0.00247 0.01320 0.01000 1
10 19 0.05470 0.23600 0.00000 1
10 20 0.00660 0.01600 0.00100 1
10 22 0.00690 0.02980 0.00500 1
11 25 0.09600 0.27000 0.01000 1
11 26 0.01650 0.09700 0.00400 1
12 14 0.03270 0.08020 0.00000 1

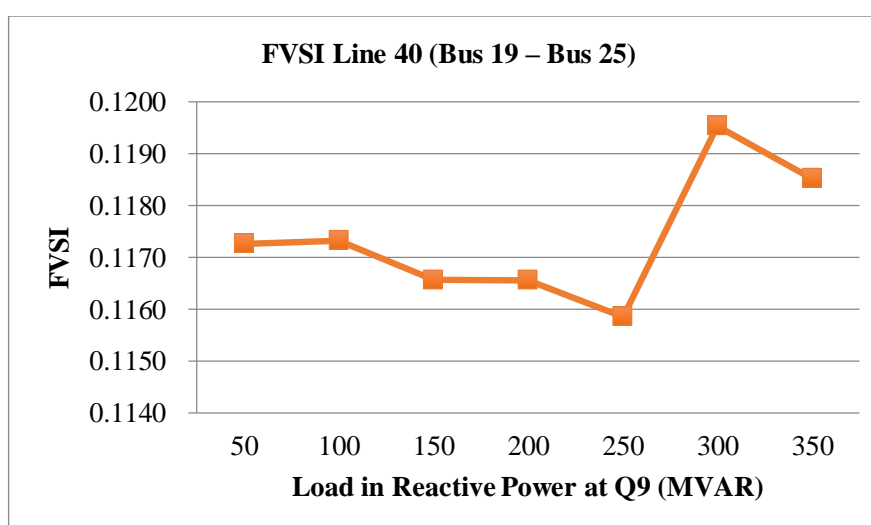
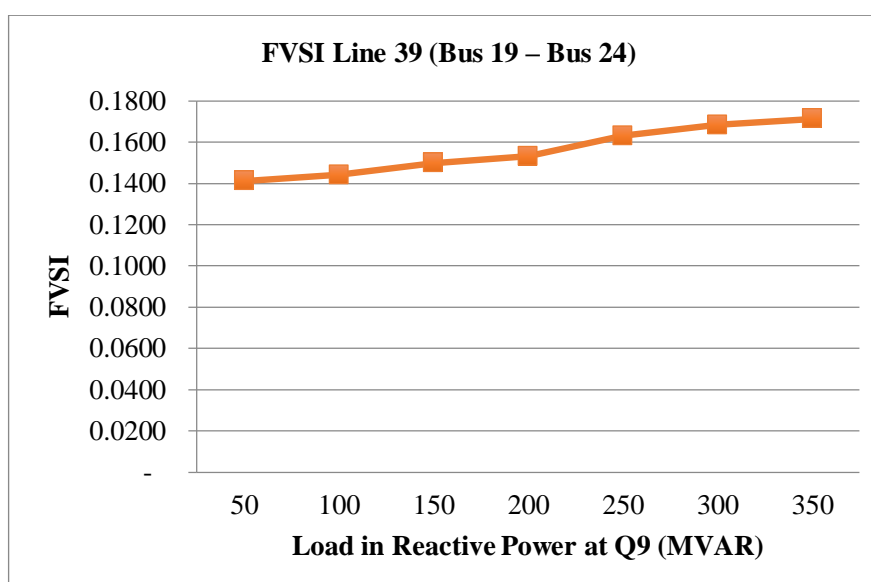
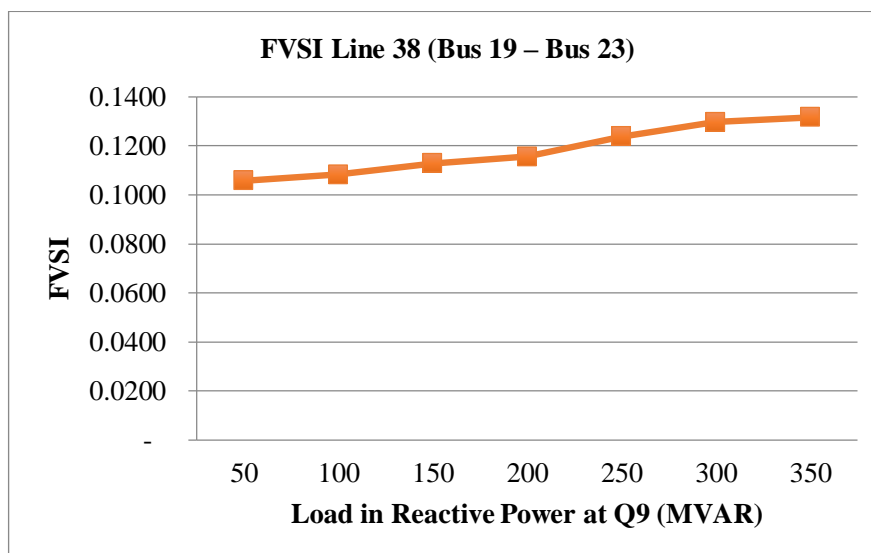
```

12	15	0.01800	0.05980	0.00000	1
13	14	0.00460	0.02710	0.00100	1
13	15	0.01160	0.06100	0.00000	1
13	16	0.01793	0.08880	0.00100	1
14	15	0.00690	0.03820	0.00000	1
15	16	0.02090	0.05120	0.00000	1
16	17	0.09900	0.06000	0.00000	1
16	20	0.02390	0.05850	0.00000	1
17	18	0.00320	0.06000	0.03800	1
17	21	0.22900	0.44500	0.00000	1
19	23	0.03000	0.13100	0.00000	1
19	24	0.03000	0.12500	0.00200	1
19	25	0.11900	0.22490	0.00400	1
20	21	0.06570	0.15700	0.00000	1
20	22	0.01500	0.03660	0.00000	1
21	24	0.04760	0.15100	0.00000	1
22	23	0.02900	0.09900	0.00000	1
22	24	0.03100	0.08800	0.00000	1
23	25	0.09870	0.11680	0.00000	1];

Appendix B: FVSI Without and with solar PV

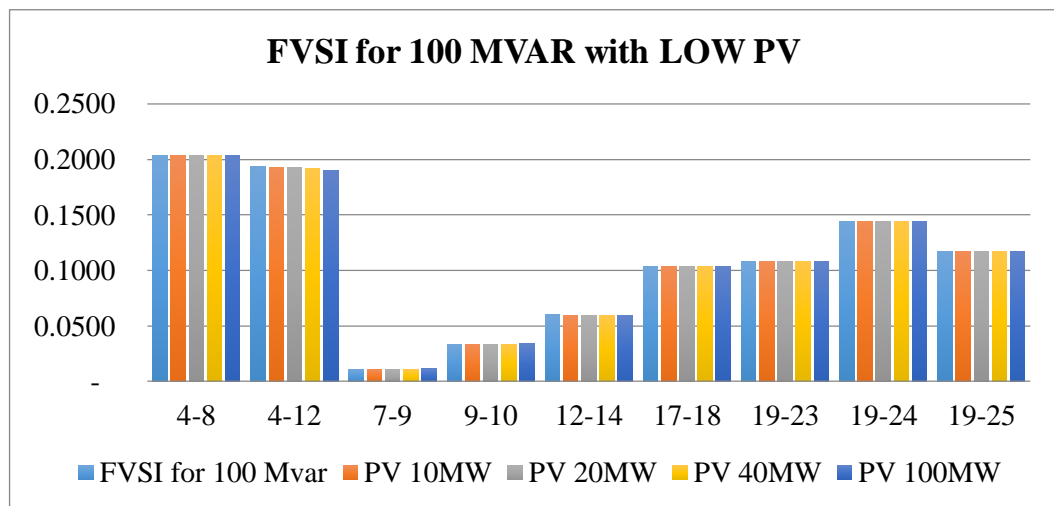




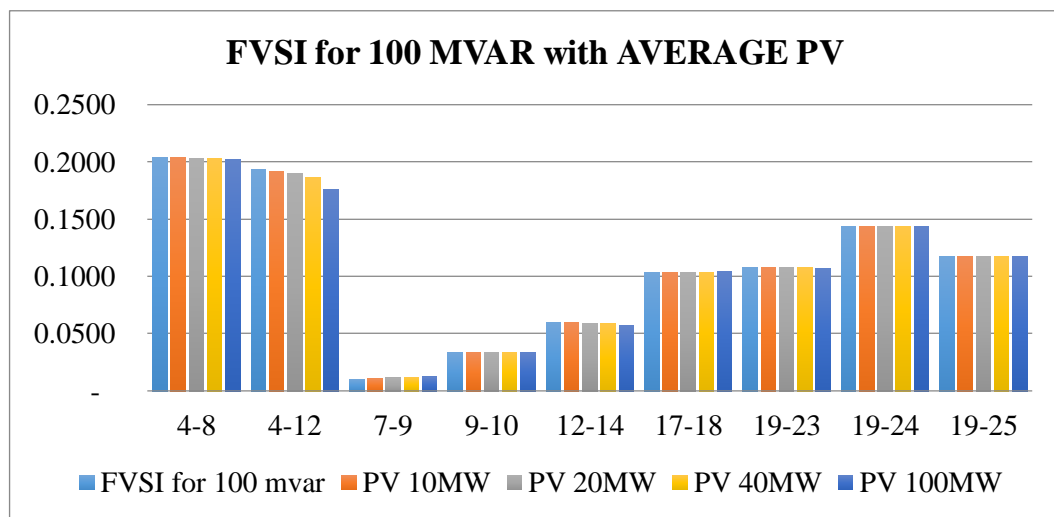


a) FVSI: Reactive Power 100MVAR, with PV (10MW, 20MW, 40MW and 100MW)

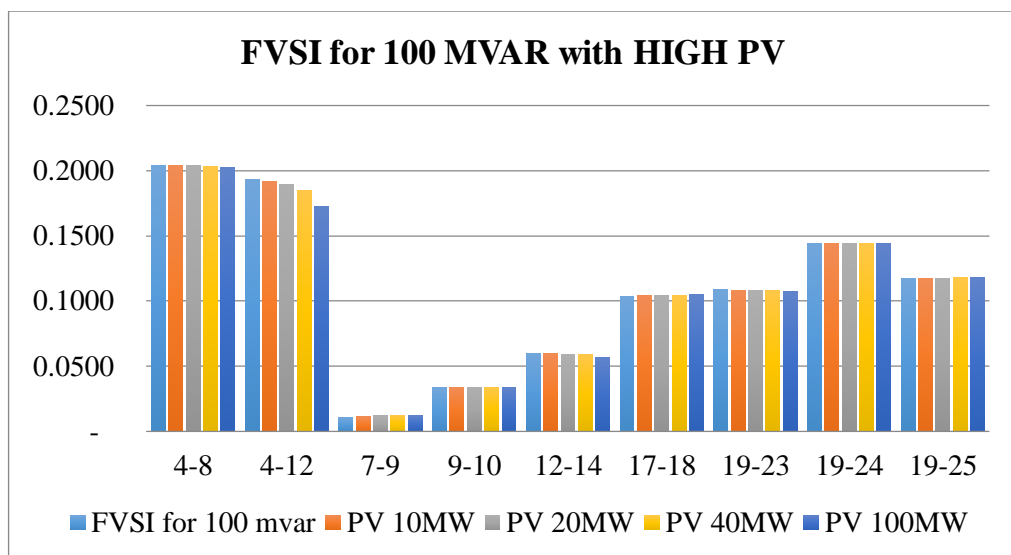
LOW (PV Output)					
Linedata	PV Capacity	10MW	20MW	40MW	100MW
	PV Output	0.859MW	1.734MW	3.485MW	8.721MW
	FVSI for 100MVAR	FVSI			
4-8	0.2038	0.2038	0.2038	0.2037	0.2035
4-12	0.1933	0.1930	0.1926	0.1920	0.1899
7-9	0.0104	0.0106	0.0107	0.0109	0.0114
9-10	0.0333	0.0333	0.0334	0.0334	0.0336
12-14	0.0598	0.0597	0.0597	0.0596	0.0592
17-18	0.1036	0.1036	0.1036	0.1037	0.1038
19-23	0.1083	0.1083	0.1082	0.1082	0.1081
19-24	0.1441	0.1441	0.1441	0.1441	0.1441
19-25	0.1173	0.1173	0.1173	0.1173	0.1174



AVERAGE (PV Output)					
Linedata	PV Capacity	10MW	20MW	40MW	100MW
	PV Output	4.475MW	8.941MW	17.891MW	44.652MW
	FVSI for 100MVAR	FVSI			
4-8	0.2038	0.2037	0.2035	0.2032	0.2023
4-12	0.1933	0.1916	0.1898	0.1865	0.1765
7-9	0.0104	0.0110	0.0114	0.0121	0.0124
9-10	0.0333	0.0335	0.0336	0.0337	0.0334
12-14	0.0598	0.0595	0.0592	0.0587	0.0572
17-18	0.1036	0.1037	0.1038	0.1039	0.1043
19-23	0.1083	0.1082	0.1081	0.1078	0.1072
19-24	0.1441	0.1441	0.1441	0.1441	0.1438
19-25	0.1173	0.1174	0.1174	0.1174	0.1176

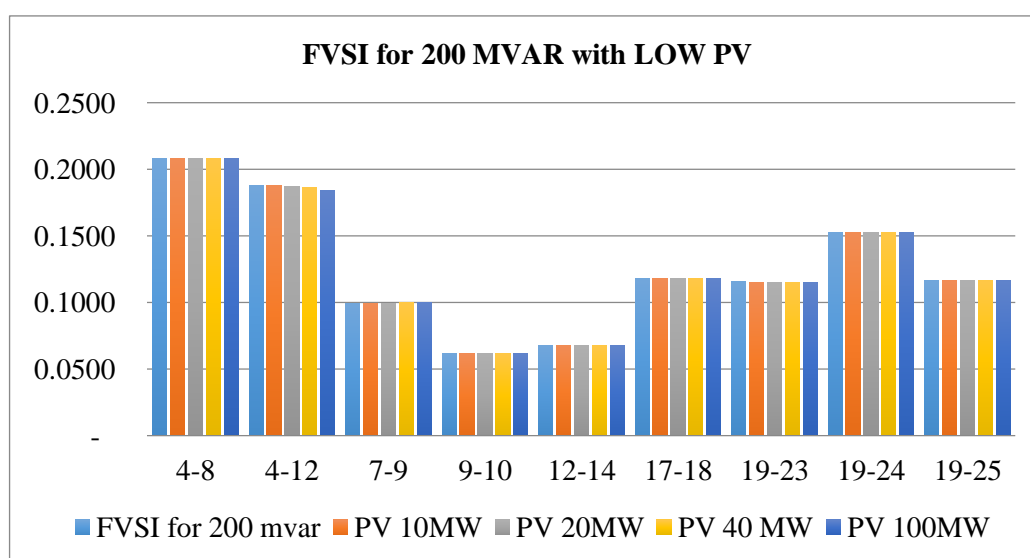


HIGH (PV Output)					
Linedata	PV Capacity	10MW	20MW	40MW	100MW
	PV Output	5.708MW	11.412MW	22.807MW	56.826MW
	FVSI for 100MVAR	FVSI			
4-8	0.2038	0.2036	0.2034	0.2030	0.2020
4-12	0.1933	0.1911	0.1889	0.1846	0.1722
7-9	0.0104	0.0111	0.0117	0.0123	0.0122
9-10	0.0333	0.0335	0.0337	0.0337	0.0336
12-14	0.0598	0.0594	0.0591	0.0584	0.0566
17-18	0.1036	0.1037	0.1039	0.1040	0.1044
19-23	0.1083	0.1081	0.1080	0.1077	0.1068
19-24	0.1441	0.1441	0.1441	0.1441	0.1435
19-25	0.1173	0.1174	0.1174	0.1175	0.1177

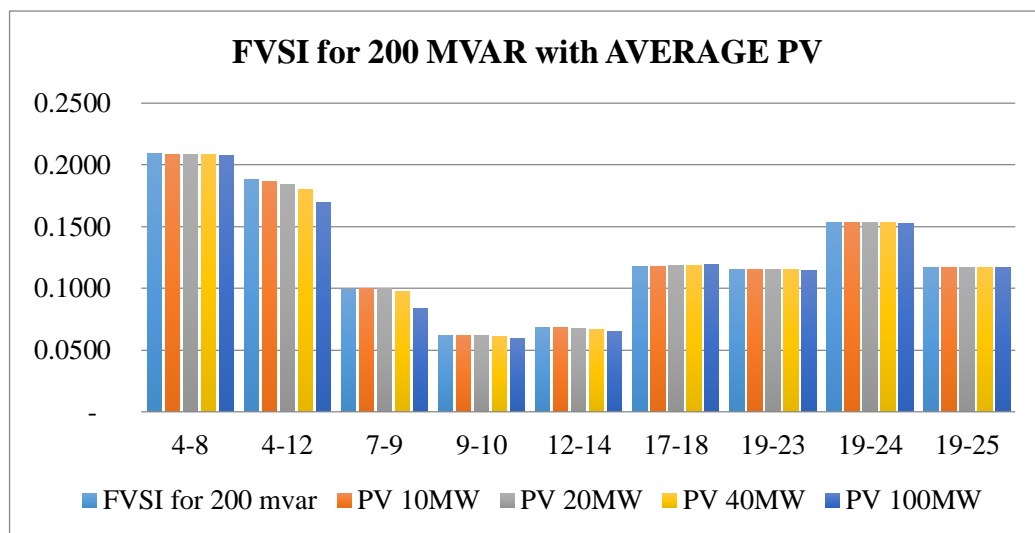


b) FVSI: Reactive Power 200MVAR, with PV (10MW, 20MW, 40MW and 100MW)

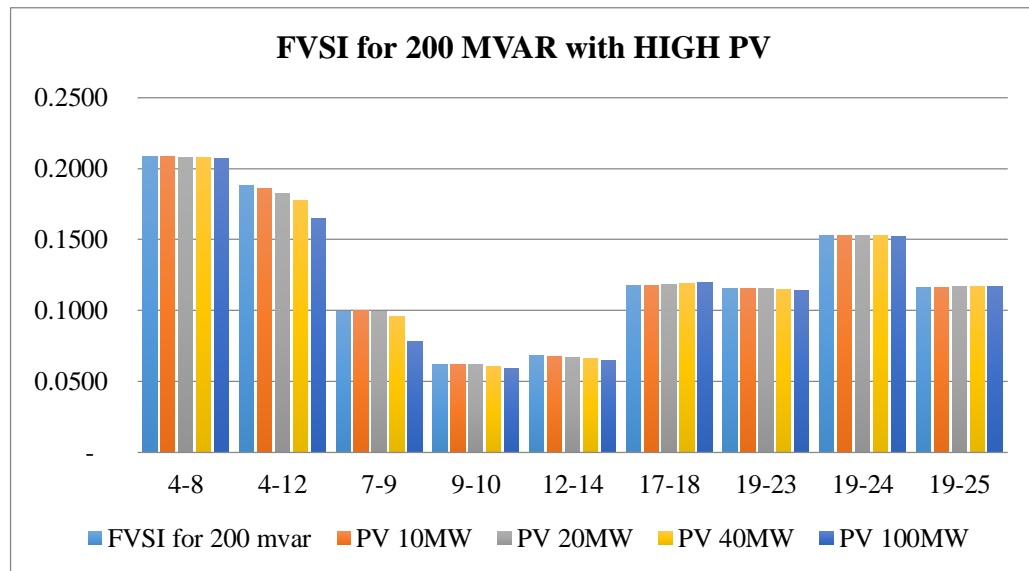
LOW (PV Output)					
Linedata	PV Capacity	10MW	20MW	40MW	100MW
	PV Output	0.859MW	1.734MW	3.485MW	8.721MW
	FVSI for 200MVAR	FVSI			
4-8	0.2088	0.2088	0.2088	0.2087	0.2085
4-12	0.1884	0.1880	0.1876	0.1868	0.1845
7-9	0.0994	0.0996	0.0998	0.1000	0.1000
9-10	0.0620	0.0620	0.0620	0.0620	0.0619
12-14	0.0682	0.0681	0.0681	0.0679	0.0676
17-18	0.1179	0.1179	0.1180	0.1180	0.1182
19-23	0.1156	0.1156	0.1156	0.1155	0.1154
19-24	0.1531	0.1531	0.1531	0.1530	0.1530
19-25	0.1166	0.1166	0.1166	0.1166	0.1166



AVERAGE (PV Output)					
Linedata	PV Capacity	10MW	20MW	40MW	100MW
	PV Output	4.475MW	8.941MW	17.891MW	44.652MW
	FVSI for 200MVAR	FVSI			
4-8	0.2088	0.2087	0.2085	0.2081	0.2073
4-12	0.1884	0.1864	0.1844	0.1800	0.1693
7-9	0.0994	0.1001	0.1000	0.0977	0.0836
9-10	0.0620	0.0620	0.0619	0.0613	0.0592
12-14	0.0682	0.0679	0.0676	0.0668	0.0653
17-18	0.1179	0.1180	0.1182	0.1188	0.1195
19-23	0.1156	0.1155	0.1154	0.1151	0.1144
19-24	0.1531	0.1530	0.1530	0.1530	0.1526
19-25	0.1166	0.1166	0.1166	0.1168	0.1169

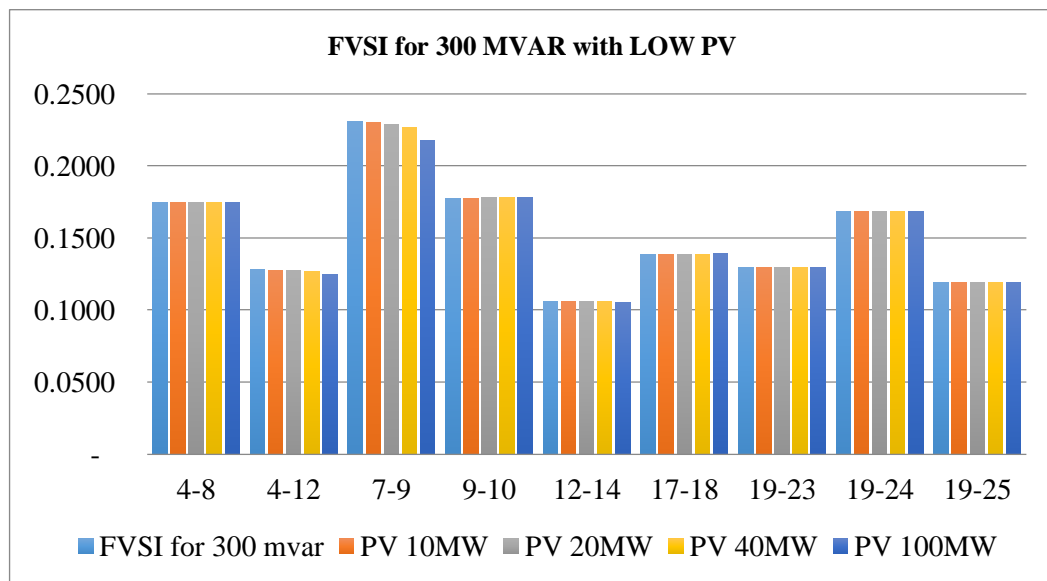


HIGH (PV Output)					
Linedata	PV Capacity	10MW	20MW	40MW	100MW
	PV Output	5.708MW	11.412MW	22.807MW	56.826MW
	FVSI for 200MVAR	FVSI			
4-8	0.2088	0.2086	0.2083	0.2079	0.2070
4-12	0.1884	0.1858	0.1828	0.1780	0.1649
7-9	0.0994	0.1002	0.0996	0.0956	0.0785
9-10	0.0620	0.0620	0.0617	0.0608	0.0591
12-14	0.0682	0.0678	0.0672	0.0665	0.0648
17-18	0.1179	0.1181	0.1186	0.1189	0.1198
19-23	0.1156	0.1155	0.1153	0.1150	0.1141
19-24	0.1531	0.1530	0.1530	0.1530	0.1523
19-25	0.1166	0.1166	0.1167	0.1168	0.1170

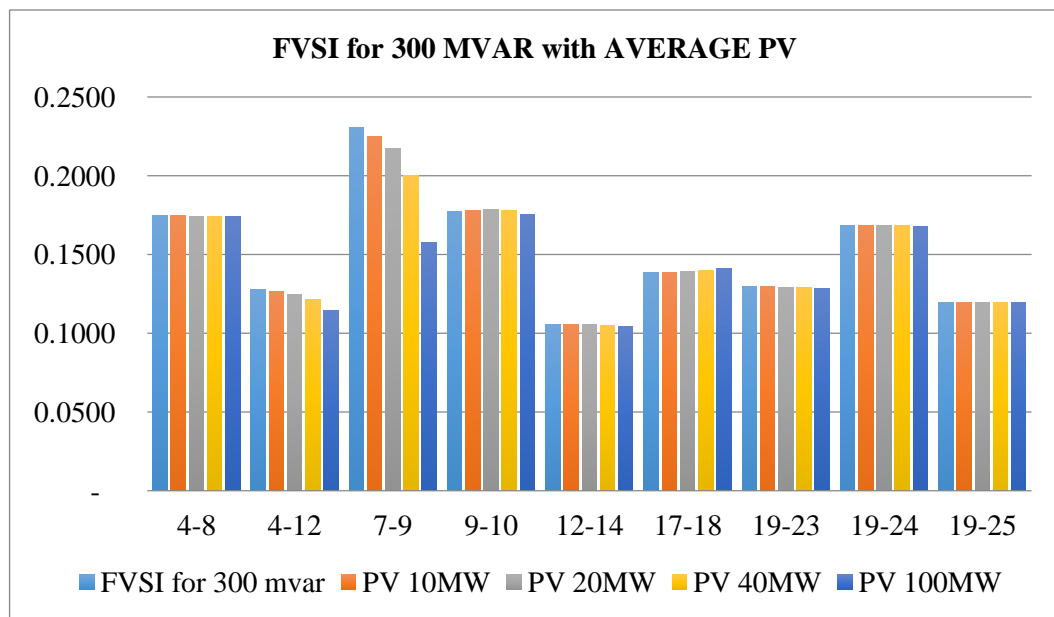


c) FVSI: Reactive Power 300MVAR, with PV (10MW, 20MW, 40MW and 100MW)

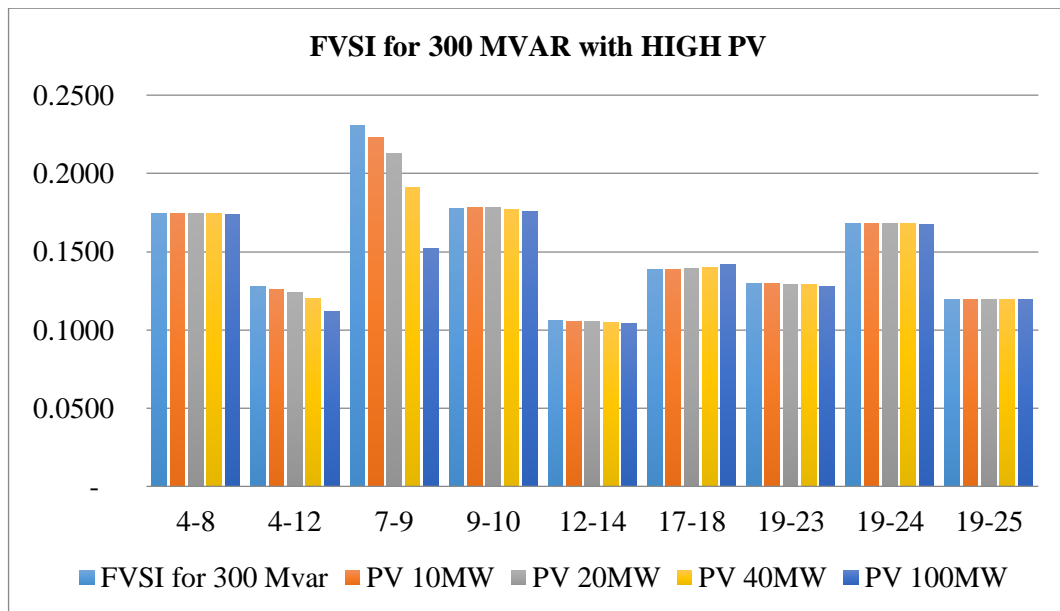
LOW (PV Output)					
Linedata	PV Capacity	10MW	20MW	40MW	100MW
	PV Output	0.859MW	1.734MW	3.485MW	8.721MW
	FVSI for 300MVAR	FVSI			
4-8	0.1747	0.1747	0.1747	0.1746	0.1746
4-12	0.1280	0.1277	0.1274	0.1267	0.1249
7-9	0.2310	0.2300	0.2289	0.2265	0.2181
9-10	0.1777	0.1778	0.1780	0.1782	0.1785
12-14	0.1059	0.1059	0.1058	0.1057	0.1055
17-18	0.1386	0.1386	0.1387	0.1388	0.1391
19-23	0.1297	0.1296	0.1296	0.1296	0.1294
19-24	0.1684	0.1684	0.1684	0.1684	0.1684
19-25	0.1195	0.1195	0.1195	0.1196	0.1196



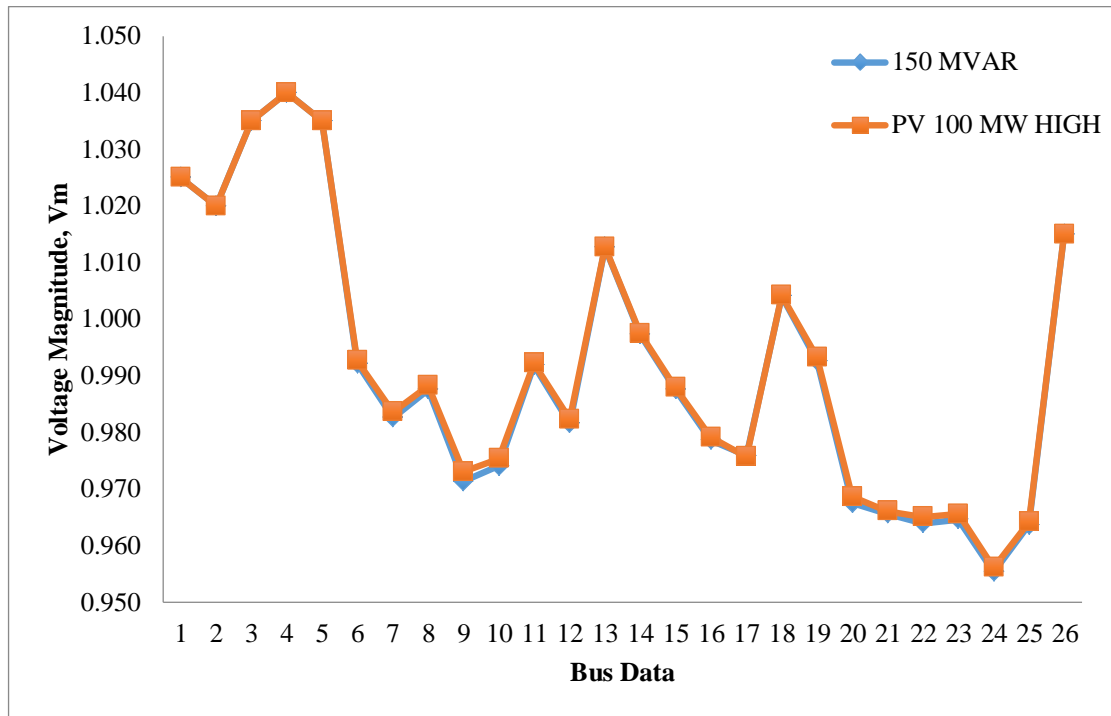
AVERAGE (PV Output)					
Linedata	PV Capacity	10MW	20MW	40MW	100MW
	PV Output	4.475MW	8.941MW	17.891MW	44.652MW
	FVSI for 300MVAR	FVSI			
4-8	0.1747	0.1746	0.1746	0.1745	0.1742
4-12	0.1280	0.1264	0.1248	0.1218	0.1144
7-9	0.2310	0.2250	0.2177	0.2006	0.1578
9-10	0.1777	0.1783	0.1785	0.1779	0.1758
12-14	0.1059	0.1057	0.1055	0.1051	0.1042
17-18	0.1386	0.1389	0.1392	0.1397	0.1412
19-23	0.1297	0.1295	0.1294	0.1292	0.1284
19-24	0.1684	0.1684	0.1684	0.1683	0.1677
19-25	0.1195	0.1196	0.1196	0.1196	0.1198



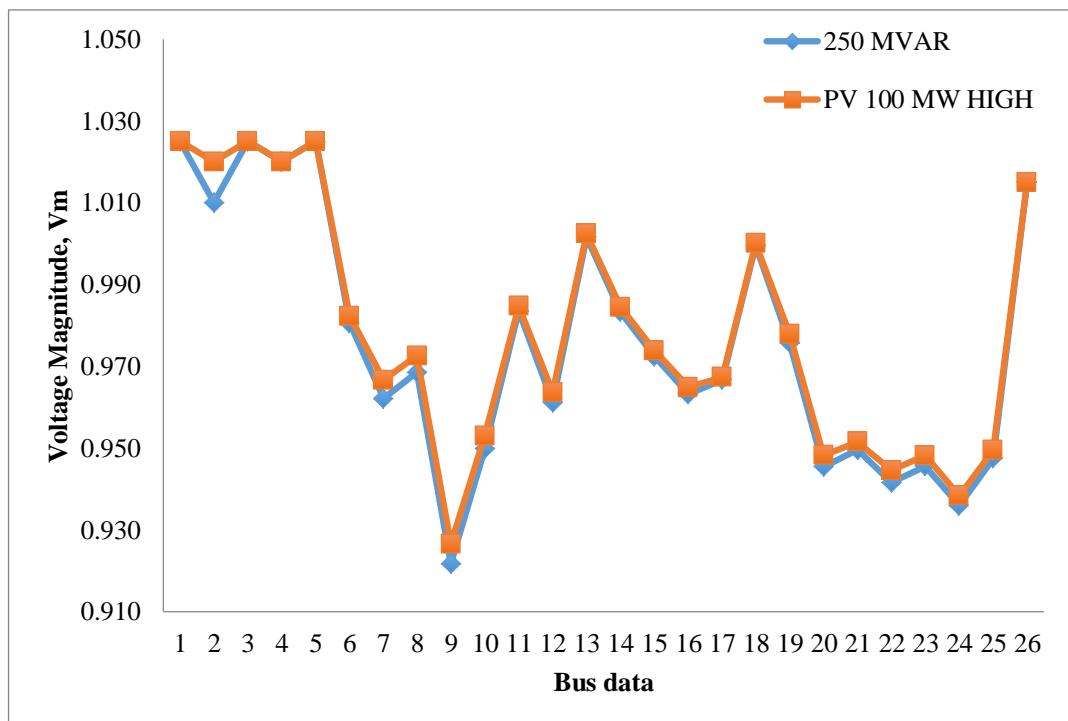
HIGH (PV Output)					
Linedata	PV Capacity	10MW	20MW	40MW	100MW
	PV Output	5.708MW	11.412MW	22.807MW	56.826MW
	FVSI for 300MVAR	FVSI			
4-8	0.1747	0.1746	0.1745	0.1744	0.1741
4-12	0.1280	0.1259	0.1239	0.1202	0.1119
7-9	0.2310	0.2231	0.2132	0.1909	0.1522
9-10	0.1777	0.1784	0.1784	0.1773	0.1761
12-14	0.1059	0.1056	0.1054	0.1049	0.1039
17-18	0.1386	0.1389	0.1393	0.1400	0.1418
19-23	0.1297	0.1295	0.1293	0.1290	0.1281
19-24	0.1684	0.1684	0.1684	0.1682	0.1674
19-25	0.1195	0.1196	0.1196	0.1197	0.1198



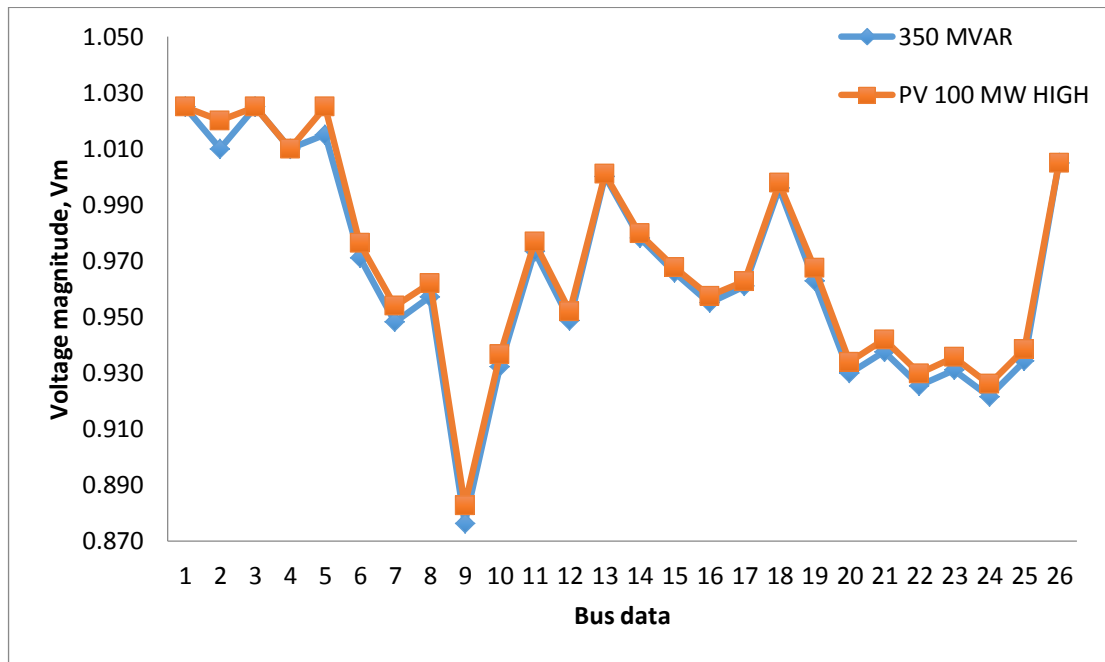
Appendix C: Voltage Profile for 26 Bus Test System



Voltage Profile for 26 Bus Test System for $Q_9=150\text{MVAR}$ reactive power loading with 100MW solar PV



Voltage Profile for 26 Bus Test System for $Q_9=250\text{MVAR}$ reactive power loading with 100MW solar PV



Voltage Profile for 26 Bus Test System for $Q_9=350\text{MVAR}$ reactive power loading
with 100MW solar PV

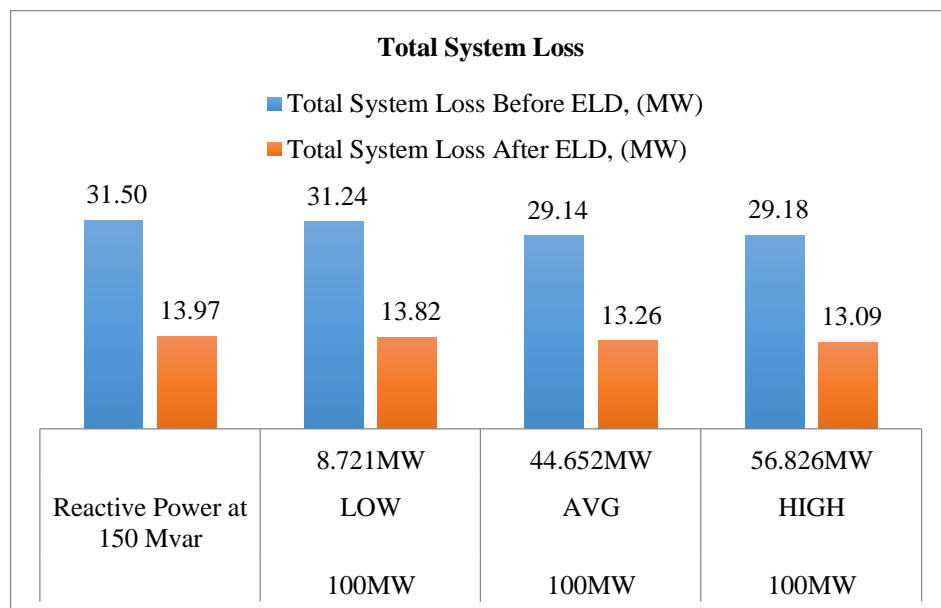
Appendix D: Economic Load Dispatch Before and After PV Placement

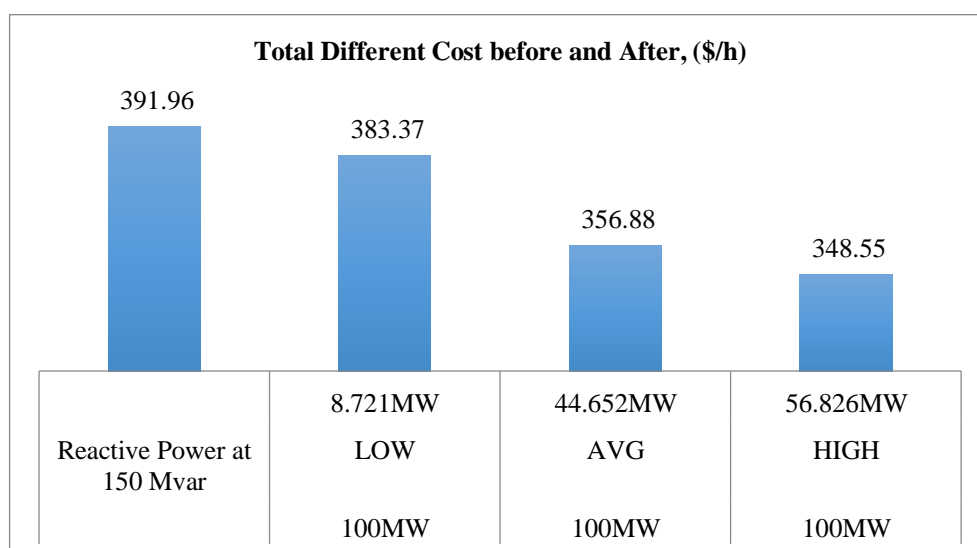
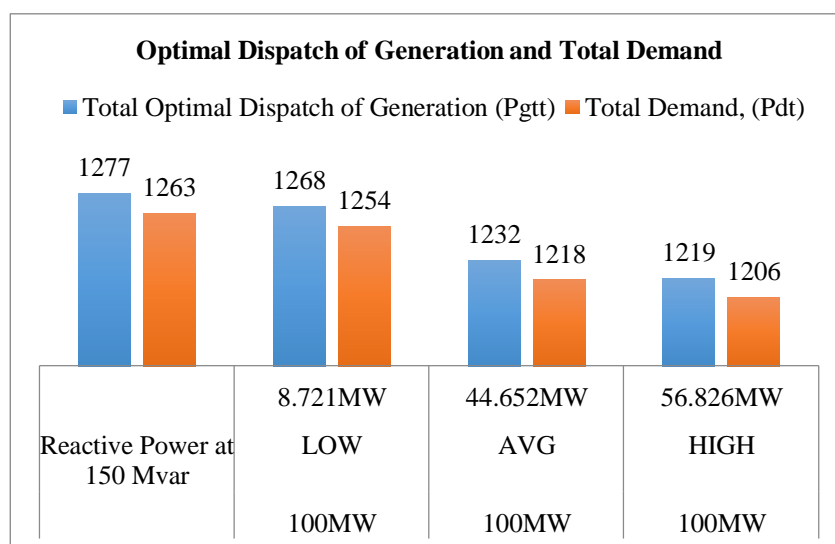
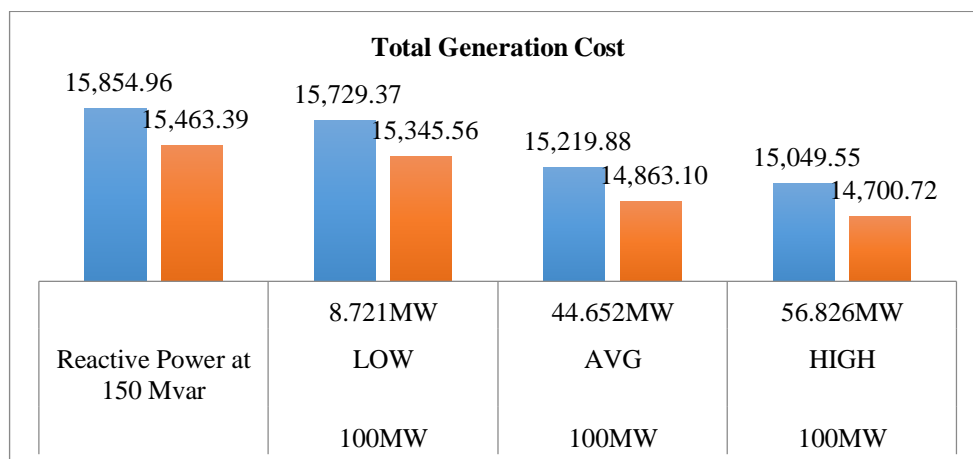
a) 100MW with Reactive Power 150 MVAR

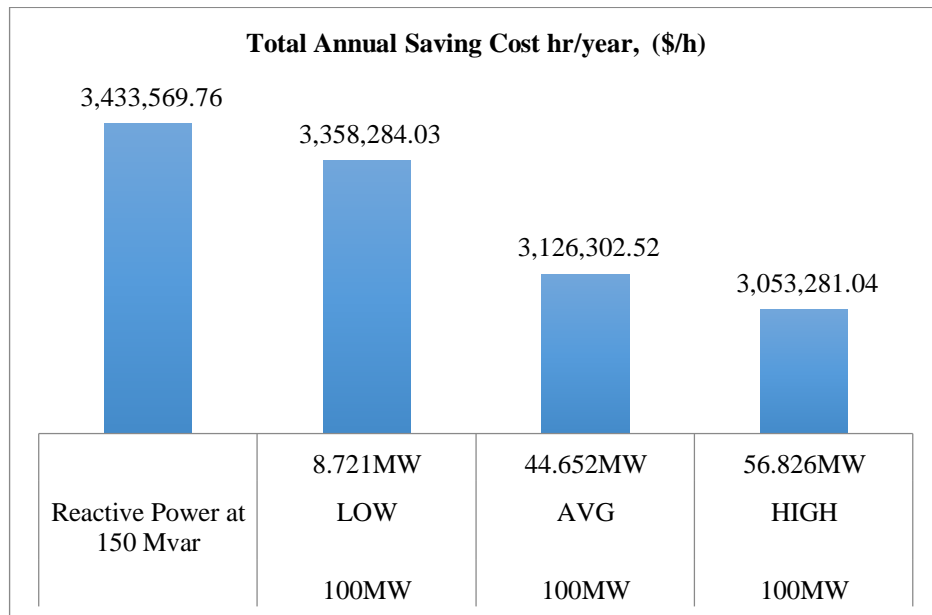
Initial Operating Condition for Reactive Power at 150 MVAR				
PV Capacity 100MW				
Case		LOW	AVG	HIGH
		PV output		
	Without PV	8.721MW	44.652MW	56.826MW
Total System Loss (MW)	31.50	31.24	29.14	29.18
Total Generation Cost, (\$/h)	15,854.96	15,729.37	15,219.88	15,049.55

After Optimization Condition for Reactive Power at 150 MVAR				
PV Capacity 100MW				
Case		LOW	AVG	HIGH
		PV output		
	Without PV	8.721MW	44.652MW	56.826MW
Total System Loss (MW)	13.97	13.82	13.26	13.09
Total Generation Cost (\$/h)	15,463.39	15,345.56	14,863.10	14,700.72
Total Optimal Dispatch of	1277	1268	1232	1219

Generation (Pgwt)				
Total Demand, (Pdt)	1263	1254	1218	1206
Total Different Cost before and After, (\$/h)	391.96	383.37	356.88	348.55
Total Annual Saving Cost hr/year, (\$/h)	3,433,569.76	3,358,284.03	3,126,302.52	3,053,281.04







b) 100MW with Reactive Power 250 MVAR

Initial Operating Condition for Reactive Power at 250 MVAR				
PV Capacity 100MW				
Case		LOW	AVG	HIGH
		PV output		
	Without PV	8.721MW	44.652MW	56.826MW
Total System Loss (MW)	32.15	29.86	27.72	27.94
Total Generation Cost, (\$/h)	15,911.00	15,784.70	15,275.08	15,105.09

After Optimization Condition for Reactive Power at 250 MVAR				
PV Capacity 100MW				
Case		LOW	AVG	HIGH
		PV output		
	Without PV	8.721MW	44.652MW	56.826MW
Total System Loss (MW)	16.90	16.75	16.19	15.86
Total Generation Cost (\$/h)	15,504.04	15,386.09	14,903.17	14,738.33
Total Optimal Dispatch of Generation (Pg_{tt})	1280	1271	1235	1222
Total Demand, (P_{dt})	1263	1254	1218	1206
Total Different Cost before and After, (\$/h)	407.00	398.70	372.08	367.09
Total Annual Saving Cost hr/year, (\$/h)	3,565,363.23	3,492,598.78	3,259,446.14	3,215,738.29

